REGULATION OF GLUT-4 EXPRESSION IN SKELETAL MUSCLE CELLS:

THE ROLES OF NUCLEAR RESPIRATORY FACTOR-1 AND CALCIUM/CALMODULIN DEPENDENT PROTEIN KINASE

EMMANUEL MUKWEVHO

Thesis presented for the Degree of

DOCTOR OF PHILOSOPHY in ANATOMY & CELL BIOLOGY

In the department of Human Biology

UNIVERSITY OF CAPE TOWN

SOUTH AFRICA

February, 2010

UCT/MRC Research Unit for Exercise Science & Sports medicine
Sports Science Institute of South Africa
Boundary Road
Newlands, 7700
Cape Town

Supervisor: Associate Professor Edward Ojuka, PhD

TABLE OF CONTENTS

ACKNOWLEDGEMENTS

I wish to acknowledge and express my sincere gratitude to the following people for their support:

Edward Ojuka: for the amazing support, input and superb guidance throughout this degree. I could have not asked for a better supervisor. His door was always open to me, and he always made time to accommodate me. He has played a tremedous role in formulating the ideas behind this research and guiding me to become a better scientist/researcher. I was able to travel to Europe, America and locally within South Africa to present my work though his support. This has given me huge exposure, confidence and passion for science. I'm deeply immensely grateful for his friendship and support.

Dr James Smith and Dr Tertius Kohn: who worked closely with me in the laboratory, for their valuable contribution to my work and for the jovial manner with which we interacted throughout my PhD program.

Dr Lester Davids, Professor Sue Kidson, Dr Sheron Prince and Prof Mike Lambert: for their support and encouragement throughout my degree.

Prof Tim Noakes: for providing me with the opportunity to do my PhD degree in his research unit. It was a priviledge to work under such an inspiring leader, who showed enthusiasm and great interest in my progress. His friendly smile, words of advice and encouragement, made me feel at home in the UCT/MRC Exercise Science and Sports Medicine Research Unit.

To my friends: Dr Sandile Ncanana, Dr Ganto Mlugiseleni, Dr Nonto Mabizela, Dr Precious Motshwene, Dr Mbhiza Freeman, Dr Ross Tucker, Dr Tamara Hew, Dr Jonathan Dugas, Dr Zandile Mciza, Dr George Mokone, Dr Zungu Makhosi, Dr Mudzunga Theophilous, John Kayembe, Godwin Magosha, Rofhiwa Takalani and Chauke Blessing, I love you all and thank you for your support.

To my family: my mother Phophi Mukwevho and my late Dad, who died at the hands of type II diabetes, this research is dedicated to you. Thank you for loving me and for your unwavering support since birth. My brothers and sisters, thank you for your support and love.

I am also grateful to the National Research Foundation (NRF), the Medical Research Council and the University of Cape Town for financial assistance.

"**I thank God for His mercies that endureth for ever and for loving me with an everlasting love, that great shepherd of the sheep**"

PUBLICATION ASSOCIATED WITH THIS THESIS

Full paper

E.Mukwevho, T.A. Kohn, D.M. Lang, E. Nyatia, J.A.H. Smith & E.O.Ojuka. Caffeine induces hyper-acetylation of histones at the MEF2 site on the *Glut4* promoter and increases MEF2A binding to the site via a CaMK-dependent mechanism. *Am J Physiol Endocrinol Metab*. **294:E582 – E288, 2008.**

Presentations at international and national conferences

1. **Experimental Biology 2010.** The role of NRF-1 in stimulating GLUT4 expression**. April 24-28, 2010. Anaheim, Carlifonia, U.S.A (to be attended, abstract already accepted).**
2. **European College of Sports Science (ECSS).** NRF-1 regulation of GLUT4 expression in C2C12 myotubes**. June 24-27, 2009. Oslo, Norway.**
3. **University of Cambridge, Department of Biochemistry.** Exercise-induced protection of type II diabetes**. June 29- July 6, 2009. Cambridge, United Kingdom.**
4. **Intergrative Biology of Exercise**. Binding of nuclear respiratory factor-1 to *mef2A* and *Alas* promoters depends on CaMK II activity in C2C12 myotubes**. September 2008, Hilton Head, South Carolina, U.S.A.**
5. **School of Biomedical Sciences, UCT**. Binding of nuclear respiratory factor-1 to *mef2A* and *ALAS* promoters depends on CaMK II activity in C2C12 myotubes. **September, 2008, Cape Town**.
6. **Physiological Society of Southern Africa (PSSA).** Caffeine induces hyper-acetylation of histones at MEF2 site in the GLUT4 promoter and increases MEF2A binding to the

site via a CaMK dependent manner. **September, 2007, Johannesburg.**

7. **The Medical Research Council Research da**y. Caffeine induces hyperacetylation of histones at MEF2 site in the GLUT4 promoter and increases MEF2A binding to the site via a CaMK dependent manner, **October 2007, Cape Town**.
8. **Physiological Society of Southern Africa (PSSA).** Activation of CaMK by caffeine causes nuclear export of HDAC-5 and increases *glut-4* content in C2C12 cells. **September. 2006, Durban.**
9. **University of Cape Town School of Biomedical Sciences Research day.** Activation of CaMK by caffeine causes nuclear export of hdac-5 and increases *glut-4* content in C2C12 cells**, September, 2006, Cape Town.**

LIST OF FIGURES

LIST OF TABLES

LIST OF ABBREVIATIONS

AcH3 –acetyl histone H3

δalas –delta aminolevulinate synthase

ADA – American Diabetes Association

ADP – adenine diphosphate

ATP- adenosine 5’ triphosphate

bp –base pairs

BSA- bovine serum albumin

C-terminus – carboxyl terminus

C2C12- mouse muscle cell line

Ca^{2+} - calcium

$CaCl_2$ –calcium chloride

CAF- caffeine

CaMK - Ca^{2+}/calmodulin dependent protein kinase

CIP –calf intestine phosphatase

CO_2 – carbon dioxide

CBP- CREB-binding protein

cDNA - complementary DNA

ChIP - chromatin immunoprecipitation

CMV-cytomegalovirus

CON – control

CREB – cAMP response element binding protein

DAG-diacylglycerol

DAPI - 4′, 6′-diamidino-2-phenylindole

DMEM – Dulbecco's modified eagles medium

DNA – deoxyribonucleic acid

dNTP – deoxyribonucleotide triphosphate

Dox - doxycycline

E.coli - Escherichia coli

EDTA – ethylene diamine tetra acetic acid

EMSA – electrophoretic mobility shift assays

F – forward

FBS- foetal bovine serum

FFM – fat free milk

Fwd - forward

GAPDH –glyceraldehyde 3-phosphate dehydrogenase

GEF –GLUT4 enhancer factor

GLUT4 – glucose transporter 4 protein or mRNA

glut4 – promoter or gene encoding for GLUT4

G418 – Geneticin

h - hour

HAT – histone acetyl transferase

HCl – hydrochloric acid

HDAC- histone deacetylase

HEPES -4-(2-Hydroxyethyl) piperazine-1-ethanesulfonic acid

HES – buffer containing HEPES, EDTA and sucrose

HRP- horse radish peroxidase

HS – horse serum

IgG – immunoglobulin G

In vitro- refers to an experiment outside a living organism in a controlled environment

In vivo – refers to a experiment conducted within a living organism

INPUT- sample used for ChIP assay prior to immunoprecipitation step

IP - immunoprecipitation

IRS1/2- insulin receptor substrate 1/ 2

KN93- CaMK II inhibitor

KOH – potassium hydroxide

L6- rat muscle cell line

L-broth – luria broth

LC –light cycler

LDH – lactate dehydrogenase

Leu – leucine

Lys –Lysine

M - molar

mA – milli ampere

MEF2- myocyte enhancer factor 2 protein/ mRNA

mef2 – gene encoding for MEF2

$MgCl_2$ – magnesium chloride

Min - minutes

MMLV –moloney murine leukemia virus

mm -millimeter

mM – millimolar

ml -milliliter

MOPS- 1 % 3-(N-morpholino) propanesulfonic acid

mRNA – messenger ribonucleic acid

N- terminus –amino terminus

Na_3VO_4 – sodium orthovanadate

$Na_3P_2O_7$ – sodium pyrophosphate

NaCl – sodium chloride

NaF – sodium fluoride

$NaHCO_3$ – sodium bircarbonate

NaOH –sodium hydroxide

-ve -negative

nm – nano meter

NP-40 – nonidet P-40

NRF-1 – nuclear respiratory factor- 1

OD – optical density

PAGE – polyacrylamide gel electrophoresis

PBST – phosphate buffered saline (PBS) containing 0.1 % Tween 20

PCAF – p300/ CBP-associated factor

PCR – polymerase chain reaction

PGC-1 – peroxisome proliferator- activated receptor gamma coactivators -1

PI3 kinase – phosphatidylinositol 3-kinase

pmol- pico mole

PMSF- phenylmethylsulphonic acid

+ve – positive

pTet-On- Tetracycline based plasmid which serves as a regulatory vector

pTRE2Hyg- Tetracycline response element (TRE) plasmid with hygromycin resistant gene (serves as reponse plamid for the Tet-On plasmid).

PVDF- polyvinylidene diflouride

qRT-PCR – quantitative real time polymerase chain reaction

RT-PCR –reverse transcriptase-polymerase chain reaction

R-primer – reverse primer

Rev - reverse

RS12 – ribosomal protein S12

RPM – rotation per minute (rpm)

RNA – ribonucleic acid

SDS – sodium dodecyl sulphate

siRNA – small interference ribonucleic acid

STZ – streptozotocin

TBST- Tris buffered saline (TBS) containing 0.1 % Tween 20

TE - buffer containing Tris-Cl and EDTA

TRE- Tetracycline response element

µg –microgram

WHO –World Health Organization

DECLARATION

I Emmanuel Mukwevho, do hereby declare that this dissertation is based is my original work (apart from the normal guidance from my supervisor and except where acknowledgements indicate otherwise) and that neither the whole work nor part of it has been, is being, or is to be submitted for another degree in the University of Cape Town or any other university.

This thesis is presented in fulfilment of the requirement for the degree of PhD in Anantomy and Cell Biology.

I hereby empower the University of Cape Town to reproduce parts, or the whole, of this thesis for the purpose of research.

SIGNATURE: ……

DATE: ……....

REGULATION OF GLUT-4 EXPRESSION IN SKELETAL MUSCLE CELLS: THE ROLES OF NUCLEAR RESPIRATORY FACTOR-1 AND CALCIUM/CALMODULIN DEPENDENT PROTEIN KINASE

EMMANUEL MUKWEVHO

Thesis presented for the Degree of

DOCTOR OF PHILOSOPHY in ANATOMY & CELL BIOLOGY

In the department of Human Biology

UNIVERSITY OF CAPE TOWN

SOUTH AFRICA

February, 2010

UCT/MRC Research Unit for Exercise Science & Sports medicine
Sports Science Institute of South Africa
Boundary Road
Newlands, 7700
Cape Town

Supervisor: Associate Professor Edward Ojuka, PhD

ABSTRACT

GLUT4 protein is the major glucose transporter in skeletal muscle and is vital in the maintenance of euglycemia (17; 108). Underexpression of GLUT4 or impairement of its translocation from intracellular compartments to the cell surface, are linked to diminished glucose transport, hyperglycemia and type II diabetes (59; 61; 153). Type II diabetes can be alleviated by increasing GLUT4 expression (223). Previous reports have shown that overexpression of NRF-1 and activation of CaMKII increases GLUT4 expression but the mechanisms involved have not be characterized (10; 173). Therefore, the objective of this thesis was to investigate the molecular mechanisms by which NRF-1 and CaMK II regulate GLUT4 expression in C2C12 myocytes.

We engineered C2C12 cells that overexpressed NRF-1 in response to doxycycline (Dox) using a Tet-On gene expression system and assessed the effects of NRF-1 overexpression on: a) MEF2A, GLUT4 and δALAS proteins by western blot, and b) the binding of NRF-1 to *mef2a* and *δalas* genes and MEF2A to the *glut4* gene, by chromatin immunoprecipitation assay (ChIP). The importance of MEF2A in NRF-1-induced increase in GLUT4 expression was investigated by silencing MEF2A expression using small interference RNA (siRNA). CaMK II was activated in wild-type C2C12 myocytes using 10 mM caffeine and was inhibited by 25 μM KN93. Acetylation of histones in the vicinity of NRF-1 and MEF2A binding sites on the *mef2a* and *glut4* genes, respectively, were assessed by ChIP assay. HDAC5 nuclear export was assessed by immunocytochemistry and mRNA levels by qRT-PCR.

Overexpression of NRF-1 resulted in ~3-fold increases in *mef2a*-bound NRF-1 and *glut4* -bound MEF2A at 6 h and 8 h post Dox treatment, respectively. MEF2A and GLUT4 proteins were both increased ~1.6-fold at 6 h and 18 h post Dox treatment. Silencing of MEF2A caused a marked downregulation of GLUT4 expression in NRF-1-overexpressing cells. The results support the

notion that NRF-1 overexpression increases GLUT4 expression via a transcriptional cascade involving NRF-1→ *mef2a*→ MEF2A→ *glut4*→ GLUT4.

CaMK II activation with caffeine for 2 h resulted in a ~2.5-fold increase in binding of NRF-1 to the *mef2a* gene 6 h after treatment, hyperacetylation of histone H3 in the vicinity of the NRF-1 binding domain on the *mef2a* gene, and ~ 2-fold increase in MEF2A expression 6 h post treatment. Moreover, we observed ~2-fold increase in the binding of MEF2A to the *glut4* gene, hyperacetylation of histones in the vicinity of MEF2A binding sites on the *glut4* gene, significant nuclear export of HDAC5, and ~2.8-fold increase in GLUT4 expression 6 h post treatment. CaMKII inhibition with KN93 resulted in significant decreases in all the observed changes; indicating that CaMK II was involved in these pathways. Collectively these results support the notion that CaMK activation remodels chromatin to increase the binding of NRF-1 to the *mef2a* gene and MEF2A to the *glut4* gene and increases their expression.

CHAPTER 1

The problem and its setting

1.1 Introduction

Type II diabetes is a non communicable metabolic disorder characterised by impaired plasma glucose disposal, resulting in hyperglycemia. This disease is most common among individuals who are physically inactive. In these individuals, the impairment in glucose transport from plasma into tissues, especially into muscle tissues, appears to result from a) down regulation of GLUT4, the insulin-sensitive glucose transporter b) the attenuation of insulin-mediated signalling cascade (162; 174) and c) insulin resistance due to impaired mitochondrial function (161; 177; 181). Physically active individuals are generally protected from type II diabetes because physical activity increases GLUT4 expression and translocation, and mitochondrial content (24; 43; 104; 179; 208). Because changes in the contents of muscle mitochondria and GLUT4 occur in parallel (10; 11), it has been suggested that they are initiated by the same signal and/or have common signalling intermediaries (10; 11; 91; 208).

It is now well established that mitochondrial biogenesis relies on the interplay of genes that are expressed from both nuclear and mitochondrial genomes. The coordinated expression of these genes is achieved through the action of transcription factors called nuclear respiratory factors (NRF)-1 and NRF-2 that belong to the cap ‘n’ collar-basic leucine zipper (CNC-bZIP) proteins (102). The expression of the *nrf-1* gene, together with the genes that depend on its expression, are down-regulated in patients with type II diabetes and those with a family history of the disease (161; 177). Lately it has been shown that NRF-1 also regulates GLUT4 expression: For example, transgenic mice that overexpress NRF-1 have markedly elevated GLUT4 levels (10). Because the

NRF-1 *cis* element is not present on the *glut4* gene, it has been hypothesised that the increase in GLUT4 expression in NRF-1 transgenic mice is a result of a transcriptional cascade involving NRF-1→ *mef2a*→ *glut4*. Support for this hypothesis comes from the fact that the *mef2a* gene has a NRF-1 binding site (185) and MEF2A is the key transcriptional regulator of the *glut4* gene (223). This hypothesis implies that NRF-1 might be one of the signalling intermediaries that link GLUT4 expression with mitochondrial biogenesis and therefore would be a suitable target for the design of therapeutic drugs for use in the treatment and management of type II diabetes. Since direct evidence for the existence of a NRF-1→ *mef2a*→ *glut4* transcriptional cascade is still lacking, one of the aims of this project was to provide evidence for or against the existence of this transcriptional cascade.

The transcriptional activity of MEF2 factors are influenced markedly by their interaction with histone modifying enzymes such as class II histone deacetylases (HDACs) and histone acetyl transferases (HATs). HDACs remove negatively charged acetyl groups from histones which condense chromatin and render it less accessible to transcriptional regulators (13). Many researchers have shown that the presence of MEF2-HDAC complexes on regulatory elements of genes harbouring MEF2 binding sites is associated with repression of those genes (79; 158). Of note is the discovery that MEF2-HDAC complexes may be dissociated when two serine-containing motifs on the deacetylase are phosphorylated by calcium/calmodulin dependent protein kinase (CaMK) II (41; 118; 143) and once phosphorylated, the HDACs are shuttled from the nucleus to the cytoplasm by chaperone molecules (25; 156; 158). The nucleocytoplasmic shuttling of HDACs relieves HDAC-mediated repression of MEF2-dependent genes and promotes association of MEF2 with HATs (79; 237). HATs catalyze the transfer of acetyl moieties to lysine residues on histones, resulting in their repulsion by the negatively charged DNA (62). This process allows increased

access of transcription factors to binding domains on DNA and is associated with increased gene transcription. Indeed, there is a growing body of evidence showing that increases in the expression of GLUT4 and mitochondrial proteins in skeletal muscle require CaMK II activation: Firstly, CaMK transgenic mice have higher mitochondrial content than wild-type mice (234). Secondly, exercise increases GLUT4 protein levels in muscle and inhibition of CaMK II activity by KN93 during exercise abrogated these effects (212). Thirdly, incubation of myotubes with caffeine to increase cytosolic calcium and activate CaMK II has also been shown to increase GLUT4 and mitochondrial proteins and inclusion of KN93 together with caffeine prevents these increases (172; 173).

Although there is ample data which demonstrate that CaMK II is required for GLUT4 expression, there is still no direct evidence that CaMK II activation affects events at the *glut4* promoter. Therefore this study also tested the hypothesis that CaMK II activation induces hyperacetylation of histones in the vicinity of the MEF2 binding site on the *glut4* gene and increases the binding of MEF2A to the site in C2C12 myotubes. Furthermore, since activation of CaMK II by caffeine increases MEF2A expression (173), and the *mef2a* gene has one NRF-1 binding domain (185), we further tested the hypothesis that CaMK II activation induces hyperacetylation of histones in the neighbourhood of the NRF-1 binding site on the *mef2a* gene to increase NRF-1 binding there.

1.2. The objectives of this study

There were two main objectives of the study: The first objective was to investigate the molecular mechanism by which NRF-1 regulates GLUT4 expression in C2C12 cell line. In this regard, we tested the hypothesis that NRF-1 regulates GLUT4 expression via a transcriptional

cascade involving NRF-1→*mef2a* → *glut4*. The second objective of the study was to investigate the molecular mechanisms by which CaMK II activation by caffeine increases GLUT4 expression in C2C12 myotubes. In this regard we tested the hypotheses that CaMKII activation: a) causes HDAC5 nuclear export, b) induces hyperacetylation of histones in the vicinity of the MEF2 binding site on the *glut4* gene, and c) increases MEF2A binding to the *glut4* gene.

CHAPTER 2

Literature Review

2.1. Introduction

A review of related literature is provided in this chapter. This review starts by discussing several studies that have provided evidence that regular physical activity protects individuals from insulin resistance and type II diabetes. Next, it looks at studies that have provided the molecular mechanisms for protection. In this regard, studies which have shown that physical activity upregulates GLUT4 expression and promote mitochondrial biogenesis, are discussed. The molecular signals that coordinate GLUT4 expression and mitochondrial biogenesis, especially NRF-1 and CaMK are reviewed in detail. Lastly, the effects of CaMK II activation on a) the remodelling of chromatin to facilitate the binding of NRF-1 to genes that code for mitochondrial and MEF2 proteins and b) the binding of MEF2A to the *glut4* gene, are examined.

2.2. A comparison of the incidence of type II diabetes amongst sedentary and physically active individuals

Epidemiological studies indicate that individuals who maintain regular physical activity are much less likely to develop type II diabetes than physically inactive persons (26; 62; 69; 86; 100; 137; 138; 148; 150; 151). The reduction in the risk of diabetes due to physical activity is, in part, due to increased glucose transport capacity and improved insulin sensitivity (95; 106; 120; 169; 189; 220).

A study by Helmrich et al., (86) investigated the association between leisure time physical activity and the risk of type II diabetes amongst 5990 male alumni from the University of

Pennsylvania from 1962-1976. They found that: a) leisure time physical activity, expressed as kilocalories expended per week in walking, stair climbing, and sports, was inversely related to the development of non-insulin dependent diabetes mellites (NIDDM); b) for each 500-kcal increment in energy expenditure, the age-adjusted risk of NIDDM was reduced by 6 %; and c) the protective effects of physical activity was strongest in persons at highest risk of NIDDM, i.e. people with high body mass index, a history of hypertension, or a family history of diabetes. Another study, "The Nurses Health Study" by Manson et al., (151) showed that physical activity also protects women: They followed 87,253 diabetic-free US women aged 34-59 years for 8 years and found that women who engaged in vigorous physical activity at least once per week had a 33 % lower risk of type 2 diabetes compared to sedentary controls that did not engaged in physical activity. Similar results were observed in other studies (51; 101; 204).

Type II diabetes is often preceded by a reduction in insulin sensitivity which is characterised by a defect in the insulin signalling pathways that may result in impaired translocation of GLUT4 to the cell surface (71). Many studies have investigated the relationship between physical activity and insulin sensitivity. For example, the "Insulin Resistance Atherosclerosis Study" by Mayer-Davis et al., (154) showed that both vigorous and mild activities were positively associated with insulin sensitivity amongst 1467 men and women of 40-69 years of age. The "British Regional Study" by Wannamethee et al., (229), which studied 5159 men aged 40-59 years, showed that light and moderate physical activities were significantly and inversely associated with serum insulin concentrations. Some studies have found that six weeks of training by insulin-resistant and diabetic patients increased insulin stimulated glucose transport by 2-fold compared to sedentary controls (179). Short et al., (208) also showed that 16 weeks of moderate-intensity aerobic exercise increased insulin sensitivity and glucose transport independent of age. In contrast, cessation of

physical activity for 14 days by endurance-trained runners or strength-trained weight lifters was associated with a decrement in insulin sensitivity.

Associations between physical activity, insulin sensitivity and glucose transport, have been shown in animal models too: For example, ten weeks of endurance training increased insulin sensitivity in rats (7; 189); exercise restores to normal the levels of insulin sensitivity and whole body glucose disposal in severely diabetic rats (39; 72; 107; 231); voluntary exercise on running wheels increased glucose transport capacity in rats (47; 90; 109; 192; 209); and male Sprague-Dawley rats that swam with weights attached to their tails for 2 h a day for 5 days exhibited 87 % and 85 % increases in glucose transport and insulin responsiveness, respectively, compared to sedentary rats; and physical activity delayed or prevented the onset of type II diabetes in rats (119).

Collectively, these studies, showing that regular physical activity improves insulin sensitivity and decreases the risk of type II diabetes in humans and animals, provide the basis for the current advocacy of regular physical activity as a way to protect individuals from these diseases. However, the molecular mechanisms of protection are not fully understood.

2.3. The mechanisms by which physical activity protects people from diabetes

Epidemiological data showing fewer cases of type II diabetes in individuals who are physically active compared to those who are sedentary have suggested that physical activity protects against type II diabetes. Controlled experiments employing exercise interventions in human and animal models have provided evidence that alterations in metabolic and gene expression profiles in skeletal muscle are responsible for the protective effects of exercise. In this section, two mechanisms by which physical activity induces protection are presented. They are: a) increase in

mitochondrial biogenesis and efficiency, and b) increased GLUT4 expression. The section ends by discussing the parallel increases in mitochondrial biogenesis and GLUT4 expression by exercise.

2.3.1. Mitochondrial biogenesis due to physical activity confers protection against type II diabetes: Skeletal muscle is endowed with mitochondria which oxidize lipids to produce ATP. Regular physical activity induces mitochondrial biogenesis (increases mitochondrial number, proteins and DNA) resulting in increased capacity for lipid oxidation and turnover (24; 83) and improved insulin sensitivity, i.e. it enhances the ability of endogenous insulin to decrease glucose in plasma by inhibiting glucose release from the liver and stimulating peripheral consumption (42; 43). In an experiment with men and women aged 21-87 years, Short et al. (208) showed that 16 weeks of aerobic physical activity increased citrate synthase and cytochrome c oxidase (markers of mitochondrial content) by 46 % and 87 %, respectively. In the same study, insulin sensitivity was increased by an average of 26 % in both women and men. Others have shown that the content of cytochrome c oxidase was increased by 42 % and 35 % in trained and untrained healthy volunteers, respectively, following a moderate training program (28; 44). In the same study, insulin sensitivity was improved by 41 % and 49 % in the trained and untrained subjects, respectively. Mitochondrial ATP production rate increased by 161 % in the vastus lateralis muscle of middle-aged men and by 170 % in elderly men after 10 days of cycling (17). Mitochondrial DNA (mtDNA) and density is 1.5-1.8-fold higher in skeletal muscle of endurance trained athletes compared to sedentary individuals (184). The above reports represent only a few examples of the vast amount of data showing that exercise increases mitochondrial content and improve insulin sensitivity in skeletal muscle.

In contrast to regular physical activity, chronic inactivity results in a decrease in mitochondrial proteins and number (96), aberrant lipid handling (155) and impaired insulin

sensitivity (24; 127). Insulin sensitivity of skeletal muscle and ATP production rates are 60 % and 30 % lower, respectively, in chronically inactive people compared to active individuals. The reduction in insulin sensitivity in these people was associated with elevated intramyocellular triacylglycerols and their derivatives, and corresponded with decreases in mitochondrial oxidative capacity and mitochondrial ATP synthesis (181). There is now strong evidence that accumulation of fats in skeletal muscle induces insulin resistance by disrupting the insulin signalling cascade (1; 48; 142; 149; 163; 170; 202; 203; 216). The insulin signalling cascade begins by the binding of insulin to the α subunit of its receptor on muscle plasma membranes. When this happens, the β-subunits, which possess tyrosine kinase activity, are activated via autophosphorylation. Activated insulin receptors phosphorylate and activate insulin receptor substrates (IRS) -1 and -2 on tyrosine residues and creates docking sites for the adaptor protein, phosphatidylinositol 3-kinase (PI3K), which catalyzes the phosphorylation of phophatidylinositol-4,5 bisphosphate (PIP_2) to form phophatidylinositol-3,4,5 triphosphate (PIP_3) which creates a lipid-based platform for the recruitment of serine/threonine kinase B (PKB) which, by a mechanism which is not fully characterized, induces GLUT4 translocation from the intracellular endosomes in muscle cells to the cell surfaces, to facilitate glucose diffusion from plasma into the muscle cells (30; 230). The ability of endogenous insulin to stimulate glucose uptake by the muscle is refered to as insulin sensitivity of the muscle. Defects in the insulin-stimulated GLUT4 translocation mechanism in the muscle diminish insulin sensitivity and induce insulin resistance and type II diabetes (4; 60; 65; 66). Insulin resistance (IR) is the condition in which normal amounts of insulin are inadequate to produce a normal insulin response from cells. It has been shown that impairment of mitochondrial function due to inactivity leads to reduction in the volume of lipids targeted for oxidation, resulting in accumulation of fatty acids and their metabolites such as long chain fatty acyl CoA (LCACoA),

diacylglycerol (DAG) and ceramide (142). Increased intracellular levels of these lipid metabolites have been functionally linked to impaired insulin sensitivity in skeletal muscle (202). It is now known that they promote phosphorylation of IRS-1 on serine residues by protein kinase C (PKC), thereby counteracting their tyrosine phosphorylation by the insulin receptor β subunit and inhibiting insulin signalling pathway. Accumulation of fats and their metabolites therefore induce insulin resistance in muscle, i.e. they interfere with the insulin signalling cascade and inhibit GLUT4 translocation to plasma membrane to enhance glucose transport (24; 48). Experimental supports for the role of lipids in inducing insulin resistance are many: For example, infusion of lipids in rats for 5 h increases IRS-1 serine phosphorylation by ~1.6-fold in soleus muscle (238). Moreover infusion of lipids for five hours has been shown to increase ceramide and LCACoA concentration, enhance PKC activity and reduce IRS-1 tyrosine phosphorylation and IRS-1 associated PI3K activity in soleus muscle. Interestingly, lipid infusion had no effect on insulin receptor tyrosine phosphorylation; demonstrating that the effects of lipids occur at the level of IRS-1 (64; 105; 121). Confirmation that lipids induce insulin resistance via serine phosphorylation of IRS-1 has come from experiments showing that mutation of the serine residue in IRS-1 to alanine rescues cells from lipid-induced insulin resistance (1).

Schenk & Horowitz (201) have shown that one session of exercise is sufficient to completely reverse fatty acid-induced impairment in insulin sensitivity. Ninety minutes of moderate-intensity exercise during a lipid-infusion protocol, which increased plasma lipid levels 4-fold above basal and impaired insulin sensitivity by 30 % in sedentary controls, not only prevented insulin resistance but also improved insulin sensitivity by 25 % above basal levels. Skeletal muscle diacylglycerol and ceramide concentration were significantly lower in the exercise group compared to the sedentary controls. Phosphorylation and activation of cytokines that are responsible for

impairing insulin signalling pathway were reduced by 50 % in the exercise group compared to the sedentary group (170). These experiments demonstrate the effectiveness of exercise in controlling the accumulation FFAs metabolites that confer insulin resistance.

Analysis of muscle samples from young, lean, normoglycemic, but insulin resistant offsprings of type II diabetics revealed that insulin-stimulated glucose transport was 60 % lower in these offspring than in control healthy subjects and this was associated with 60 % higher intramuscular lipid content. Skeletal muscle mitochondrial density was lower by ~38 % in these offsprings. These changes were associated with ~50 % increase in IRS-1 serine phosphorylation and reduced tyrosine phosphorylation. Moreover, Akt, a signalling molecule in insulin signalling cascade, was also reduced by 60 %. These data provide insight into early defects that may be responsible for the development of type II diabetes and support the idea that reduction of mitochondrial content predisposes offsprings of diabetic patients to intramuscular lipid accumulation that cause defects in insulin signalling in the muscle (163). These data further suggest that the reduction of mitochondrial content that results from a sedentary lifestyle may also cause intramuscular lipid accumulation, defects in insulin signalling, insulin resistance, and ultimately type II diabetes.

In summary, insulin resistance can be reversed by interventions that reduce the intramuscular contents of LCACoA, ceramide and DAGs. Bruce et al. (24) and others (170; 201) have shown that moderate-intensity endurance training decreases intramuscular ceramide, LCACoA and DAGs. The decreases in these metabolites were associated with improvement in insulin sensitivity and in mitochondrial fat oxidative capacity. These data clearly show that increased mitochondrial content due to exercise protects against insulin resistance and type II diabetes by increasing the capacity of the mitochondria to oxidize fats and its derivatives.

2.3.2. Increased GLUT4 content by physical activity protects against type II diabetes:

Skeletal muscle is the major site for whole body insulin-stimulated glucose disposal and is responsible for about 70-80 % of glucose uptake from plasma (43). As discussed before, glucose enters muscle cells predominantly via GLUT4 protein which resides in intracellular compartment vesicles but is translocated to the cell membrane to enhance glucose transport. Like insulin, exercise also induces GLUT4 translocation to cell membranes: Hansen et al., (81) showed that after 3.5 h of exercise, there was a 2-fold increase in plasma membrane GLUT4 and a similar increase in glucose transport in rat muscle, compared to controls. Kennedy et al., (120) showed that 45-60 min of cycling at 60-70 % VO_2max caused plasma membrane GLUT4 protein to increase to the same extent (~71-74 %) in the vastus lateralis muscles of diabetic patients and non diabetic subjects. King et al., (122) showed that a single bout of exercise increased plasma membrane GLUT4 content in severely insulin resistant obese Zucker rats (fa/fa) by ~ 2.2-fold and this was accompanied by ~ 4.1-fold increase in glucose transport, compared to controls. Collectively, these results show that unlike insulin, acute exercise effectively translocates GLUT4 to the cell surface and increases glucose transport in insulin resistant and diabetic animals. Goodyear et al (71) also reported that in rats, insulin injection increased tyrosine phosphorylation of IRS-1 and IRS/PI3K, whereas contraction had no effect. Addition of wortmannin, an inhibitor of PI3K, significantly reduced glucose transport and GLUT4 translocation in insulin-stimulated muscle whereas addition of higher a concentration of wortmannin (1μM) had no effect on exercise-induced GLUT4 translocation and glucose transport. Lund et al., (144) further showed that PKB activity was increased ~4-fold with insulin stimulation but exercise had no effect. Collectively, these observations indicate that GLUT4 translocation by exercise is mediated by a signalling pathway which is distinct from that induced by

insulin and suggest that insulin and exercise probably use different pools of GLUT4 transporters (38).

Many researchers have shown that exercise increases insulin sensitivity: Hansen et al., (81) showed that insulin sensitivity increased by 60 % in rats that were exercised for 3.5 h compared to the sedentary controls. In humans, Short et al., (208) have shown that 4 months of exercise training in elderly people result in 26 % increase in insulin sensitivity. In young people, insulin sensitivity increases after a single session of exercise but in middle and old age people, the increase in insulin sensitivity only appears after a few sessions. The increase in insulin sensitivity by exercise disappears 3-6 days after session of exercise (87).

A conspicuous increase in glucose transport and GLUT4 protein expression occur in skeletal muscle in response to exercise training. This observation is supported by a large body of evidence from different studies (33; 61; 85; 92; 97). For example, Houmard et al., (99) have reported ~1.8-fold increase in GLUT4 protein concentration in middle- aged men after 14 weeks of exercise training from the vastus lateralis muscle. Seven days of cycle ergometer training was reported to increase GLUT4 ~2.0-2.8-fold in the vestus lateralis muscle (78; 98). Physical training increases GLUT-4 protein by 40 % and mRNA by 52 % in a long term aerobic physical training accompanied by 26 % improvement in insulin sensitivity in aged subjects and in patients with type II diabetes (167; 205; 208). In a study where diabetic patients performed one-legged ergometer bicycle training for 9 weeks (6 days/week; 30 min/day), GLUT4 mRNA and protein increased by 30 % and 22 %, respectively on the trained leg compared to the untrained leg. GLUT4 protein increased by ~74 % and 71 % and glucose transport by ~47 % and 28 % in type II diabetes patients and normal healthy individuals respectively in response to exercise training (45; 120; 225). In many studies, diabetics tend to show more pronounced increases in GLUT4 due to exercise compared to

non-diabetic people. In insulin resistant obese Zucker rats, exercise also increased insulin sensitivity primarily by increasing GLUT4 protein content (36; 37; 61). In one study using obese Zucker rats, seven weeks of training induced a ~2.3-fold increase in GLUT4 compared to sedentary rats and was accompanied by ~4.5-fold glucose transport (122).

Regular exercise increases GLUT4 expression and insulin sensitivity in parallel (129). In a study involving rats, it was found that 2 hours of swimming per day for 5 days increased GLUT4 protein concentration and insulin sensitivity by 87 % and 85 %, respectively, relative to controls. Forty two hours after training, GLUT4 protein concentration and insulin sensitivity were still higher by 52 % and 51 % respectively in muscle from trained rats compared to controls. GLUT4 protein concentration and insulin sensitivity in trained muscle returned to sedentary control level within the 90 h after training. These results show that changes in insulin sensitivity during detraining is directly related to muscle GLUT4 protein content (119). The increases in GLUT4 content and glucose transport capacity seen after long-duration low-intensity exercise also occur in high-intensity short-duration intermittent exercise in rats (222) and in humans (120; 208).

Skeletal muscle of type II diabetic and insulin resistant rats and mice is characterised by deficiency in insulin stimulated recruitment of GLUT4 to the cell surface (196; 243). In these animals, specific overexpression of GLUT4 restores insulin sensitivity to normal. Insulin stimulated glucose transport is impaired in diabetic obese *db/db* mice despite unaltered GLUT4 expression (126); indicating that the translocation of GLUT4 to the cell surface is the main cause. Overexpression of GLUT4 in these mice normalizes oral glucose tolerance and increases insulin sensitivity (68). In streptozotocin-induced diabetic rats, skeletal muscle GLUT4 mRNA and protein are reduced concomitantly with whole body insulin sensitivity (21; 29; 167). Overexpression of GLUT4 in skeletal muscle also improves insulin action and reduces basal plasma glucose levels in

these rats (134). These data demonstrate that impaired insulin action in these diabetic rats arise from reduced GLUT4 expression. As mentioned earlier, several studies have shown that exercise can increase GLUT4 content and glucose uptake in individuals who are insulin resistant or in type II diabetics. Collectively, results from all the above studies are consistant with the notion that increased GLUT4 content, whether by overexpression, as is the case with GLUT4 transgenic animals or by means of exercise training, prevents hyperglycemia and enhances whole-body glucose disposal (103).

Exercise can also increase glucose transport and GLUT4 translocation through adenosine monophosphate (AMP)-activated protein kinase (AMPK) activation (93). AMPK is a signalling intermediate that is increased during moderate to -intensity exercise which reduces the ATP and phosphocreatine concentration in muscle cells and increases AMP. In rats, activation of AMPKα2 by AICAR has been shown to increase skeletal muscle glucose disposal by increasing the translocation of GLUT4 to the sarcolemma (117). In transgenic mice expressing the dominant negative mutant of AMPKα2, there is a significant impairement of glucose uptake in response to exercise. These observations have led researchers to conclude that AMPK is also a suitable target for anti-diabetic drugs (84; 117).

In summary, impaired insulin-stimulated GLUT4 expression and translocation in muscle cells are important causes of insulin resistance and type II diabetes. Since exercise increases GLUT4 content, GLUT4 translocation to the plasma membrane, and glucose uptake in type II diabetes patients--thereby improving whole body glucose disposal and insulin sensitivity--it is therefore an important therapeutic modality for insulin resistance and type II diabetes (95). Hence studies such as this one, which seek to elucidate the molecular mechanisms involved in exercise-induced upregulation of GLUT4 content, could identify molecular targets for drugs to treat type II diabetes and insulin resistance.

2.3.3. Physical activity induces mitochondrial biogenesis and increases GLUT4 expression in parallel:

Many studies have shown that stimuli that increase mitochondrial biogenesis also increase GLUT4 expression (10; 11; 19; 57; 91; 208). For example, Short et al., (208) has shown that 16 weeks of moderate aerobic exercise intensity increases GLUT4 protein and mRNA by ~30-50 % and mitochondrial biogenesis by ~45-76 % simultaneously. Expression of muscle-specific inactive form of AMPK results in abrogation of the increases in both GLUT4 and mitochondrial proteins by exercise, indicating that AMPK may signal their regulation during exercise (32; 63; 186; 191; 232). CaMKII activation by exercise or caffeine has been shown to increase both GLUT4 and mitochondrial proteins in animal and cell culture models, respectively (57; 172; 173; 211; 212). It is well established that mitochondrial biogenesis is regulated by NRF-1 (46; 133; 199; 226). As expected, overexpression of NRF-1 in transgenic mice results in augmented mitochondrial proliferation (10). Intriguingly, NRF-1 transgenic mice also have increased GLUT4 expression (10).These observations have prompted us to speculate that there is cross talk between the signalling pathways for mitochondrial biogenesis and GLUT4 expression.

2.4. The role of NRF-1 in regulating mitochondrial and GLUT4 expressions.

This section reviews the role of NRF-1 in regulating mitochondrial biogenesis and in the expression of MEF2 transcription factors; and how these impact on GLUT4 expression.

2.4.1. NRF-1 is one of the transcription factors that regulate mitochondrial biogenesis:

NRF-1 is a transcriptional factor that regulates mitochondrial biogenesis (53; 73). The biogenesis of mitochondria involves the interaction of two genomes, namely those located in the nucleus and those housed in the mitochondria. Mitochondrial genome codes for 13 respiratory chain polypeptides, 2 ribosomal RNAs and 22 transfer RNAs. The nuclear genome encodes all the rest of the proteins necessary for a complete maintenance and expression of mitochondria. NRF-1, and

other transcription factors, acts on nuclear genes that express the proteins involved in heme biosynthesis, oxidative phosphorylation, mitochondrial gene transcription and replication, protein import into the mitochondria, and numerous respiratory chain subunits that are involved with cellular respiration (53). Regulation of the expression of this multitude of genes by these transcription factors culminates in a well coordinated program of activities in the nucleus and in the mitochondria that result in mitochondrial biogenesis. Because the mitochondrion is crucial in generating ATP from substrates, the activity of NRF-1 in cells must match the ATP demand in the cells. Therefore, NRF-1 can be regarded as a critical component of the energy sensing machinery in mammalian cells which converts physiological signals that arise during conditions of energy demand, e.g. physical activity, into improved ability for energy generation (135).

Sequence analysis shows that NRF-1 is a putative bZIP transcriptional factor and has a gene map locus at 7q32 in humans which spans approximately 65 kb with 12 exons and 11 introns (73). NRF-1 was initially known as an activator of cytochrome c expression but was later found to regulate many genes encoding subunits from all five respiratory complexes (46; 52; 199). It functions together with other transcription factors including NRF-2, stimulating protein -1(Sp1) and MEF-2; and transcriptional coactivators such as peroxisome proliferator-activated receptor gamma coactivator-1 (PGC-1α) alpha (125; 160; 215). NRF-1 binds as a homodimer to the GC-rich palindromic sequence (T/C)GCGCA(C/T)GCGC(A/G) and forms a strong affinity bond with less tolerance for non compliance (164; 185).

NRF-1 is amongst the seven identified transcription factors that are frequently found in the proximal promoters of ubiquitously expressed genes (56). Chromatin immunoprecipitation (ChIP) and ChIP-on-chip assays have shown that of the 13000 human promoters surveyed, 691 genes were occupied by NRF-1 in living cells and the majority of those genes were involved in

mitochondrial biogenesis and metabolism (27; 188). A few of the NRF-1 target genes that code for key mitochondrial proteins are discussed here illustrate the role that NRF-1 plays in mitochondrial biogenesis: Firstly, for mitochondrial DNA (mtDNA) to replicate, a nuclear-encoded transcriptional factor called mitochondrial transcription factor A (TFAM) is required. TFAM expression requires the binding of NRF-1 on the *tfam* gene (35). Choi et al. (35) showed that when NRF-1 sites on the *tfam* promoter were mutated, approximately 90 % *tfam* activity was lost. Since NRF-1 controls *tfam* expression to regulate mtDNA, it can therefore be concluded that NRF-1 regulates both nuclear and mitochondrial genome resulting in complete and normal mitochondrial functions. Secondly, NRF-1 also regulates the expression of δ-aminolevulinic acid synthase (δALAS), a rate-limiting enzyme in the synthesis of heme (135). NRF-1 binding sites are present in the *δalas* gene and are highly conserved in human, mouse and rat species (22; 32). δALAS catalyses the condensation of glycine and succinyl-CoA to form 5-aminolevulinate, and first step in heme synthesis. Heme is part of the respiratory cytochromes that play an important role in the transfer of electrons from fuels to oxygen in the electron transport chain to generate ATP. The activity of δALAS determines the respiratory capacity of the mitochondria. Thirdly, another important mitochondrial enzyme that relies on NRF-1 activity is cytochrome c oxidase (COX). COX is a transmembrane protein found in the inner membranes of the mitochondria of eukaryotic cells. It is the terminal enzyme in the electron transport chain which binds molecular oxygen and reduces it to water. This enzyme is responsible for over 90 % of the oxygen consumption by living organisms. It also pumps protons across the mitochondrial membrane and contributes to the proton gradient that exists across the inner mitochondrial membrane. It is a multi-subunit holoenzyme consisting 13 polypeptides; ten of which are encoded in the nucleus and their expression controlled by NRF-1 (46). Genomic sequence analysis show that the

promoter regions of some skeletal muscle-specific COX isoforms, such as COX6A, COX7A and COX8, which are nuclear encoded, lack NRF cis elements but have conserved MEF2A binding sites (133; 185; 228; 238). It has now been shown by many independent researchers that NRF-1 coordinates the expression of these COX isoforms by binding to the *mef2a* gene to increase MEF2A expression and MEF2A then binds to these COX isoforms (46; 133; 185; 228). These studies suggest that the coordinated expression of many proteins that form part of the mitochondria involves a transcriptional cascade involving NRF-1$\rightarrow$ *mef2a* $\rightarrow$ nuclear gene.

2.4.2. Does NRF-1 play a role in regulating GLUT4 expression? Baar et al., (10) showed that transgenic mice that overexpressed NRF-1 had elevated levels of mitochondrial proteins as well as GLUT4. The increase in GLUT4 was not expected because NRF-1 has no binding sites on the *glut4* gene. The mechanism through which NRF-1 up-regulates GLUT4 expression has not been studied and forms one of the aims of this study. What is known is that *glut4* gene expression is regulated by the binding of MEF2A/D heterodimer together with the GLUT4 enhancing factor (GEF) to their respective sites on the *glut4* promoter (162; 223). It is quite conceivable that NRF-1 regulates GLUT4 expression indirectly via MEF2. As discussed in section 2.4.1, there is growing body of evidence that suggest a cordial relationship between NRF-1 and MEF2A whereby NRF-1 regulates the expression of MEF2A and MEF2A in turn regulates other genes (10; 133; 165; 185; 228). An example of this relationship was discussed in the case of COX genes. Since *glut4* gene is a target of MEF2A (223), it is logical to hypothesise that the increase in GLUT4 expression reported in NRF-1 transgenic mice is due to a transcriptional cascade involving NRF-1 $\rightarrow$ *mef2a* $\rightarrow$ *glut4.* This hypothesis would also suggest that NRF-1 is responsible for coordinating the increase in GLUT4 expression and mitochondrial biogenesis in response to exercise. However, direct evidence to support this hypothesis is still lacking.

2.4.3. Evidence that NRF-1 might play a role in exercise-induced increase in the expression of GLUT4 and mitochondrial proteins: Although it has been consistently reported that both GLUT4 and mitochondrial proteins are upregulated in parallel by stimuli such as exercise, the signal that coordinates their parallel upregulation has not been identified. In NRF-1 transgenic mice, GLUT4, MEF2A and mitochondrial proteins are all increased (10). Mimicking the effects of exercise with caffeine in myotubes increased NRF-1 binding to mitochondrial genes and upregulated the expression of MEF2A, GLUT4 and selected mitochondrial proteins (172; 173).The fact that NRF-1 controls the *mef2a* gene to induce the expression of respiratory subunits (185), suggests that NRF-1 may also induce the expression of GLUT4 since GLUT4 is also regulated by MEF2A (223). Therefore, it may be hypothesized that the simultaneous increases in both GLUT4 and mitochondrial proteins by exercise may be due to the actions of NRF-1 on *mef2a.* However evidence for this hypothesis is still lacking.

2.5. The impact of CaMK II activation on chromatin remodelling, mitochondrial biogenesis and GLUT4 expression.

CaMK II has been implicated in the regulation of gene expression. For example, it phosphorylates HDACs and causes their export out of the nucleus. HDACs suppress gene transcription and their export from the nucleus favours the action of HATs, which favour gene transcription. In this section the mode of action of CaMK II is described and the mechanism by which it regulates GLUT4 expression and mitochondrial biogenesis is discussed.

2.5.1. CaMK II regulates GLUT4 & mitochondrial protein expression: CaMK II is a calcium/calmodulin (Ca^{2+}/CaM) dependent protein kinase which mediates a myriad of physiological responses. It is a holoenzyme consisting of 8 to 12 subunits (206); each subunit consisting of a conserved N-terminal regulatory domain and a C-terminal domain. The regulatory

domain is formed by an auto-inhibitory domain, a calmodulin binding domain and numerous autophosphorylation threonine sites. Binding of Ca^{2+}/CaM to the CaM binding domain is presumed to disrupt the auto-inhibitory interactions and allow substrates and ATP to gain access to the catalytic site. This interaction results in auto-phosphorylation of threonine which increases its sensitivity to Ca^{2+}/CaM by ~1000-fold (178).

In skeletal muscle, CaMK II modulates gene transcription and various signalling pathways that enable muscle to adapt to stimuli such as exercise (57; 178). CaMK II is not active at rest but its activity is triggered by increases in free calcium concentration that is displayed during muscle contraction (178). With regard to GLUT4 regulation, CaMK II activation by exercise has been shown to result in increased GLUT4 and MEF2A protein expressions in rats (211; 212). Incubation of L6 myotubes with caffeine, an agent that raises cytosolic calcium levels in an exercise-like manner, also increases GLUT4 and MEF2A proteins (172).

CaMK II has also been reported to be involved in mitochondrial biogenesis. Using L6 myotubes, Ojuka et al., (173) showed that activation of CaMK II increased mitochondrial markers such as δALAS, COX-1 and cytochrome c. Wright et al., (233) also showed that incubation of isolated rat epitrochlearis muscle with caffeine, to activate CaMK II resulted in augmented levels of mitochondrial mRNA, and proteins such δALAS, COX and citrate synthase. The strongest evidence implicating CaMK in mitochondrial biogenesis has come from Wu et al. (234) who used muscle specific CaMKIV transgenic mice. Skeletal muscles from these mice had increased levels of proteins for mitochondrial DNA replication, transcription, fatty acid metabolism, and electron transport.

2.5.2. CaMK II activation influences mef2a and nrf-1 gene transcription through acetylation: Chromatin, which is composed of DNA wound around histone proteins, has a dynamic

structure which influences gene transcription. A compact structure retards transcription whereas a relaxed configuration favours gene expression. In general, acetylation of histones by HATs relaxes chromatin (217) and enables transcriptional factors (e.g. NRF-1 or MEF2A) to have access to their respective binding domains on the DNA. Conversely, deacetylation of histones by HDACs generally represses genes (23; 31; 213; 218). HDACs also repress MEF2-dependent genes by associating with MEF2 transcription factors to form gene-repressing complexes on MEF2 binding sites (79; 159). External signals, such as stress or exercise activate CaMK II which phosphorylate two serine-containing motifs on HDACs within the HDAC/MEF2 complex and induces HDAC nuclear export by chaparones. HDAC nuclear export relieves HDAC-mediated repression of MEF2-dependent genes (156; 159) and favours increased HAT activity. HATs, such as p300, also acetylate MEF2 to increase binding and transcriptional activity (198). The binding activity of NRF-1 has also been shown to be increased by posttranslational acetylation (110) and phosphorylation (77). Our group has previously shown that activation of CaMK II by caffeine in L6 myotubes increases NRF-1 binding to *δalas* gene by 90 % (172).

CHAPTER 3

Description and Optimization of Experimental Procedures

3.1. Introduction

This study was conducted to investigate the molecular mechanism by which a) NRF-1 regulates GLUT4 expression and b) CaMK II activation brings about a coordinated expression of GLUT4 protein in skeletal muscle. The studies were conducted using the C2C12 muscle cell line. In this chapter, a justification for the use of the cell culture model is provided, the experimental procedures and protocols used to answer the various experimental questions are described, and evidence showing that these procedures and protocols were optimized is presented.

3.2. Justification for the use of a cell culture model

C2C12 cells, a skeletal muscle cell line of mouse origin, have been used widely in various studies and have proved to be easy to work with. They serve as an excellent model system for investigating complex biochemical adaptations that occur in skeletal muscle. Like skeletal muscle they have a well formed mitochondria and differentiate into multinucleated myotubes. They also exhibit most, if not all, the principles of mechano-biochemical adaptations associated with contractility (123; 166; 182; 207). Cell culture experiments are more convenient than *in vivo* experiments in establishing molecular pathways that arise from a specific stimulus because they are conducted in an isolated system which removes the influences of the brain, hormones and other physiological interferences. In human and animal models, exercise triggers many physiological and biochemical responses at the same time, which makes it difficult to isolate the mechanism responsible for the changes observed.

For the part of our studies, in which we characterized the role played by NRF-1 in regulating GLUT4 expression, we found it quite easy to induce forced overexpression of NRF-1 in C2C12 myoblasts using Tet-On gene expression system. In the studies where the role of CaMK II activation in coordinating the expression of GLUT4 was investigated, CaMK II activation was easily accomplished by incubating the cells with caffeine (172; 173; 233).

3.3. General cell culture protocol

C2C12 myocytes were maintained at 37 ^{o}C in 5 % CO_2 on 100 mm collagen-coated plastic petri-dishes containing DMEM (Dulbecco's modified eagles medium) supplemented with 10 mM creatine, 100 μU/ml streptomycin, 100 μU/ml penicillin, 0.25 μg/ml fungizone and 10 % heat-inactivated fetal calf or bovine serum. Cells were maintained in continuous passage by trypsinization of sub-confluent cultures with 0.25 % trypsin versene. Myoblast differentiation was induced by introduction of medium containing 2 % heat-inactivated horse serum once myocytes were ~80 % confluent. Cells were kept in this medium for 8-13 days until myotubes were well formed.

3.4. Development of the Tet-On gene expression system in C2C12 myocytes

To develop a system that controls the expression of NRF-1, we employed the Tet-On gene expression system (Clonotech, Paulo, CA) that is based on the use of the *E. coli* tetracycline-resistance operon (74). Two plasmids were inserted into C2C12 myocytes to form a double stable cell line: The first, pTet-On, produces a regulatory protein called reverse tetracycline transactivator (rtTA) and the second plasmid, pTRE2Hyg, into which mouse NRF-1 cDNA was cloned, is the response plasmid which expresses NRF-1 when rtTA binds to its tetracycline response element (TRE) in the presence of the tetracycline derivative doxycycline (Dox). Because

the plasmid lacks strong enhancer elements, no expression of NRF-1 is expected in the absence of bound rtTA and Dox.

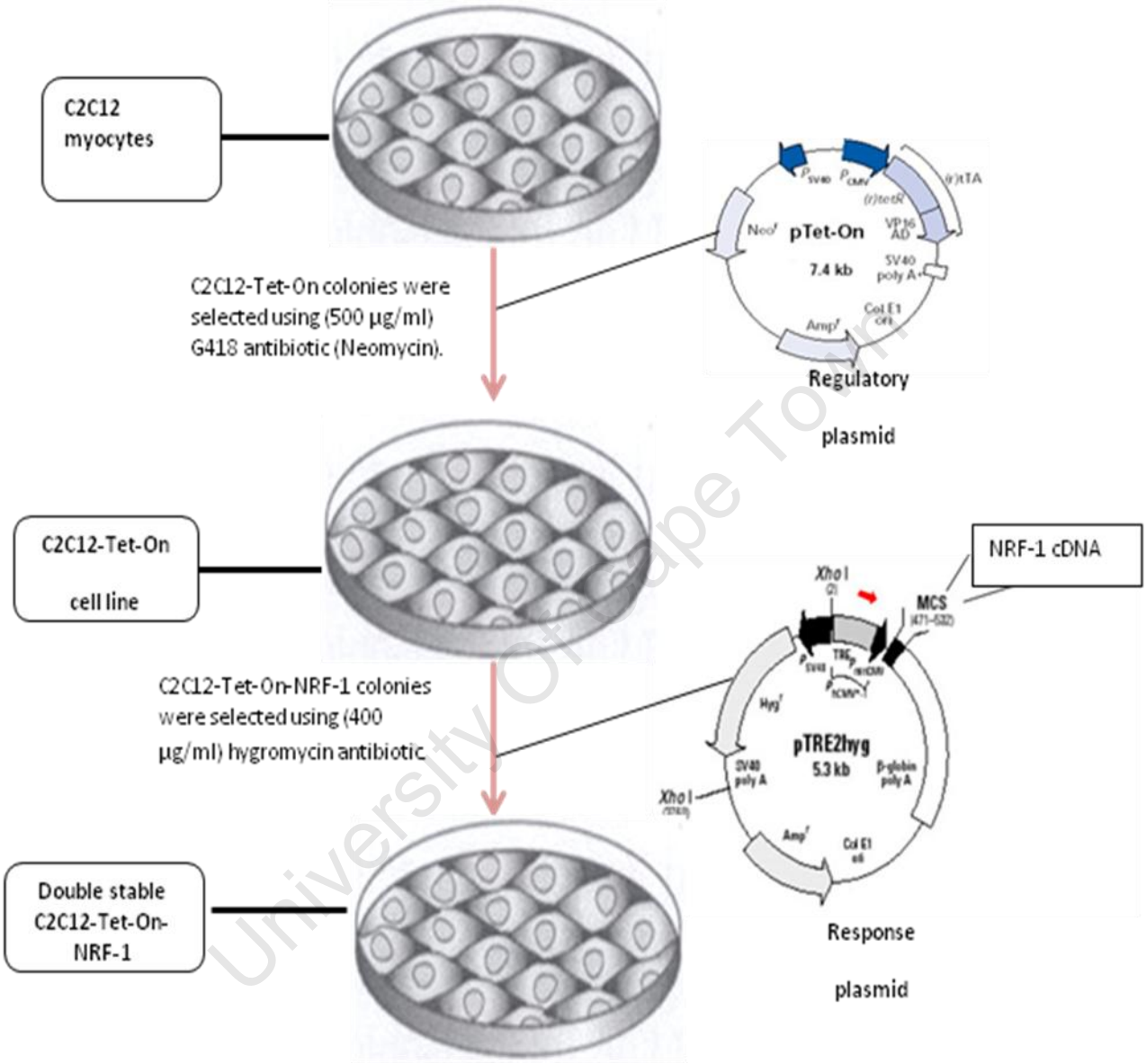

Figure 3.1: An overview of the stages in the development of the double stable C2C12-Tet-On-NRF-1 cell line. The first plasmid to be introduced to C2C12 myoblasts was pTet-On. The C2C12-Tet-On resistant clones were selected using G418 antibiotic (Neomycin). The second plasmid, pTREHyg-NRF-1, which is the response plasmid was introduced to the C2C12-Tet-On clones. Selection of C2C12-Tet-On-NRF-1 resistant clone was achieved using hygromycin antibiotic. Western blot was used to determine the clones that had high induction of NRF-1 when treated with Dox but with low background. These clones were used as the C2C12-Tet-On-NRF-1 cell line for all subsequent experiments.

To develop the Tet-On system in C2C12 cells we generated the mouse NRF-1 cDNA, cloned cDNA into the pTRE2Hyg and transfected Tet-On and pTRE2Hyg-NRF-1 plasmids into C2C12 myotubes (Fig. 3.1). These procedures are described in detail below:

3.4.1. NRF-1 cDNA generation: Total RNA was isolated using Trizol (Ambion, Austin, TX) according to manufacturer's protocol. Briefly, a triceps muscle was excised from mouse and stored in a cryovial in liquid nitrogen. The frozen tissue was disrupted using a pestle and mortar in liquid nitrogen and 1 ml of Trizol reagent was added to the homogenized tissue sample. Tissue homogenates were mixed, incubated for 5 min at room temperature, centrifuged at 12000 x g for 10 min at 4 ^{o}C and the supernatant transferred to a fresh clean tube. Two hundred μl of chloroform was added to the supernatant and incubated at room temperature for 15 min and centrifugated at 12000 x g for 10 min at 4 ^{o}C. The aqueous phase was transferred to a fresh tube containing 500 μl of isopropanol and the mixture vortexed for 10 s and incubated for 10 min at room temperature. This was centrifuged at 12000 x g for 8 min at 20 ^{o}C and the supernatant discarded. The pellet, containing RNA, was washed with ethanol, air dried, and re-suspended in 20 μl nuclease-free water. RNA concentration and optical density at 260 and 280 nm was measured in triplicates using 1 μl of RNA in a Nanodrop ND 100 spectrophotometer (Nanodrop Technology, Wilmington, DE, USA). RNA was accepted as pure from contamination when the 260/280 nm ratio was between 1.9 and 2.1. The integrity of RNA was verified as follows: 3 μg of RNA was diluted in a 10 μl buffer containing 6 % glycerol, 1 % MOPS, 2 M formaldehyde, 0.5 % formamide and bromophenol blue. The mixure was heated at 55 ^{o}C for 15 min and separated by electrophoresis on a 1 % agarose gel containing 1 x MOPS, 0.66 M formaldehyde and 35 μg ethidium bromide. RNA was visualised under UV and deemed usable (undegraded) if the 28S and 18S ribosomal bands were observed intact.

Primers for the NRF-1 cDNA which amplify a 1.74 kb section of the coding region of the mouse NRF-1 cDNA from position 161 to 1901 bp (Gen Bank™ accession no. NM_010938) are: Forward primer: 5'-GTT GGATCC CTC TCA CCC ATT G -3' (Position 161-182; BamH1 restriction sites underlined). Reverse primer: 5'- CCA AGTCGAC GAG ACT TAA TTC C-3' (Position 1881– 1901; Sal1 restriction sites underlined). Primers for the NRF-1 cDNA were designed to contain BamH1 and Sal1 restriction sites to permit cloning of the transcripts into pTRE2Hyg and are present in the multiple cloning site of pTRE2Hyg. Real Time-Polymerase Chain Reaction (RT-PCR) was performed using a Qiagen OneStep RT-PCR Kit as per manufacturer's protocol (Valencia, CA). Briefly, each reaction contained a cocktail consisting of 400 μM dNTPs, 2.5 mM $MgCl_2$, 10 units of RNase inhibitor, 1 x RT-PCR buffer, 2 μl Qiagen OneStep RT-PCR enzyme mix for reverse transcription (Omniscript and Sensiscript transcriptases) and HotStarTaq DNA polymerase, 0.8 μM forward and reverse primers and 2 μg RNA template. The RT-PCR reaction consisted of 30 min of reverse transcription at 50 ^{o}C, and 15 min of PCR reactions at 95 ^{o}C using HotStarTaq DNA polymerase which simultaneously inactivates the reverse transcriptases. RT-PCR step cycling was done as follows: 35 cycles of amplification (1 min denaturing at 94 ^{o}C, 1 min annealing at 70 ^{o}C, and 1 min of extension at 72 ^{o}C) and 1 cycle of 10 min final extension at 72 ^{o}C. The amplified NRF-1 cDNA from RT-PCR was run on 0.5 % agarose gel. It migrated at ~1.74 kb as predicted. Shown below are: a) the tabulated RT-PCR conditions used to generate the mouse NRF-1 cDNA (Table 3.1) and agarose gel of the amplified NRF-1 cDNA (Figure 3.2).

Table 3.1. RT-PCR Thermal cycle conditions

Conditions	Reaction time	Temperature	Enzyme used
Reverse transcription	30 min	50 ^{o}C	Omniscript & Sensiscript Reverse transcriptases
Initial PCR activation step	15 min	95 ^{o}C	HotStarTaq DNA polymerase.

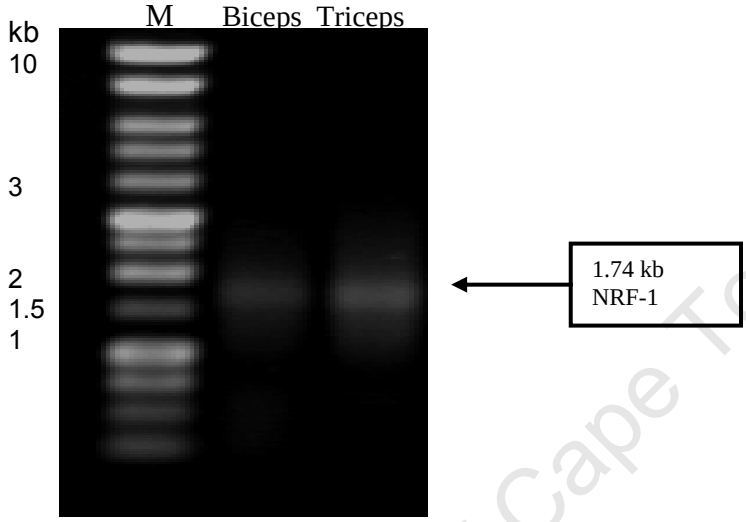

Figure 3.2: Mouse NRF-1 cDNA from biceps and triceps muscles. M represents molecular size marker. The NRF-1 cDNA migrated at the expected 1.74 kb after electrophoresis.

In order to verify that the amplified cDNA contained a correct NRF-1 nucleotide sequence, a dideoxy sequencing procedure using the Applied Biosystems Big Dye Terminator v3.1 Cycle sequencing kit was performed as described in the manufacture's protocol (Applied Biosystems, Foster City, CA, USA). Briefly, the generated NRF-1 cDNA was used as template in four separate DNA amplification reactions containing 1.1 µl terminator premix (consisting of dNTPs and one of the four dideoxyribonucleoside triphosphates (ddNTPs) in a ratio of 100:1), 2.9 µl Bioline Half dye, 50 ng template and 1 µl of 5 µM primer and deionized water to a final volume of 10 µl using Applied Biosystems GeneAmp PCR System9700 (Applied Biosystems, Foster City, CA, USA). PCR was initiated by 1 cycle of 1 min denaturing at 96 ^{o}C, 20 s of annealing at 50 ^{o}C and 4 min of extension at 60 ^{o}C followed by 25 cycles of 10 s denaturing at 96

^{o}C, 20 s of annealing at 50 ^{o}C and 4 min of extension at 60 ^{o}C. Denaturing produced a single stranded DNA which was hybridized to a synthetic deoxyribonucleotide primer during the annealing phase. When a ddNTP is added at the position of the corresponding normal dNTPs during PCR, chain termination occurs because ddNTPs lacks a hydroxyl group to facilitate chain elongation. Therefore, the reaction mixture would contain a mixture of prematurely terminated chains ending at every occurrence of each ddNTPs. The PCR product thus generated was cleaned up using the Sigma Sephadex G-50 columns, spun at 3200 rpm for 2 min and eluted with 20 μl distilled water. The ddNTP-generated fragments were electrophoresed on a DNA capillary sequencer genetic analyser (Applied Biosystems 3130 Genetic analyser) as recommended by the manufacturer (Applied Biosystems, Bedford, MA). The fragments produced during PCR are of different sizes and carry one of the four colour dyes. The colour and size of each fragment was detected using a laser beam and the data collected by computer software which generated the chromatographs from which the sequence of nucleotides on the sequenced template DNA (NRF-1 cDNA) was determined. The sequenced DNA template was then compared with the posted genomic bank mouse NRF-1 cDNA sequence, NM_010938, (NCBI, Pubmed) and found to be homologous (See Figure 3.3). The sequenced-verified NRF-1 cDNA was subsequently cloned into the pTRE2Hyg plasmid.


```
Seq       CACCTCCACAGCCTGGCCATCCATGGTGACTGCGCTGTCCGATATCCTGGTGGTCACTGG   99
          ||||||||||||||||||||||||||||||||||||||||||||||||||||||||||
Genbank   CACCTCCACAGCCTGGCCATCCATGGTGACTGCGCTGTCCGATATCCTGGTGGTCACTGG   1661

Seq       GGCCATGGCCACCTGCACCGGCCCGTTGCCCTGGGCGAGGCTGGTTACCACAGTCTGGTA   159
          ||||||||||||||||||||||||||||||||||||||||||||||||||||||||||
Genbank   GGCCATGGCCACCTGCACCGGCCCGTTGCCCTGGGCGAGGCTGGTTACCACAGTCTGGTA   1601

Seq       CATGCTCACAGGTATCTGGACCAGGCCATTAGCATCTTGGACTCCAGTAAGTGCTCCGAC   218
          ||||||||||||||||||||||||||||||||||||||||||||||||||||||||||
Genbank   CATGCTCACAGGGATCTGGACCAGGCCATTAGCATCTTGGACTCCAGTAAGTGCTCCGAC   1541
```

Figure 3.3: Illustration of the sequenced mouse NRF-1 cDNA as aligned with the Genbank, mouse NRF-1 gene, NM_010938. Seq. refers to the sequenced NRF-1 cDNA, whereas the Genbank represents the NCBI gene bank sequence, NRF-1, NM_010938. This sequence depicts just a small section of the 1.7 kb NRF-1 gene that was aligned against in NCBI gene bank and found to be homologous. The NRF-1 cDNA was subsequently cloned to the pTRE2Hyg.

***3.4.2. Transformation and amplification of pTRE2Hyg plasmids*:** pTRE2Hyg was used as the carrier for NRF-1 cDNA. It is a Tet-On response plasmid which is controlled by CMV promoter and a Tet response element (TRE). pTRE2Hyg was transformed in competent DH5α cells by the method described by Ausubel et al., (9). Briefly, 50 ng of pTRE2Hyg was added into 100 µl of DH5α competent cells and gently mixed. The mixture was incubated on ice for 30 min and heat-shocked for 2 min at 37 ^{o}C. Nine hundrend µl SOC medium (2 % bactotryptone, 0.5 % yeast extract, 10 mM NaCl, 2.5 mM KCl, 10 mM $MgCl_2$, 10 mM $MgSO_4$ + 20 mM glucose) medium was added to each tube and incubated at 37 ^{o}C for 30 min. Ten µl of the transformation mixture was plated onto SOB agar plates (2 % bactotryptone, 0.5 % yeast extract, 10 mM NaCl, 2.5 mM KCl, 10 mM MgCl2, 10 mM MgSO4 + 1.5 % agar) containing 100 µg/ml ampicillin and 100 µg/ml hygromycin antibiotics. Isolatable colonies were formed after overnight incubation at 37 °C. When competent cells without any DNA (negative control) were plated on SOB agar plates with 100 µg/ml ampicillin and 100 µg/ml hygromycin antibiotics and incubating for 12-14 h at 37 °C, no colonies were observed. Colonies were picked using a sterilized toothpick and used to inoculate 5 ml SOC culture medium containing 100 µg/ml ampicillin and 100 µg/ml hygromycin and grown for approximately 16 h at 37 ^{o}C with shaking. A 1 ml aliquot of this culture was used to inoculate 100 ml of SOC medium which was incubated for another 16 h at 37 °C with shaking. Cells were pelleted from the medium by centrifugation at 12,000 x g for 30 s at 4 ^{o}C in a microfuge. Plasmids were isolated from the pellets using the alkaline lysis method (9) with minor modifications as

follows: the pellet containing cells were re-suspended in 100 µl ice-cold solution containing 50 mM glucose, 25 mM Tris-HCl, 10 mM EDTA (pH 8.0) by vigorous vortexing. Two hundred µl of freshly prepared solution containing 0.2 M NaOH and 1 % SDS was added to the 100 µl of re-suspended cells, mixed, incubated on ice and 150 µl of 3 M potassium acetate (pH 5.5) added. The tube was inverted gently for 10 s to disperse the solution through the viscous bacterial lysate, incubated on ice for 5 min, and centrifuged at 12000 x g for 5 min at 4 ^{o}C. The supernatant containing the plasmids was transferred to a new tube. An equal volume of phenol: chloroform was added and mixed by vortexing and the mixture centrifuged at 12000 x g for 5 min at 4 ^{o}C in a microfuge. The supernatant containing the plasmids was transferred into a fresh tube. Plasmid DNA was precipitated in 2 volumes of 100 % ethanol at room temperature for 10 min and then centrifuged at 12000 x g at 4 ^{o}C on a microfuge. The supernatant was gently removed by aspiration and the plasmid DNA pellet rinsed in 70 % ethanol. Following centrifugation, the supernatant containing water and ethanol was discarded and the pellet was allowed to dry for 10 min before it was resuspended in 20 µl DNAse free water containing pancreatic RNAse (20 µg/ml). The plasmid (pTRE2Hyg) was verified by enzymatic digestion with Xho1 which produces 1.5 kb and 3.75 kb fragments as expected. An agarose gel of the Xho1 restriction digest is shown below in figure 3.4.

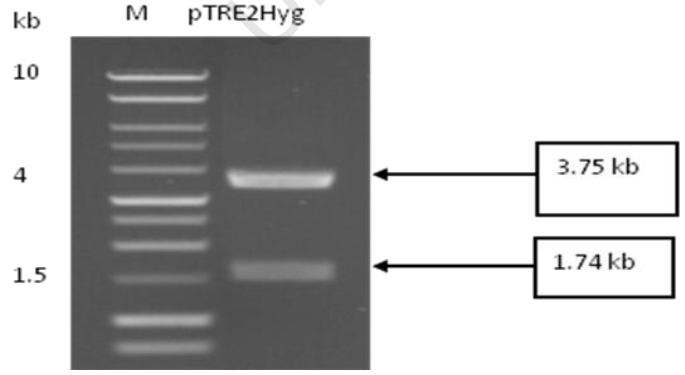

Figure 3.4: Agarose gel showing fragments of pTRE2Hyg after restriction digests with Xho1. According to the vector construction map the observed 1.74 kb and 3.7 kb fragments are expected.

3.4.3. Cloning of the NRF-1 cDNA to the pTRE2Hyg vector: NRF-1-cDNA was directly cloned to the BamH1 and Sal1 sites in the multiple cloning sites of the pTRE2Hyg. pTRE2Hyg was linearised by BamHI and Sal1 and then treated with calf intestine phosphatase (CIP). Briefly, the CIP reaction composed of 500 ng pTRE2Hyg, 1 x CIP buffer and CIP enzyme at a concentration of 0.01 u/µl. The reaction mixture was incubated at 37 ^{o}C for 30 min after which a fresh 0.01 u/µl CIP enzyme was added and incubated for additional 30 min. A "stop" buffer was added to end the CIP reaction and the plasmids extracted using phenol: cholorform method. To precipitate pTRE2Hyg, 0.5 volume of 7.5 M ammonium acetate (pH 5.5) followed by 2 volumes of 100 % ethanol were added to the final aqueous phase. pTRE2Hyg pellet was washed with 70 % ethanol and resuspended in 20 µl DNase free water. Ligation of NRF-1 insert to the pTRE2Hyg vector was carried out using T4 DNA ligase (promega). The ligation mixture, consisting of 400 ng vector (pTRE2Hyg), 100 ng for the insert (NRF-1 cDNA), 1 unit T4 DNA ligase and 1 x ligase buffer, was mixed gently and incubated at 15 ^{o}C for 16 h. The vector/insert is shown diagrammatically in figure below.

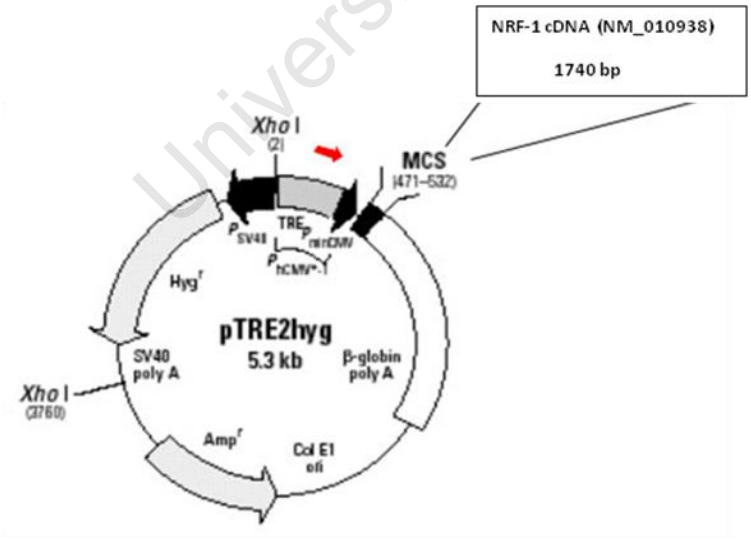

Figure 3.5: Vector construction of pTRE2Hyg depicts the multiple cloning sites where the mouse NRF-1 cDNA was cloned. The CMV promoter is shown downstream the Tetracycline response element (TRE). The two Xho1 restriction sites, which produce fragments of 1.74 kb and 3.75 kb, are also shown.

The ligation mixture was then transformed into DH5α competent cells as described in section 3.4.2. Alkaline lysis, followed by Xho1 restriction digestion and agarose gel electrophoresis were used to identify clones that had taken up the pTRE2Hyg-NRF-1 cDNA vector. In figure 3.6 below, lanes 1 and 3 show the undigested pTRE2Hyg-NRF-1 positive clone. Lane 2 shows a pTRE2Hyg-NRF-1 positive clone after digestion with Xho1 which contains the expected 5.3 kb and 1.74 kb fragments. Lane 4 indicates a clone that did not produce the expected fragments after digestion with Xho1 and hence was disregarded.

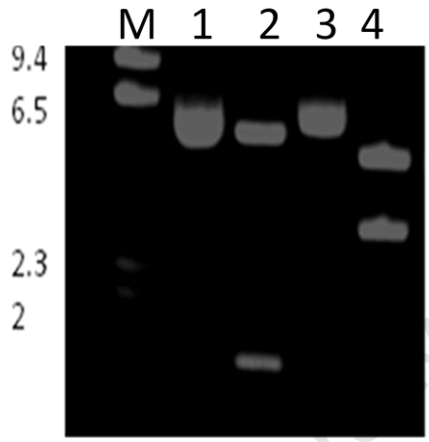

Figure 3.6: Restriction digests of various clones to identify those containing pTRE2Hyg-NRF-1 construct. Clones were digested with Xho1 and separated on 0.5 % agarose gel. Lane M, represent molecular weight marker, lanes 1 and 3 represent the undigested plasmid. Lane 2 represents the positive clone which exhibited the 5.3 kb fragment representing the pTRE2Hyg and the 1.74 kb representing the fragment for NRF-1 cDNA. Lane 4 represents a clone that did not produce the expected sizes for the pTRE2Hyg-NRF-1 when digested with Xho1.

3.4.4. Generation of Tet-On plasmids. The other plasmid which is a constituent of the Tet-On gene expression system kit is the Tet-On plasmid (figure 3.7) which is 7.4 kb in size. This plasmid is known as the regulatory plasmid since it produces the 37 kb reverse tetracycline-controlled transactivator protein (rtTA) consisting of a reverse Tet repressor (rTetR) protein fused

to the Herpes simplex virus VP16 domain (which is required by the pTRE2Hyg response plasmid for gene activation). The rtTA binds to the TRE on pTRE2Hyg-NRF-1 to activate gene transcription only in the presence of Dox. The vector construction map for the Tet-On plasmid is shown below in figure 3.7. Note that this plasmid contains neomycin and ampicillin resistance genes which permit selection of cells that have taken up the plasmid.

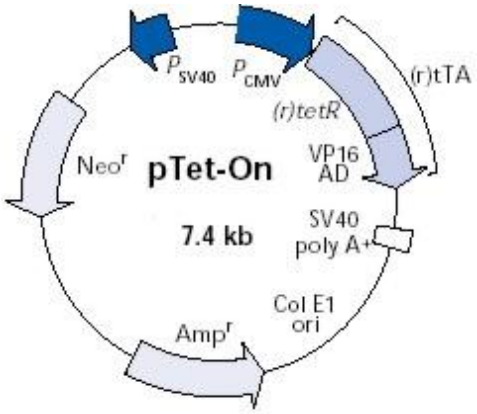

Figure 3.7: Illustration of the Tet-On plasmid. The Tet-On plasmid is the regulatory plasmid that produces the rtTA protein (reverse tetracycline controlled transcriptional activator) which binds on to the response plasmid in the presence of doxycycline; resulting in gene activation.

The Tet-on plasmid was amplified by transformation into competent DH5α cells, cultured and verified as described in section 3.4.2 with minor modifications as follows: The pTet-On plasmid is reported to be a low copy number plasmid, and has a very low plasmid yield upon culturing (74; 236). To enhance plasmid yield during culturing, we added 170 µg/ml of chloramphenicol in the growth medium and incubated for 14 h. The plasmid was verified by restriction digests using Xho1 and HindIII restriction enzymes. Figure 3.8 below shows that upon restriction digestion the expected 0.9, 1.5, 2.2, and 2.9 kb bands (Clontech, Paulo, CA) were observed after electrophoresis.

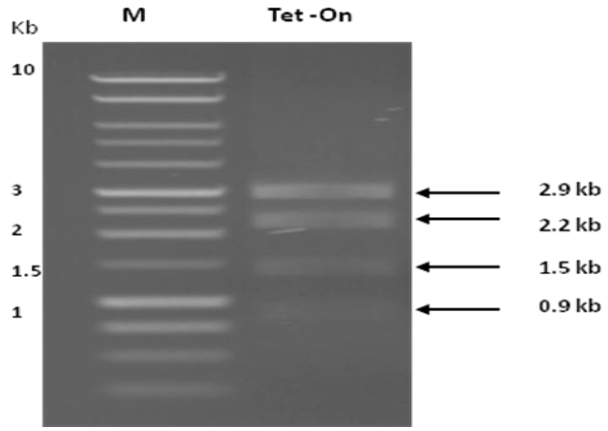

Figure 3.8: Verification of the presence of the Tet-On plasmid. M: The 1 kb marker**.** The different bands are restriction digests with Xho1 & HindIII to produce the expected 0.9, 1.5, 2.2 and 2.9 kb fragments.

***3.4.5. Production of stable Tet-On C2C12 myocytes*:** C2C12 myoblasts were allowed to grow to 70-90 % confluence and were transfected with 4 µg pTet-On vector (Clontech, Paulo, CA) using cationic liposomes (Lipofectamine, Life Technologies, Inc.). Lipofectamine (Life Technologies, Inc.) transfection into C2C12 myotubes in one well of a 6-well plate was done as follows: 4 µg DNA (Tet-On) was diluted into 250 µl Opti-MEM and mixed gently and allowed to stand at room temperature for 5 min. Ten µl of Lipofectamine was also diluted into 250 µl Opti-MEM, mixed gently and allowed to incubate for 5 min at room temperature. The diluted DNA and Lipofectamine were mixed together and allowed to incubate for 25 min at room temperature to allow DNA-Lipofectamine complexes to form. After incubation, the mixture was added to plated cells in a 6-well plate. Two days after transfection, cells were transferred into a 10 cm diameter cell culture dish and allowed to grow to a density of ~2.0 x 10^5 cell/plate. After 24 h growth in a 10 cm culture dish, Neomycin (G418) antibiotic was added to the culture to a concentration of 500 µg/ml and used to select stably transfected C2C12-Tet-On cells. Neomycin was a choice antibiotic since the Tet-On plasmid contains a Neomycin resistance gene. Neomycin-resistant clones were isolated using cloning cylinders (Sigma) and plated sequentially

in 96, 24 and 6-well plates and then finally to 10 cm plates where they were cultured for ~2 weeks until there was ~2.0 x 10^5 cell/plate. Thereafter cells were harvested and stored at -80 ^oC in cryotubes until they were needed.

Each cryotube of frozen C2C12-Tet-On cells was revived in a 10 cm culture dish, grown to 70-90 % confluency, and transfected with 4 μg of pTRE2Hyg-NRF-1 vector construct using Lipofectamine as described above. Twenty four hours post transfection, 400 μg/ml hygromycin was added to the culture to select clones that had taken up the vector. The pTRE2Hyg-NRF-1 contains the hygromycin resistance gene which allows for selection of cells that have taken up the plasmid. These clones, which are referred to here as double stable C2C12-Tet-On-NRF-1 cells were cultured in medium for 2 weeks until they had been sufficiently amplified. The clones were cultured in the presence or absence of Dox and its NRF-1 content was assessed by western blot. Approximately 60 clones were tested and clones that were not responsive to Dox and those with high NRF-1 levels in the absence of Dox (figure 3.9A) were discarded. Only clones that expressed low levels of NRF-1 in the absence of Dox and high NRF-1 under 1 μg/ml Dox treatment were selected (Fig 3.9B), amplified and used for subsequent experiments.

Figure 3.9: Identification of appropriate C2C12-Tet-On-NRF-1 clones for use in experiments. Western blot was performed to identify C2C12-Tet-On-NRF-1 clones that had high NRF-1 induction upon Dox treatment and low background. A is a representative western blots from a rejected clone: It shows a clone with a high NRF-1 background and poor response to Dox. B is a blot from a clone with low NRF-1 content in the absence of Dox and high NRF-1 induction with Dox. Such clone was accepted and used in subsequent experiments.

***3.4.6. Experiments performed with the C2C12-Tet-On-NRF-1 cell line*:** The double stable C2C12-Tet-On-NRF-1 cell line was used to study the effects of NRF-1 overexpression on the contents of: a) NRF-1, GLUT4, MEF2A, δALAS and α-tubulin using convectional western blotting, b) *mef2a* and *δalas* promoter-bound NRF-1, and c) *glut4* promoter-bound MEF2A. The effects of silencing MEF2A expression on the variables described in (a-c) above were also studied in these C2C12-Tet-On-NRF-1 cells to determine if the effects of NRF-1 overexpression occur via MEF2A. Details of all the protocols used in silencing MEF2A are described in sections 3.5; 3.7; 3.9 and 3.11.

3.5. Silencing MEF2A expression by small interference RNA

To test the hypothesis that NRF-1 regulates GLUT4 expression via MEF2A, we silenced MEF2A expression in Dox-treated C2C12-Tet-On-NRF-1 myotubes using small interference RNA (siRNA) which targeted MEF2A mRNA.

3.5.1. siRNA technology: The small interference RNA (siRNA) technology involves introduction of a double stranded RNA to a cell to induce a homology-dependent degradation of its own cognate mRNA (2; 50). The MEF2-siRNA (Santa Cruz) which was used in this experiment is a pool of 3 target-specific 20-25 nucleotides designed to knock down MEF2A mRNA, in a process called small interfering RNA (siRNA). The introduction of this MEF2- siRNA triggers the assembly of endoribonuclease-containing complexes known as RNA-induced silencing complexes (RISCs), which unwind the double stranded siRNA and promote base pairing interactions between the siRNA anti-sense strand and complementary mRNA. The bound mRNA is cleaved and degraded, resulting in gene silencing (2; 50; 67; 219).

3.5.2. Transfection protocol: A 20-80 pmol duplex MEF2A-siRNA was diluted with 100 µl DMEM and incubated for 5 min at room temperature. Five µl Lipofectamine (Life Technologies,

Inc.) was also diluted in DMEM and incubated at room temperature for 5 min. Both the diluted MEF2A-siRNA and Lipofectamine were mixed gently together with a pipette and incubated for 25 min at room temperature. The MEF2A-siRNA-Lipofectamine complexes formed were overlaid onto cells and incubated for 12 h. After 12 h of transfection, the medium was then aspirated and the cell washed. The medium was replaced with a fresh normal growth medium containing serum and the cells were further incubated for 48 h and used for western blots.

***3.5.3. Optimization of MEF2A-siRNA protocol*:** C2C12-Tet-On-NRF-1 cells were allowed to form myotubes in 6-well plates and 1 μg/ml Dox was added to initiate NRF-1 overexpression. Twelve hr after Dox treatment was initiated 30, 60 or 90 pmols of MEF2A-siRNA(sc-35895; Santa Cruz, CA, U.S.A) or 50 pmol of control siRNA (sc-37007; Santa Cruz, CA, U.S.A) which does not degrade mRNA, were transfected (see section 3.5.2) into myotubes to assess the optimal quantity needed to silence MEF2A expression. Transfected myotubes were cultured for 60 h in the presence of Dox and conventional western blotting (see Section 3.7.3) was used to verify MEF2A protein content. Figure 3.10 is a typical result.

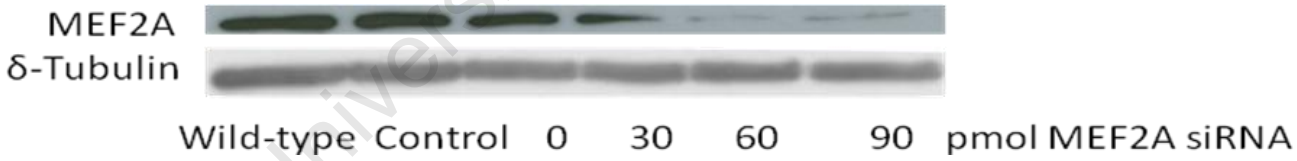

Figure 3.10: A western blot showing the effectiveness of siRNA-MEF2A on native MEF2A protein. Myotubes were treated with varying amounts of the siRNA-MEF2A to establish the optimum concentration to silence wild type MEF2A. Note that α-tubulin was not degraded by the MEF2A-siRNA or control-siRNA.

For all subsequent MEF2A silencing experiments, C2C12-Tet-On-NRF-1 myotubes were treated with 1 μg/ml Dox and incubated for 12 h and then transfected with 60 pmol of MEF2A-siRNA or 50 pmol of control siRNA, incubated for a further 60 h in the presence of 1 μg/ml Dox, harvested and the protein content assayed by conventional western blot.

3.6. CaMK II activation in C2C12 myotubes

In previous studies, Ojuka and co-workers showed that GLUT4 and MEF2A contents in muscle were increased when CaMK II activity was increased in L6 myotubes in culture (172; 173). In these studies, CaMK II was activated by incubation of myotubes in medium containing caffeine, an agent which induces Ca^{2+} release from the sarcoplasmic reticulum (SR) and increases cytosolic calcium levels. Because NRF-1 has been shown to upregulate the expression of both MEF2A and GLUT4, we investigated the role that NRF-1 might play in the caffeine-induced increases in MEF2A and GLUT4 expression in cultured myotubes.

Well differentiated C2C12 myotubes were incubated in serum-free medium for ~12 h before incubation in medium containing 10 mM caffeine (Sigma) in the presence or absence of 10 μM dantrolene (a compound that inhibits Ca^{2+} release from the SR) or 25 μM KN93 (CaMK II inhibitor) (Sigma) for 2 h. After treatment, myotubes were harvested and assayed for: a) NRF-1 binding to *mef2a* and *δalas* genes, b) acetylation of the NRF-1 binding site on *mef2a* and *δalas* promoters, c) MEF2A binding to the *glut4* gene, d) acetylation of the MEF2A binding site on the *glut4* promoter, e) GLUT4 and MEF2A expression, and f) HDAC5 trafficking between the nucleus and cytosol. Detailed protocols of the above assays are presented in sections 3.7-3.11.

3.7. Protein assays

After treatments of C2C12-Tet-On-NRF-1 cells with Dox (Section 3.4.5) or C2C12 myotubes with caffeine (Section 3.6) were completed, myotubes were washed twice with ice-cold PBS containing 1 x complete protease inhibitors (Roche). Total cellular proteins (Crude extracts), cytosolic proteins or nuclear proteins were extracted by the methods described below:

3.7.1. Crude extracts: Myotubes were scraped loose from the plates in 300 μl of RIPA buffer (56 mM Tris-HCl pH 7.4, 150 mM NaCl, 1 mM EDTA, 0.1 % SDS, 1 % Triton-X100, 10

mM $Na_4P_2O_4$, 20 mM NaF, 0.15 µM okadaic acid, 4 mM Na_3VO_4, 1 x complete protease inhibitors). The cells were then transferred to clean eppendorf tubes, incubated for 20 min on ice and then sonicated for 5 s. The homogenate was centrifuged at 10,000 rpm for 10 min at 4 °C, the supernatant (the crude extract) collected, and the protein concentration measured using the Bradford assay method.

3.7.2. Nuclear and cytosolic fractions: After washing myotubes twice with ice-cold PBS, 300 µl of homogenization buffer (10 mM Tris, 1 mM EDTA, 5 mM $MgCl_2$, 1.4 M sucrose, 10 mM $Na_4P_2O_4$, 20 mM NaF, 0.15 µM okadaic acid, 4 mM Na_3VO_4, 1 x complete protease inhibitor, 30 µM MG132, pH 7.4) was then added and cells were scraped loose from the plate and homogenized with a Dounce homogenizer. The homogenate was centrifuged at 600 x g for 10 min at 4 °C and the supernatant, containing the crude cytosolic fraction, was centrifuged a second time (same speed for 5 min) to produce the final cytosolic extract. The pellet, containing nuclei, was washed in 300 µl homogenization buffer, centrifuged as above, and resuspended in 75 µl of nuclear extraction buffer (25 % glycerol, 0.2 mM EDTA, 15 mM $MgCl_2$, 20 mM HEPES, 450 mM NaCl, 0.5 % Triton X-100, 100 mM KCl, 25 µM MG132, 4 mM Na_3VO_4, 20 mM NaF, 1.5 µM okadaic acid, 10 mM $Na_4P_2O_7$, 1 x complete protease inhibitors) and sonicated on ice for 5 s. After centrifugation at 600 x g for 5 min, the supernatant, containing the nuclear extract, was collected. Protein concentrations of the extracts were measured using the Bradford method as follows: Five microliters of the extracted protein and 95 µl of water were added to 900 µl of Bradford reagent consisting (0.02 % coomassie brilliant blue G250, 4.75 % ethanol, 8.5 % phosphoric acid) and incubated for 10 min and the optical density (OD) measured at 595 nm. Bovine serum albumin (BSA) was used to make a standard curve from which the concentration of proteins in the extracts was deduced.

To determine whether the extraction protocol was effective in separating the cytosolic from the nuclear proteins, the activity of lactate dehydrogenase (LDH), a cytosolic protein, and the contents of α-tubulin (cytosolic protein) and histone H3 (nuclear protein) were measured in both extracts. LDH activity was measured spectrophotometrically by assessing the rate at which NADH was oxidized to NAD^+ in an LDH-catalyzed reaction that is coupled to the conversion of pyruvate to lactate.

Pyruvate $\xrightarrow{\text{LDH}}$ Lactate

NADH $\longrightarrow$ $NAD^+ + H^+$

Fifteen µg of cytosolic or nuclear extracts was added to a 1 ml of reaction buffer [50 mM Tris (pH 7.5), 4 mM EDTA, 2 mM pyruvate, and 0.14 mM NADH] and the absorbance measured at 340 nm every 12 sec for ~1 min. The contents of α-tubulin and histone H3 proteins in the nuclear and cytosolic extracts were measured by western blot (Section 3.7.3). Figure 3.11A. and 3.11 B, showing typical results from these measurements indicate that our extraction protocol effectively separated cytosolic and nuclear proteins.

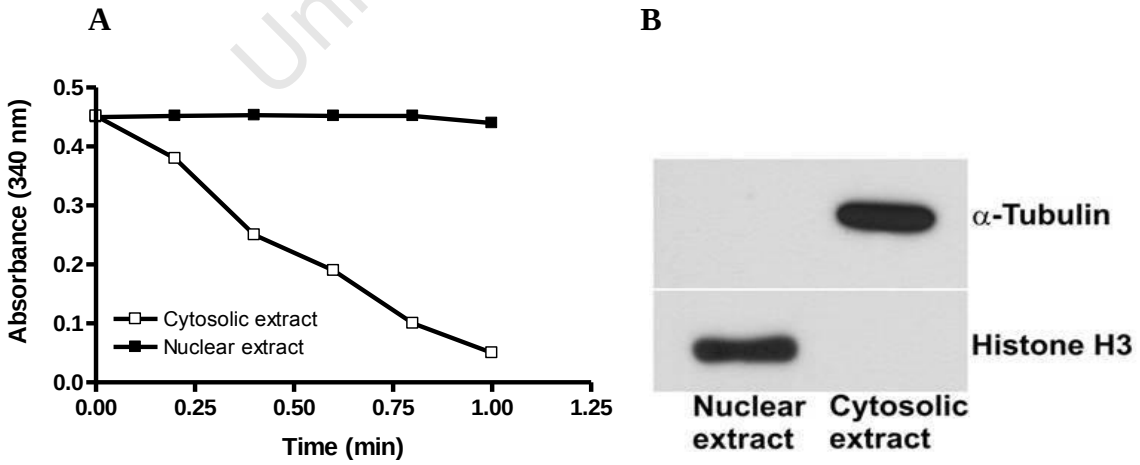

Figure 3.11: Separation of nuclear and cytosolic cell compartments. ***A****:* Lactate dehydrogenase (LDH) activity in cytosolic and nuclear extracts. LDH activity is evident in the cytosolic fraction but absent in the nuclear fraction. ***B***: α-tubulin (a cytosolic protein) is detectable in the cytosolic fraction but not in the nuclear fraction, whereas histone H3 (a nuclear protein) is enriched in the nuclear fraction but absent in the cytosolic fraction. Collectively, these control experiments show that the nuclear extraction protocol was effective.

3.7.3. Western blots: Crude extracts were solubilised in 2 x Laemmli sample buffer (250 mM Tris-HCl pH 6.8, 2 % glycerol, 10 % SDS, 0.01 % of Bromophenol blue and ± 5 % mercaptoethanol), heated at 95 ^{o}C for 1-5 min and proteins separated by size using SDS PAGE. A kaleidoscope precision standard marker (Bio-Rad, Hercules, CA) was used to indicate the size of the proteins of interest. Proteins from SDS-PAGE were transferred to polyvinylidene diflouride (PVDF) membrane (Amersham, Cape Town, South Africa) in a transfer buffer (25 mM Tris-HCl, 192 mM glycine and 20 % methanol; 4 ^{o}C) at 90 mA overnight or 180 mA for 2 h. Membranes were blocked in 5 % non-fat dry milk or 5 % BSA (Sigma, St Louis, MA) dissolved in 1x PBS-T for 1 h at room temperature or overnight at 4 ^{o}C and thereafter incubated with antibodies against NRF-1, MEF2A, GLUT4, δALAS, or α-tubulin overnight at 4 ^{o}C. Dilutions and buffers used for the antibodies used are summarized in Table 3.2. After washing the membranes for 3 x 7 min in PBS-T, they were incubated for 2 h at room temperature with appropriate HRP-conjugated secondary antibody (Dako, Carpinteria, CA). Membranes were washed for 2 x 7 min in PBS-T followed by 1x 7 min in PBS, incubated for 2-5 min in enhanced chemiluminescence (ECL) solution (Amersham, Cape Town, South Africa) and exposed to film (Kodak) for 20 to 60 min and the film developed using the protocol prescribed by the manufactures. The film was scanned using UN-SCAN-IT gel 6.1 software (Silk scientific, Orem, USA) and the density of signals from MEF2A, GLUT4 (Cell signalling, Charlottesville, VA), NRF-1 (Abcam) and δALAS (SCBT, Santa Cruz, CA) blots was measured and normalized to α-tubulin and expressed relative to controls.

3.7.4. Stripping of membranes: Where it was necessary to detect multiple proteins from the same PVDF membrane, sequential western blots, with different primary antibodies on the same membrane, were performed. The antigen-antibody interactions on a membrane that had already been probed with one antibody was disrupted by incubation (with shaking), in a stripping buffer consisting of 100 mM 2-mercaptoethanol, 2 % SDS, 62.5 mM Tris-HCl pH 6.7 at 50 ^{o}C for 20 min and washed twice in either PBS-T or TBS-T at room temperature. The stripped membrane was then blocked as described in section 3.7.3 before incubation with another primary antibody.

Table3.2: Antibody concentration for western blots, immunocytochemistry and ChIP assay.

Protein to be identified	1° Antibody	1°Antibody incubation conditions	2° Antibody	2°Antibody incubation conditions
MEF2A	Anti-MEF2A (Cell signalling) diluted 1:500 in TBS-T	Overnight at 4°C	Anti-rabbit diluted in 1:10000 TBS-T)	2 h at R.T
GLUT4	Anti-GLUT4 (Cell signalling) diluted in 1:2000 in TBS-T	Overnight at 4°C	Anti-rabbit diluted in 1:10000 TBS-T)	2 h at R.T
NRF-1	Anti-NRF-1 (Abcam) diluted 1:2000 in PBS-T)	Overnight at 4°C	Anti-rabbit diluted in 1:10000 PBS-T)	2 h at R.T
δALAS	Anti-δALAS (Santa Cruz) diluted 1:500 in PBS-T)	Overnight at 4°C	Anti-goat diluted in 1:10000 PBS-T)	2 h at R.T
α-TUBULIN	Anti α-tubulin (Santa Cruz) diluted 1:500 in PBS-T)	Overnight at 4°C	Anti-mouse diluted in 1:10000 PBS-T)	2 h at R.T
MEF2A, HDAC5, Fluorochrome conjugated anti-mouse and anti-rabbit		All these antibodies were used for immunocytochemistry and diluted 1:200 for 1^{o} and 2^{o} diluted 1:1000		

All antibodies were diluted in TBS-T/PBS-T containing 1% Fat free milk (Santa Cruz antibodies) or 5% BSA (Cell signalling antibodies) when used for western blot; BSA = Bovine serum albumin; TBS=Tris-buffered saline; T = Tween20; R.T = Room temperature1^{o} = primary antibody; 2^{o} = secondary antibody; HDAC5= Histone deacetylase 5.

3.8. Immunocytochemical analysis of MEF2A and HADC5 localization in C2C12 myotubes in response to CaMK II activation

In order to study the effects of CaMK II activation on MEF2A and HDAC5 trafficking, immunocytochemical analyses of C2C12 myotubes were performed on myotubes that were treated with caffeine or vehicle.

3.8.1. Treatment of myotubes for immunocytochemistry: Myotubes were kept in serum-free medium for ~12 h before treatments. The treatments involved incubation in medium containing 10 mM caffeine in the presence or absence of 10 µM dantrolene (calcium release inhibitor) or 25 µM KN93 for 2 h.

3.8.2. Immunocytochemistry: Immediately after treatments as described in section 3.7.1, myotubes were washed in ice-cold PBS and fixed with 3:1 methanol/glacial acetic acid at –20 °C for 10 min. Thereafter, they were washed in PBS, blocked in 1 % BSA for 30 min, and incubated overnight at 4 °C with antibodies against HDAC5 (Santa Cruz) and MEF2A (Cell signalling). The following day, cells were washed and incubated with fluorochrome-conjugated anti-rabbit (Cy3) (Dianova) and goat anti-mouse (Alexa) secondary antibodies (diluted 1:1000) for 2 h at room temperature. Nuclei were stained using a 1:50 dilution of 0.05 µg/ml DAPI for 10 min at room temperature. After washing the cells, a coverslip was mounted on the cells with a solution consisting of 40 % glycerol, 20 % Mowiol, 8 % n-propyl gallate, and 0.2 M Tris buffer (pH 7.4). Subcellular location of HDAC5 and MEF2A was viewed using a Zeiss Axiovert 200M fluorescence microscope equipped with plan-neofluar optics set at 15 (Cy3), 10 (Alexa 488), and 1 (DAPI) as well as an Axiocam HR charge-coupled device camera. Adobe Photoshop 7 software was used for image processing.

3.9. Chromatin immunoprecipitation (ChIP) assays

ChIP assay was used to assess the amount of: a) NRF-1 that was bound to *mef2a* and *δalas* promoters, b) MEF2A that was bound to the *glut4* promoter, in Dox-treated C2C12-Tet-On-NRF-1 myotubes or caffeine treated C2C12 myotubes, and c) Acetylation levels of histones in the vicinity of NRF-1 binding domain on *mef2a* promoter and of histones in the neighbourhood of the MEF2A binding site on the *glut4* promoter in C2C12 myotubes.

3.9.1. Primer design for ChIP assay: Primers were designed using Primer 3 software using the genome sequences posted in the NIH genome database (PUBMED). Primer pairs (forward and reverse), were designed to span the NRF-1 binding site on *mef2a* and *δalas* promoters and the MEF2 site on the *glut4* promoter. These are refered to as positive (+ ve) primers in this thesis. Negative control primers (-ve), which span a sequence of DNA without NRF-1 or MEF2 binding sequences were designed to be a least ~3 kb away from primers at corresponding NRF-1 or MEF2 binding sites. The following criteria were used for selection of primers: a) they had to have least potential to form inter- or intra primer dimmers and hairpins, b) the GC content was between 50-66 % , c) the melting temperature was 55-70 ^{o}C, d) they contained 18-24 bp of nucleotides, and e) transcript size was between 250-340 bp.

Table 3.3: Primers used in the ChIP assays.

Designed Primer name	Amplicon size	Forward (F) and Reverse primer (R)
GLUT4-MEF2A (+VE)	268 bp	F: 5'- CAG GCA TGG TCT CCA CAT ACA C-3' R: 5' –GGT AAC TCC AGC AGG ATG ACA-3'
GLUT4-MEF2A (-VE)	315 bp	F: 5' – CCA ACA GCT CTC AGG CAT-3' R: 5' – CCA TTC CAC AGG CAA GCA G-3'
MEF2A-NRF-1 (+VE)	315 bp	F: 5' – CCT TCC TGT GCC GGG TGA TCT-3' R: 5' –CTA TTT TTA GGA GTC AGG CCC GG-3'
MEF2A-NRF-1 (-VE)	250 bp	F: 5' –AGT TGT GCC ACC TGT CCC A-3' R: 5' –CAA TGT CAG CTC ACA CTC A-3'
ALAS-NRF-1 (+VE)	260 bp	F: 5'-TAG AAG GAG CAG AGG GAC GA-3' R: 5'-TGT TCA CGA GCA GCC TAA GG-3'
ALAS-NRF-1 (-VE)	339 bp	F: 5'-TCT CGT AGA CTC CAC GTG CAT-3' R: 5'-AGT GCC CAG GAC AGG ATT AC-3'

***3.9.2. Treatment of myotubes for ChIP assay*:** C2C12-Tet-On-NRF-1 cells were grown for 10-13 days to form myotubes as described in section 3.3. To stimulate NRF-1 overexpression, 1 μg/ml Dox was added to and kept in the medium for 6 h. After the Dox treatment, cells were washed with 1 x PBS to remove Dox and incubated in fresh medium for additional 6-8 h. C2C12-Tet-On-NRF-1 cells that were treated with vehicle (No Dox) served as controls. Differentiated wild type C2C12 myotubes were treated with 10 mM caffeine in the presence or absence of 25 μM KN93 and incubated for 2 h after which cells were washed and incubated in DMEM only for further 6 h.

3.9.3. The ChIP assay protocol: To assess changes that occurred in the amount of NRF-1 that bound to *mef2a* and *δalas* promoters and MEF2A that bound to the *glut4* promoter in response to Dox or caffeine, ChIP assays were used (146). After treatments, formaldehyde was added to the medium to a concentration of 1% (v/v) to crosslink protein to DNA and protein to protein. Crosslinking was allowed to proceed for 10 min and stopped by adding glycine to the medium to a concentration of 0.125 M. Cells were then washed twice with cold PBS containing 1 x complete protease inhibitors (Roche), scraped into an eppendorf tube on ice and centrifuged (1200 x g, 4 min, 4 ^{o}C) on a bench top microfuge. After removal of the supernatant, the pellet was sonicated in 500 μl nuclear lysis buffer (1 % SDS, 50 mM Tris-HCl, pH 8.0, 10 mM EDTA + 1 x complete protease inhibitors) on ice to shear chromatin using a Virsonic 60 sonicator (Virtis). With the sonicator set at 33 % of maximal power, chromatin was sheared to the desired size of ~300-1000 bp by 8 cycles (60 s rests between cycles) of 20 s pulses of sonication. The tube containing sonicated solution was centrifuged at 13000 rpm for 10 min and the supernatant (containing chromatin fragments) transferred to a new tube. Endogenous immunoglobin was pre-cleared by incubating with 30 μl (60 μg) of 50 % salmon sperm DNA/protein A agarose slurry (Santa Cruz) for an hour at 4 ^{o}C (with

shaking) followed by centrifugation at 1000 x g for 1 min. The resultant supernatant containing chromatin was referred to as the 'input' sample (IN). Chromatin from 100 µl of the input sample was diluted 1:10 in ChIP dilution buffer (0.1 % SDS, 1 % Triton X-100, 1.2 mM EDTA, 16.7 mM, Tris-HCl, pH 8.1, 167 mM NaCl and 1 x complete protease inhibitors). This was incubated with 5 µl MEF2A (Cell signalling) or NRF-1 (Abcam) antibodies, or with 5 µl IgG (Cell signalling) on a rocking platform at 4 ^{o}C for 24-48 h. After the incubation, the immuno-complexes were precipitated with 60 µl (120 µg) of the 50 % salmon sperm DNA/protein A agarose bead slurry (Santa Cruz) for 2 h in a rocking platform at 4 ^{o}C. The beads were pelleted by centrifugation at 5500 x g for 1 min at 4 ^{o}C and the pellet, washed sequentially with low salt buffer (0.1 % SDS, 1 % Triton X-100, 2 mM EDTA, 20 mM Tris-HCl, pH 8.0, 150 mM NaCl), high salt buffer (0.1 % SDS, 1 % Triton X-100, 2 mM EDTA, 20 mM Tris-HCl, pH 8.0, 500 mM NaCl), Lithium chloride buffer (250 mM LiCl, 1 % NP-40, 1 % sodium deoxycholate, 1 mM EDTA, 10 mM Tris-HCl, pH 8.0) and twice with TE buffer (10 mM Tris-HCl pH 8.1, 1 mM EDTA). The washing steps were done by adding 1 ml of each buffer, shaking the tubes for 5 min on a rocking platform and centrifuging at 5500 x g at 4 ^{o}C except during the last wash (with TE buffer) which was carried out at room temperature. Elution was done with 150 µl elution buffer (1 % SDS, 100 mM $NaHCO_3$) for 15 min at room temperature and repeated twice to make a 300 µl final volume. The eluted immunoprecipitated sample (IP), and equal volume of IN sample were decross-linked by incubation in 0.3 M NaCl at 65 °C for 6 h. After digestion of proteins by proteinase K (10 µg/µl) for 1 h at 45 ^{o}C, DNA fragments were purified, using the phenol-chloroform extraction method, to yield IP and IN DNA samples respectively. Phenol-chloroform extraction was performed as follows: One volume of Phenol was added the DNA sample, mixed for 5 min and centrifugation at 12000 x g for 3 min. The aqueous phase was added to an equal volume of phenol:chloroform:isoamyl alcohol

(25:24:1), shaken for 5 min, and centrifuged at 12000 x g. The aqueous portion was mixed with an equal amount of chloroform:isoamyl alcohol (24:1) and centrifuged as before. The aqueous portion was transferred to a new tube containing 100 % ethanol, 0.3 M sodium acetate and glycogen and the DNA precipitated overnight at -20 ^{o}C. After centrifugation at 12000 x g for 15 min, the DNA pellet was washed in 70 % ethanol, air dried and then re-suspended in 20 µl dH_2O. The DNA concentration was determined by measuring absorbance at 260 nm in a quartz cuvette using a spectrophotometer and DNA concentration was calculated by the dilution multiplying the absorbance obtained dilution factor and 50 µg/ml.

3.9.3.1. Assessment of mef2a promoter-bound NRF-1: To assess the amount of NRF-1 that was bound to the mouse *mef2a* gene (AC120123), a 315 bp fragment corresponding to nucleotides -308 to +7 of the mouse *mef2a* gene containing the NRF-1 *cis*-element was PCR amplified from purified IN DNA and from the NRF-1 antibody co-immunoprecipitated DNA (IP). To control for antibody specificity, purified DNA from sample that had been treated with IgG was also PCR amplified. The PCR reaction consisted of 30 pmol of forward and reverse *MEF2A*-NRF-1 (+ve primers) (Table 3.3), 1 µl of purified IP DNA, 1 µl IN DNA or 1 µl IgG immunoprecipitate, 0.2 mM $MgCl_2$, 0.5 U of SuperTherm Taq polymerase, 1 x SuperTherm buffer and 2 mM dNTPs). A 250 bp fragment corresponding to nucleotides +2904 to +3154 (relative to the start of transcription), which does not contain the NRF-1 site, was used as a negative control. In this case the PCR reaction consisted of 30 pmol of forward and reverse *MEF2A*-NRF-1 (-ve primers) (Table 3.3), 1 µl of purified IP DNA, 1 µl IN DNA or 1 µl IgG immunoprecipitate, 1-3 mM $MgCl_2$, 0.5 U of SuperTherm Taq polymerase, 1 x SuperTherm buffer, 0.2 mM dNTPs). The PCR reaction was conducted as follows: 1 cycle of denaturing at 94 ^{o}C for 4 min followed by 35 cycles of 4 min of

denaturing at 94 ^{o}C, 30 s annealing at 63.5 ^{o}C, extension for 1 min at 72 ^{o}C and lastly, 1 cycle of final extension at 72 ^{o}C for 5 min.

The PCR reactions were conducted under identical conditions as described above. Five to 10 μl of PCR products was separated by 2 % agarose gel electrophoresis to verify amplicon sizes. Figure 3.12, showing a typical gel, indicates that the primers used amplified fragments of 315 bp (+ve) and 250 bp (-ve) as expected. Lane 3 represents a PCR product after immunoprecipitation (IP) with IgG and amplification using +ve primers. No signal is seen as expected. Lanes 2 and 5, which represents NRF-1- IP samples which underwent PCR using *MEF2A*-NRF-1 (+ve) and *MEF2A*-NRF-1 (-ve) primers (Table 3.3), showed a signal (lane 2) and no signal (lane 5) respectively as was expected. Lanes 1 & 4 represents PCR of Input samples using both *MEF2A*-NRF-1 (+ve) and *MEF2A*-NRF-1 (-ve) primers which produced 315 bp and 250 bp products, respectively, as expected.

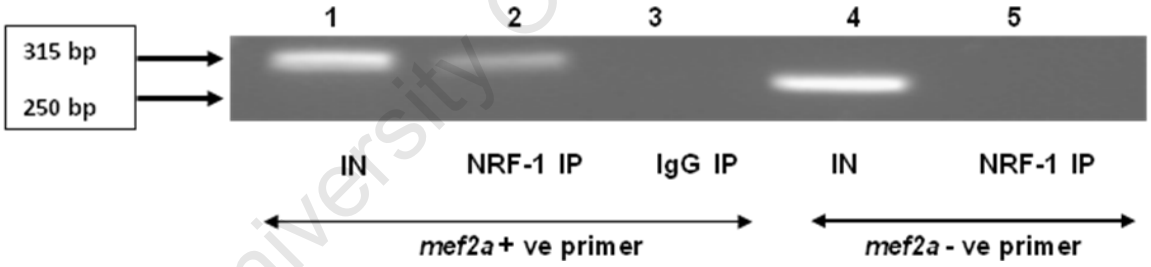

Figure 3.12: The typical agarose gel from a ChIP assay performed in either C2C12-Tet-On-NRF-1 cells treated with Dox or C2C12 myotubes treated with caffeine. Lanes 1 & 4 shows PCR conducted on input samples (IN) with positive (315 bp) and negative primers (250 bp), respectively. Lanes 2 & 5 show a PCR conducted on IP (NRF-1 immunoprecipitation) samples with both positive (315 bp) and negative primers (250 bp) respectively. Lane 3 shows PCR done with positive primers on IgG IP samples used as a control. These results demonstrate the high specificity of our assay.

3.9.3.2. Assessment of δalas promoter-bound NRF-1: For measurement of *δalas* promoter-bound NRF-1, a 260 bp fragment corresponding to nucleotides -236 to +24 of the mouse *δalas* gene

containing NRF-1 binding site was amplified by PCR. In this case, the PCR reaction consisted of 20 pmol of forward and reverse *δALAS*-NRF-1 (+*ve* primers) (Table 3.3), 1 μl of purified IP DNA, 1 μl IN DNA or 1 μl IgG immunoprecipitate, 3 mM $MgCl_2$, 0.5 U of SuperTherm Taq polymerase (Medox Biotech, Chennai, India), 1 x SuperTherm buffer and 0.2 mM dNTPs. The PCR reaction was conducted as follows: 1 cycle of 4 min denaturing at 94 ^oC followed by 35 cycles of 30 s denaturing at 94 ^oC, 30 s annealing at 63 ^oC, 1 min extension at 72 ^oC and lastly, 1 cycle of 5 min final extension at 72 ^oC.

Like wise, a 339 bp fragment corresponding to nucleotides -8404 to -8065 (relative to the start of transcription), which does not contain the NRF-1 site, was used as a negative control. This site was amplified using *δALAS*-NRF-1 (-ve primers) (Table 3.3). In this case the PCR reaction was conducted similarly as for the δ*ALAS*-NRF-1 (+ve primers) described above.

3.9.3.3. Measurement of glut4 promoter-bound MEF2A: A 268 bp fragment corresponding to nucleotides –604 to –336 of the mouse *glut4* promoter containing the MEF2A binding site was amplified by PCR using 20 pmol of forward and reverse *GLUT4*-MEF2A (+ve primers) (Table 3.3), 1 μl of purified IP DNA, 1 μl IN DNA or 1 μl IgG immunoprecipitate, 2.5 mM.$MgCl_2$, 0.5 U of SuperTherm Taq polymerase, 1 x SuperTherm buffer, 0.2 mM dNTPs. The PCR reaction was conducted as follows: 1 cycle of denaturing at 94 ^oC for 4 min followed by 35 cycles of 30s denaturing at 94 ^oC, 30 s annealing at 64 ^oC, 1 min extension at 72 ^oC and lastly, 1 cycle of 5 min final extension at 72 ^oC.

A 315 bp fragment corresponding to nucleotides +2,868 to +3,183 (relative to the start of transcription), which does not contain the MEF2A site, was used as negative control. This site was amplified using similar conditions used for the *GLUT4*-MEF2A (+ve primers) described above. The amplified DNA fragments were separated by electrophoresis on 2 % agarose gels as described

under section 3.9.3.1. Figure 3.13, shows a typical gel. The figure verifies that the positive primers amplified 268 bp fragments (lanes 1 and 2) and the -ve primers amplified 315 bp fragments (lane 4), as expected. Lane 3 represents immunoprecipitation with IgG which did not produce any signal as expected. Lanes 1 & 4 represents PCR of Input samples using both *GLUT4*-MEF2A (+ve) and *GLUT4*-MEF2A (-ve) primers which produced 268 bp and 315 bp products, respectively, as expected.

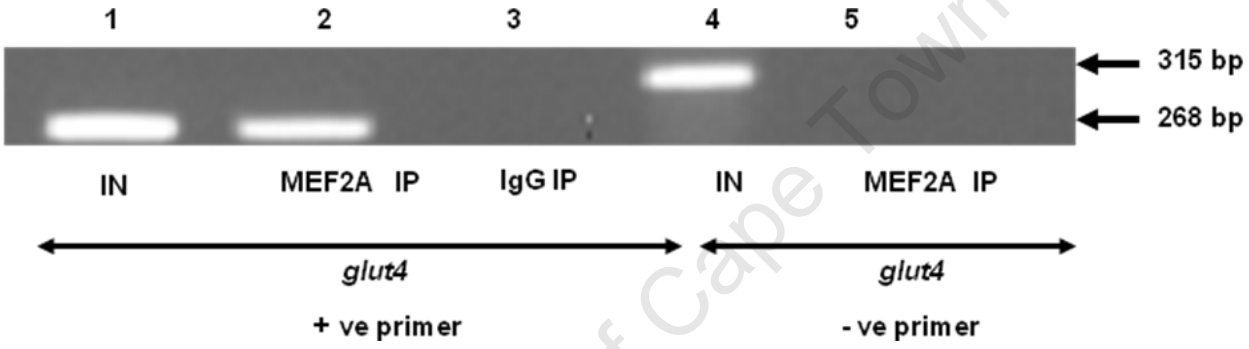

Figure 3.13: The typical agarose gel showing a ChIP assay performed in either C2C12-Tet-On-NRF-1 treated with Dox or C2C12 myotubes treated with caffeine. Lanes 1 & 4 show PCR conducted on input samples (IN) with positive (268 bp) and negative (315 bp) primers respectively. Lanes 2 & 5 show a PCR conducted on IP (MEF2A immunoprecipitation) samples with positive (268 bp) and negative (315 bp) primers respectively. Lane 3 shows PCR done with positive primers on IgG IP samples used as a control.

3.9.3.4. Assessment of acetylation of histones at NRF-1 and MEF2A binding domains:

For assessment of histone acetylation, ChIP assay was performed as described in sections 3.9.3.1-3. We assessed the levels of acetylation of histone H3 in the vicinity of the NRF-1 binding site on the mouse *mef2a* gene, and MEF2A binding domain on the *glut4* gene. Immunoprecipitation was done using antibodies against histone H3 and acetyl histone H3 (Cell signalling). The amount of co-immunoprecipitated *mef2a* and *glut4* gene sections were assessed by PCR using appropriate primers (i.e. the same +ve and –ve primers shown in table 3.3).

Table 3.4: Antibodies and antibody dilution for ChIP assays.

Antibodies used for ChIP assay	antibody dilution
Acetyl histone H3 (Lys9/Lys14); Histone H3; Mouse IgG (Cell Signalling).	(5 µl of antibody in 1 ml ChIP assay sample)
MEF2A (Cell signalling) and NRF-1 (Abcam)	In ChIP assay, a 5 µl of each antibody was added into 1 ml ChIP assay sample.

3.10. RNA analysis

After analysing the binding levels of NRF-1 and MEF2A on *mef2a* and *glut4* promoters respectively after CaMK II activation, we investigated how the levels of MEF2A and GLUT4 mRNA under the same conditions were. C2C12 were grown as before until they had formed myotubes. They were treated with caffeine or caffeine with KN93 for 2 h, washed and incubated in fresh DMEM medium for 6 h, and harvested.

Primers for quantitative real time PCR, and semi quantitative RT-PCR were designed to span exon-exon boundary segments to avoid amplifying genomic DNA. Exons were mapped using SPIDEY program (www.ncbi.nlm.nih.gov/spidey). The primers were designed using the Roche light cycler (LC) probe design and Primer 3 software from sequences posted from gene bank (NIH genome database, PUBMED). For oligonucleotides to qualify as primers, they had to have: a) low potential to form inter-or intra primer dimmers and hairpins, b) a GC content of 50-60 %, and c) 16–21 bp.

3.*10.1. RNA gels and preparation:* Gel tanks, trays, and combs were thoroughly washed with detergent and thereafter rinsed well with water. The agarose powder was dissolved in 10 % of 10 x MOPS (0.2 M MOPS pH 5.5, 0.05 M sodium acetate, 0.01 M) in DEPC water. The powder was heated and dissolved in a microwave and then cooled to 60 ^{o}C. Formaldehyde (4.9 % of 12.3 M) and 0.5 µg/ml ethidium bromide were added and mixed and poured onto trays and allowed to

set. The gel was then placed in a tank wherein 1 x MOPS running buffer was added. RNA (2-5 μg) samples were mixed with RNA formaldehyde loading buffer (0.8 % of 0.5 M EDTA, 7.2 % formaldehyde, 20 % glycerol, 30 % formamide, 40 % 10 x MOPS, 0.8 % Bromophenol blue dye) vortexed, centrifuged, heated at 55 ^{o}C for 15 min, and loaded onto wells and separated by electrophoresis. Electrophoresis was performed at 50 V until the RNA bands were well separated and a photograph of the bands taken. The 28S rRNA and 18S rRNA bands were inspected visually to assess the integrity of the RNA. When the integrity of the RNA was acceptable, the concentration of RNA was determined spectrophotometrically at 260 nm and the RNA used in the experiments.

3.10.2. Measurement of MEF2A and GLUT4 mRNA: Well differentiated myotubes were serum-starved overnight and incubated with 10 mM caffeine in the presence or absence of 25 μM KN93. Myotubes were harvested 6 h post treatment and RNA was isolated using 1 ml of Trizol reagent according to the manufacturer's instructions (Ambion). Briefly, the medium was sucked from the plates after treatments and 1 ml of Trizol reagent added directly to the cells and the cells scraped loose from the plates. Cells were passes through the thin bore of a pipette several times to lyse the cells. The lysate were transferred to an RNase-free eppendorf tube and incubated at room temperature for 5 min to allow nucleoprotein complexes to dissociate completely. Thereafter, 200 μl of chloroform was added. The tubes were tightly capped and vigorously shaken and then incubated further for 10 min at room temperature. The lysate were centrifuged at 12000 x g for 10 min at 4 ^{o}C and thereafter the aqueous phase was transferred to a fresh clean tube. Fifty μl of isopropanol was added and the mixture vortexed and incubated for 10 min at room temperature and finally centrifuged at 12000 x g for 8 min at 4 ^{o}C. The supernatant was removed without disturbing the pellet containing RNA. One ml of 75 % ethanol was added to wash the pellet followed by

centrifugation at 7500 x g for 5 min at 4 ^{o}C. Ethanol was removed and the pellet was air-dried and dissolved in DEPC-treated water and stored at -85 ^{o}C. The RNA quantity was assayed by measuring the absorbance at 260 nm and the integrity of the RNA was checked by running samples on a 1 % formaldehyde agarose gel as described above. Genomic DNA was eliminated from the samples by digestion with DNAse-1 for 90 min at 37 ^{o}C. DNAse-1 was subsequently deactivated by incubation at 75 ^{o}C for 5 min. cDNA was synthesized from 1 μg of total RNA using 200U of M-MLV reverse transcriptase (Promega) for 1 h in a reaction mixture containing 2 mM dNTPs, 2.5 mM $MgCl_2$, 20 U RNAsin and 1 x RT buffer. Real time PCR was performed in triplicate on the cDNA in a Light Cycler PCR machine (Roche) using SYBR Green PCR reagents from Roche and primers which amplify a 187 bp region in the mouse *mef2a* gene (Fwd 5'-GTG TAC TCA GCA ATG CCG AC-3′; Rev 5'-AAC CCT GAG ATA ACT GCC CTC-3'). For GLUT4: primers that amplify a 270 bp region in the mouse *glut4* gene (forward 5'-GCAGCGAGTGACTGGAACA-3'; reverse 5'-CCA GCC ACG TTG CAT TGT AG-3'). Relative mRNA concentrations were calculated using the PCR threshold cycle according to the method described by (140). Mean values were corrected to mouse GAPDH (Fwd 5'–GCA CAG TCA AGG CCG AGA AT-3'; Rev 5'-GCC TTC TCC ATG GTG GTG AA-3') and Ribosome S12 (Fwd 5-GGA AGG CAT AGC TGC TGG AGG TGT-3'; Rev 5'-CGA TGA CAT CCT TGG CCT GAG-3') genes (internal controls) and expressed relative to a control in each experiment.

Table 3.5: Characteristics of the primers used to amplify the mouse cDNA and mRNA.

Name	Primers	Product size	mRNA	cDNA
GLUT4	F: 5'-GCA GCG AGT GAC TGG AAC A-3' R: 5'-CCA GCC ACG TTG CAT TGT AG -3'	270 bp	X	
MEF2A	F: 5'- GTG TAC TCA GCA ATG CCG AC -3′ R: 5′- AAC CCT GAG ATA ACT GCC CTC -3′	187 bp	X	
GAPDH	F-5'-GCA CAG TCA AGG CCG AGA AT-3' R-5-GCC TTC TCC ATG GTG GTG AA-3'	100 bp	X	
RS12	F-5'-GGA AGG CAT AGC TGC TGG AGG TGT-3' R- 5'-CGA TGA CAT CCT TGG CCT GAG -3'	380 bp	X	
NRF-1	F: 5'-GTT GGA TCC CTC TCA CCC ATT G - 3' R: 5' - CCA AGT CGA GAC TTA ATT CC-3'	1740 bp		X

Mouse GAPDH- Glyceraldehyde 3-phosphate dehydrogenase; RS12-Ribosomal protein S12; GLUT4-Glucose transporter 4; MEF2-myocyte enhancing factor 2; mRNA-messenger ribonucleic acid; cDNA- complementary deoxyribonucleic acid. F- Forward primer; R- Reverse primer, bp= base pair.

3.11. Statistics

Data were presented as means ± SD. Statistical differences between treatments were determined using a one-way ANOVA. Significance was accepted at $p < 0.05$. When the ANOVA test showed a significant difference, *post hoc* analysis was performed using LSD or Fisher's test. STATISTICA 9 software was used for these analyses.

CHAPTER 4

Study One:

Stimulation of GLUT4 expression by NRF-1 is mediated by MEF2A

4.1. Introduction

As mentioned in Section 1.1, overexpression of NRF-1 in transgenic mice induce significant increases in MEF2A and GLUT4 proteins, and enhanced glucose transport capacity in muscle (10) (Baar et al., 2003). The aim of our first study was to investigate the mechanisms involved in the increase in GLUT4 protein in response to NRF-1 overexpression. We hypothesized that NRF-1 overexpression stimulates MEF2A expression, which in turn induces GLUT4 up-regulation. Our hypothesis was derived from the following observations: a) NRF-1 *cis*-element is absent in the *glut4* gene but present in the *mef2a* gene (10; 185) b) overexpression of NRF-1 increases MEF2A protein content (10) c) *glut4* gene is regulated by MEF2 transcription factors (223), and d) overexpression of MEF2A in myotubes increases GLUT4 expression (197).

The study was performed using the NRF-1 overexpressing C2C12-Tet-On-NRF-1 cell line which was developed as described in Section 3.4. The first set of experiments was conducted to verify that the transgenic myotubes that we engineered effectively overexpressed NRF-1 in the presence of Dox. Following this verification, we measured the contents of GLUT4 and MEF2A proteins to ascertain that they were increased as expected (10). Having determined that our cell culture system effectively increased GLUT4 and MEF2A proteins in response to NRF-1 overexpression, we performed experiments to determine: a) if the increase in MEF2A was necessary for GLUT4 up-regulation using MEF2A-siRNA and b) the amount of NRF-1 that was bound to the

mef2a promoter and MEF2A bound to the *glut4* promoter. A description of the experimental methods and our findings are presented and discussed below.

4.2. Methodology

4.2.1. Treatment of myotubes: The C2C12-Tet-On-NRF-1 clones that had high NRF-1 protein expression in response to Dox and low background (without Dox) were verified by western blot as described in section 3.7.3. Myoblasts were incubated in medium containing 2 % horse serum for a period of up to 13 days to form myotubes. To overexpress NRF-1 protein in these myotubes, they were incubated in medium containing 1 μg/ml Dox for 6 or 72 h. Myotubes that were incubated with an equal volume of vehicle, and wild type C2C12 myotubes, served as controls. After 72 h treatments (Dox or vehicle), cells were washed and incubated in Dox-free medium for 0, 6 or 18 h, homogenized and the total protein content was measured using the Bradford assay. The protocols used for protein extraction and assay were presented in detail in sections 3.7.1-3. For binding assays, C2C12-Tet-On-NRF-1 myotubes we incubated with Dox or vehicle for 6 h, washed with PBS, incubated in medium for 6-8 h and fixed in 1 % formaldehyde for 10 min.

4.2.2. Assessment of NRF-1 overexpression: One hundred μg of protein homogenate from the crude extracts was loaded onto a 7.5 % SDS-polyacrylamide gel and the component proteins separated by electrophoresis at 100 mV for 1-2 h. Subsequently, proteins from the gel were transferred onto a PDVF membrane in a BioRad transfer unit at 150 mA for 3 h at 4 ^{o}C and the membrane was blocked in 5 % fat-free milk or BSA overnight. The contents of NRF-1 and α-tubulin (used as a control) were then measured by western blot as described before (Section 3.7.3). Briefly, the membrane was incubated overnight at 4 °C (with rotation) in PBS-T containing a 1:2000 dilution of anti-NRF-1 antibody (Abcam) in PBST and 1 % fat-free milk or BSA, washed in PBST and again

incubated in a solution containing a 1:10000 dilution of anti-rabbit secondary antibody (Dako) in PBST for 2 h at room temperature (see table 3.2). The signal was detected using enhanced chemiluminescence (ECL, Amersham) and the relative abundance of NRF-1 protein from the blot quantified using densitometry, as described in section 3.7.3. The NRF-1 signal was normalized to α-tubulin signal for comparison.

4.2.3. Measurement of MEF2A, GLUT4 and δALAS contents: After establishing that C2C12-Tet-On-NRF-1 myotubes overexpress NRF-1 in response to Dox treatment, we then measured the contents of MEF2A, GLUT4 and δALAS proteins in Dox-treated myotubes and compared them to the contents in vehicle-treated and wild-type C2C12 myotubes using western blot. The western blot protocol used was described in section 4.2.2, except for the following modifications: For assessment of GLUT4, MEF2A and δALAS contents, 20 μg of total protein was used in the SDS-PAGE. Anti-GLUT4 (diluted 1:2000, Cell signalling), anti-MEF2A (1:2000 dilution, Cell signalling), and anti-δALAS (1:500, Santa Cruz) specific antibodies in TBST containing 5 % BSA (Sigma) were used. After washing the membrane with TBST, it was incubated in a solution containing anti-rabbit (Dako, Carpinteria, CA) or anti-goat HRP-linked secondary antibody (1:10000 dilution, Dako, Capinteria, CA) for 2 h at room temperature. After incubation in ECL (Amersham) reagent for 3-5 min, membranes were autographed using Kodak film and the magnitude of the signals quantified using densitometry as described in section 3.7.3.

4.2.4. Silencing of MEF2A expression: To test whether MEF2A was responsible for the increase in GLUT4 expression in Dox-treated C2C12-Tet-On-NRF-1 myotubes, we transfected the myotubes (in 6 well plates) with 60 pmol MEF2A-siRNA (sc-35895; Santa Cruz) or control-siRNA (sc-37007; Santa Cruz) for 60 h using Lipofectamine as described previously in section 3.5.2. The concentration of MEF2A-siRNA and Control-siRNA (Santa Cruz) that we used was based on the

results of pilot experiments described in section 3.5.3. Myotubes were treated with 1 μg/ml Dox 12 h prior the transfection and cultured for further 60 h in the presence MEF2A-siRNA or Control-siRNA (Santa Cruz). C2C12-Tet-On-NRF-1 myotubes that were not incubated with Dox or transfected with either MEF2A-siRNA or control-siRNA (Santa Cruz) served as further controls.

4.2.5. ChIP assays: The relative amounts of NRF-1 that bound to *mef2a* and *δalas* promoters in Dox- and vehicle-treated C2C12-Tet-On-NRF-1 myotubes were assessed using ChIP assay. The assay protocol is described in detail in section 3.9.3. Briefly, the formaldehyde-fixed myotubes (described in section 4.2.1) were sonicated to fragment the chromatin to 300-1000 bp and the chromatin fragments immunoprecipitated using anti-NRF-1 (Abcam) or anti-MEF2A (Cell Signalling) antibodies. IgG (Cell signalling), which does not recognize NRF-1 and MEF2A proteins, was used as a control antibody. Co-immunoprecipitated DNA was PCR amplified using primers that recognize the NRF-1 sites on the *mef2a* and *δalas* genes or MEF2 site on the *glut4* gene. Control primers that targeted regions which do not contain the NRF-1 binding site on the *mef2a* and *δalas* genes, or MEF2 site on the *glut4* gene were also used as controls. Criteria for primer selection were described in detail in section 3.9.1 and primer sequences are shown in table 3.3. PCR products were electrophoresed on 2 % agarose gel and the signals quantified by densitometry. Signal from the immunoprecipitated chromatin (IP) was normalised to its corresponding input signal (IN) i.e. signal from chromatin that did not undergo immunoprecipitation.

4.3. Results & Discussion

4.3.1. Verification of NRF-1 overexpression in C2C12-Tet-On-NRF-1 myotubes*:* We began by verifying that C2C12-Tet-On-NRF-1 myotubes effectively overexpressed NRF-1 protein in the presence of Dox. Figures 4.1A and 4.1B indicate that, unlike wild-type C2C12 myotubes which were non-responsive to Dox treatment, C2C12-Tet-On-NRF-1 myotubes expressed ~ 6-fold higher NRF-1

when treated with 1 µg/ml Dox for 72 h relative to vehicle-treated controls. This result confirms that the double-stable C2C12-Tet-On-NRF-1 myotubes that we used caused high induction of NRF-1 with Dox treatment with low background (without Dox). Clones that were not responsive to Dox, and those with high NRF-1 levels in the absence of Dox (high background), were not used in the experiments. High induction of NRF-1 in the absence of Dox may occur if the two transfected plasmids become co-integrated into the chromosome (15; 74) whereas non-responsiveness to Dox may occur in clones that failed to incorporate the pTRE2Hyg-NRF-1 (the second plasmid) in their genome after transfection (15; 236). Because Dox treatment caused overexpression of NRF-1 in transgenic but not wild-type C2C12 myotubes, it may be concluded that Dox increases NRF-1 expression via the transfected plasmids and not via endogenous *nrf-1* gene. Unlike NRF-1, the content of α-tubulin was not altered by Dox treatment in both C2C12-Tet-On-NRF-1 and C2C12 myotubes; indicating that Dox treatment does not increase protein expression globally.

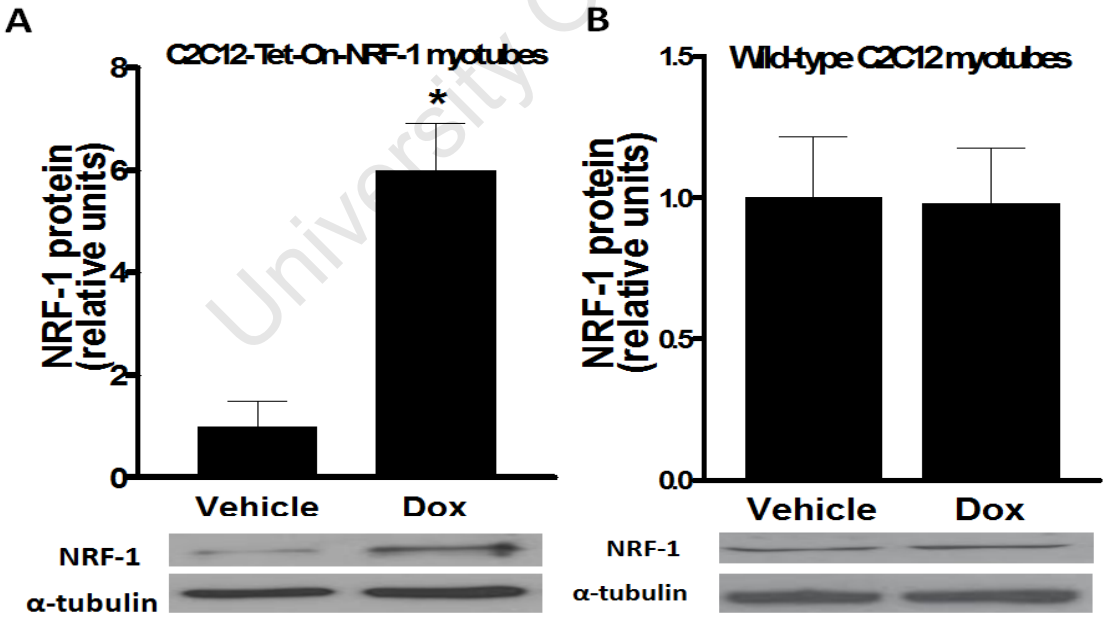

Figure 4.1: NRF-1 expression in C2C12-Tet-On-NRF-1 and wild-type C2C12 myotubes in response to Dox treatment. Western blot for NRF-1 protein from double stable C2C12-Tet-On-NRF-1 **(A)** or wild-type C2C12 **(B)** myotubes harvested 18 h after 72 h treatment with 1 µg/ml Dox or vehicle. Representative blots for NRF-1 (~68 kDa) and α-tubulin (~51 kDa) are shown below the graphs. n = 4, * P = 0.004 vs vehicle. Data presented as means ± SD.

4.3.2. Overexpression of NRF-1 increases the expression of MEF2A, GLUT4 and δALAS proteins:

The contents of MEF2A, GLUT4, δALAS and α-tubulin in C2C12-Tet-On-NRF-1 myotubes that were treated with 1 μg/ml Dox or equal volume of vehicle for 72 h were measured by western blot 18 h post treatment. Wild-type C2C12 myotubes that were similarly treated with Dox or vehicle served as further controls. The contents of MEF2A, GLUT4 and δALAS but not α-tubulin were ~4-fold higher in Dox-treated C2C12-Tet-On myotubes compared to vehicle-treated controls (Fig 4.2A). Similar increases in these proteins have previously been reported in NRF-1 transgenic mice (10). The increase in δALAS protein, which we used here as an index for mitochondrial biogenesis (135), validates our research model since overexpression of NRF-1 in an animal model (10) increased the expression of δALAS as it does in our cell culture system. Because no significant increase in MEF2A, GLUT4 or δALAS was observed in wild-type C2C12 myotubes in response to Dox treatment (Fig 4.2B), it is logical to conclude that the increases in these proteins in C2C12-Tet-On-NRF-1 myotubes resulted from NRF-1 overexpression. It is not surprising that NRF-1 overexpression would increase the expression of MEF2A and δALAS but not α-tubulin because functional NRF-1 *cis*-elements are present on *mef2a* and *δalas* promoters (135; 185) but absent on the *α-tubulin* promoter (NCBI database DNA sequence search).

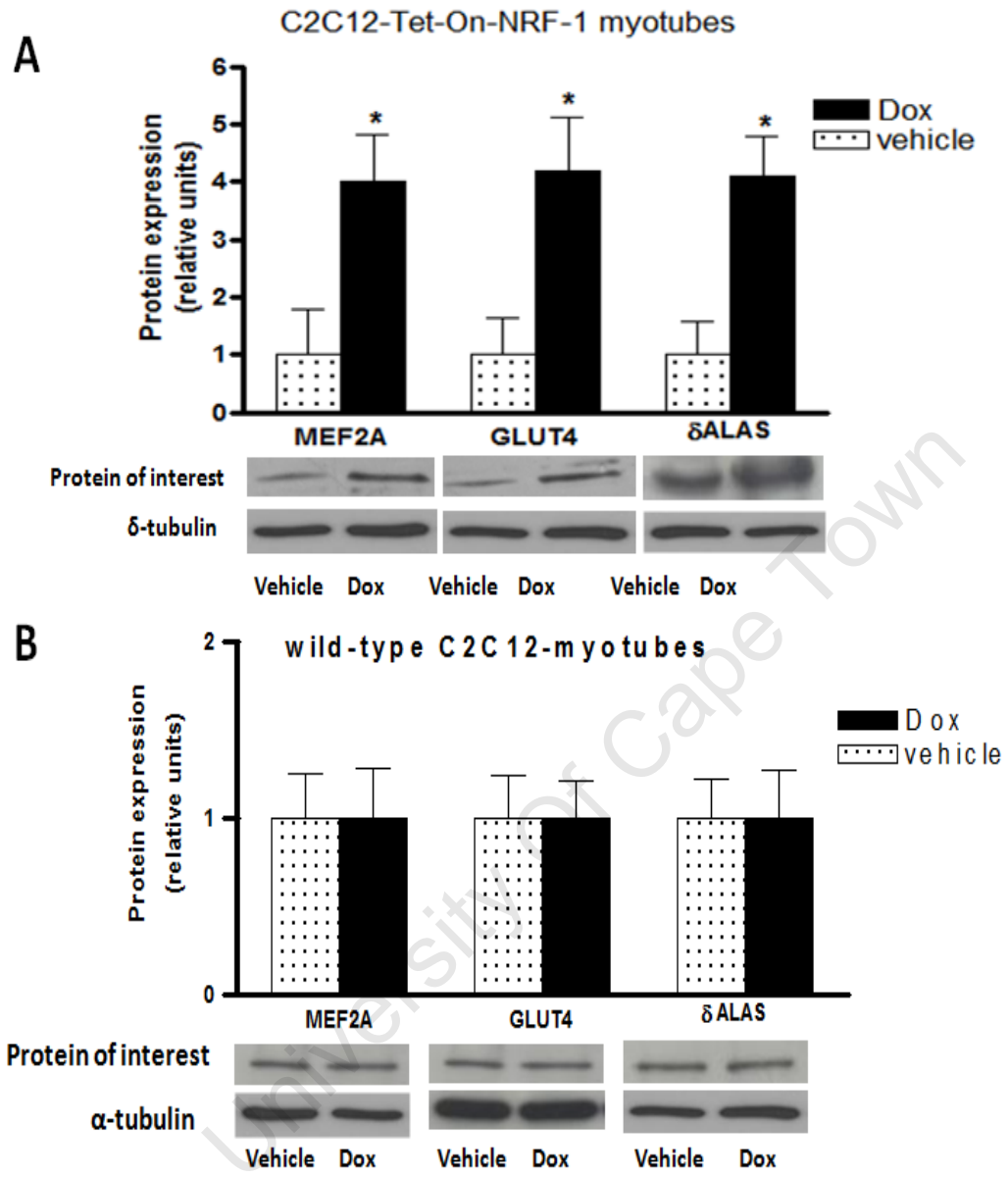

Figure 4.2: MEF2A, GLUT4 & δALAS expression in C2C12-Tet-On-NRF-1 and wild type C2C12 myotubes in response to Dox treatment. Western blot was performed to assay MEF2A, GLUT4 & δALAS protein levels from double stable C2C12-Tet-On-NRF-1 (A) or wild-type C2C12 (B) myotubes when incubated with 1 µg/ml Dox or vehicle for 72 h. Representative blots for MEF2A (~54 kDa) * P = 0.007 vs vehicle, GLUT4 (~45 kDa) P =0.002 vs vehicle & δALAS (~67 kDa) * P = 0.004 vs vehicle and α-tubulin (~51 kDa) are shown below the graphs. n = 4, * P < 0.05. Data presented as means ± SD.

4.3.3. Timeline of the increases in NRF-1, MEF2A and GLUT4*:* Although GLUT4 up-regulation in response to NRF-1 overexpression has been observed before (10), the mechanism responsible remains unclear. In this experiment, we hypothesised that it occurs because of the increase in MEF2A content since numerous studies (94; 162; 223) have shown that MEF2A activates GLUT4 expression when it binds to its domain on the *glut4* promoter. For our hypothesis to be true, the increase in NRF-1 ought to preceed the increase MEF2A which in turn should preceed the increase in GLUT4. To check if the increases in NRF-1, MEF2A and GLUT4 followed this predicted timeline, we cultured C2C12-Tet-On-NRF-1 myotubes for 6 h in Dox and measured the contents of NRF-1, MEF2A and GLUT4 at 0, 6, and 18 h post treatment. Figure 4.3 B shows that, in Dox-treated myotubes, NRF-1 tended to be higher at 0 h ($p=0.052$), was significantly higher at 6 h and remained elevated for up to 18 h, compared to vehicle-treated controls. MEF2A was increased at 6 h and 18 h (Fig 4.3 B) but not at 0 h post Dox, whereas GLUT4 was only significantly increased after 18 h (Fig 4.3 B). The timeline of the increases in NRF-1, MEF2A and GLUT4 is consistant with our hypothesis, and provides preliminary evidence that the increase in GLUT4 expression in NRF-1 overexpressing cells occurs via cascade of events involving NRF-1→MEF2A→GLUT4 expression.

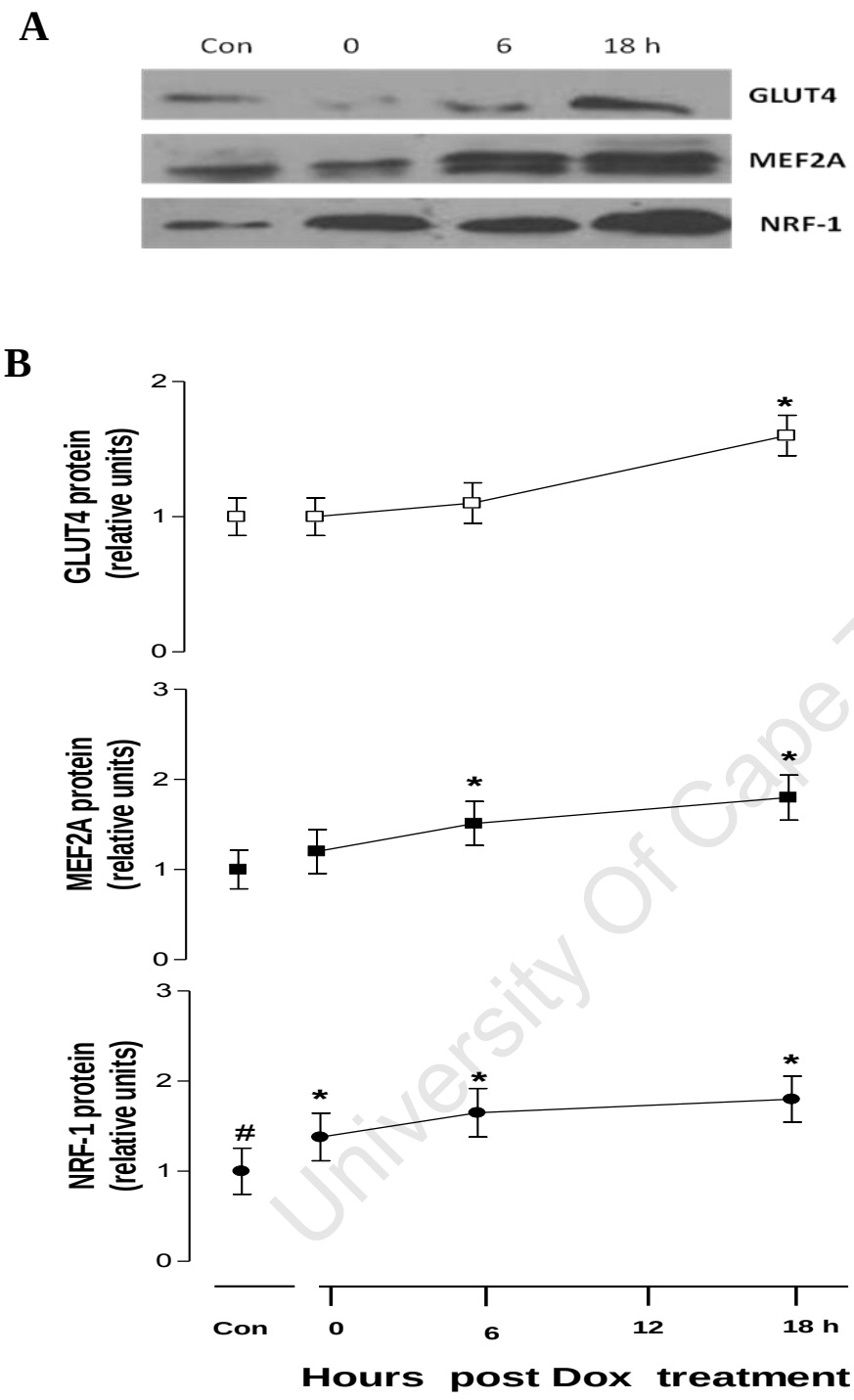

Figure 4.3: Contents of NRF-1, MEF2A and GLUT4 proteins in C2C12-Tet-On-NRF-1 myotubes after 6 h Dox treatment. A: Western blots were performed to assay NRF-1 (68 kDa), MEF2A (54 kDa) and GLUT4 (45 kDa) protein levels from double stable C2C12-Tet-On-NRF-1 myotubes at 0 h, 6 h and 18 h after 6 h treatment with with 1 μg/ml Dox or vehicle. **B:** Graphic representation of NRF-1, MEF2A, and GLUT4 proteins at various time points. n = 4, * $P < 0.05$; # $P = 0.052$. Data presented as means ± SD.

4.3.4. MEF2A is necessary for the increase in GLUT4 protein in response to NRF-1 overexpression

overexpression. To test if the increase in MEF2A content was responsible for GLUT4 up-regulation in Dox-treated C2C12-Tet-NRF-1 myotubes, we transfected the myotubes with either the MEF2A-siRNA or control-siRNA, incubated the transfected myotubes in medium containing 1 μg/ml Dox for 60 h, and performed western blots for MEF2A, GLUT4 and α-tubulin. Figure 4.4A shows that MEF2A expression was silenced by MEF2A-siRNA (treatments B vs. C) but not by control-siRNA (treatments B vs. D) in Dox-treated cells; indicating that transfection of MEF2A-siRNA specifically, and not transfection of siRNA per se, was the cause of MEF2A downregulation. Alpha-tubulin was not affected by control-siRNA or MEF2A-siRNA; indicating that MEF2A siRNA selectively silenced MEF2A expression.

Changes in GLUT4 expression in C2C12-Tet-On-NRF-1 myotubes followed the same pattern as changes in MEF2A expression: i.e. Dox-treatment increased GLUT4 significantly and the increase was blocked by MEF2A-siRNA and not by control-siRNA (Fig 4.4B). This data provides the first strong evidence that the increase in GLUT4 expression that occurs in response to NRF-1 overexpression requires a parallel increase in MEF2A expression. This result is not surprising because MEF2A is one of the major regulators of GLUT4 expression (162; 223).

There are four isoforms of MEF2 transcription factors, namely MEF2A, MEF2B, MEF2C and MEF2D (18; 145) which dimerize in order to bind to a well conserved consensus sequence on genes. It has been reported that the MEF2A/D heterodimer and the MEF2A/A homodimer regulate the *glut4* gene (124; 157; 162). It is therefore not surprising that when the MEF2A isoforms is silenced, as we did in our experiments, GLUT4 expression would be compromised because neither the MEF2A/D nor the MEF2A/A would be available. In conclusion, the results of our experiment show that MEF2A is necessary for the increase in GLUT4 protein in response to NRF-1 overexpression.

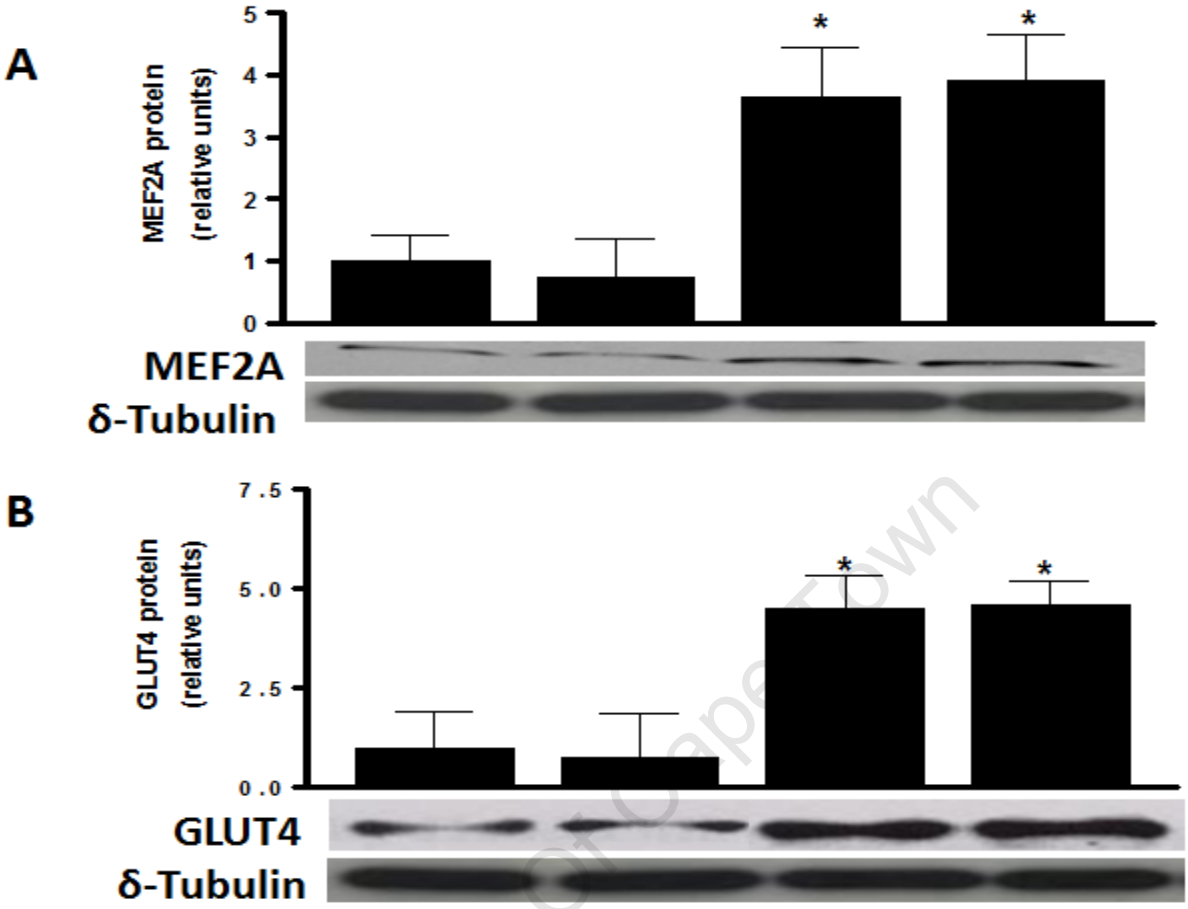

Treatment	A	B	C	D
DOX	-	+	+	+
MEF2A-siRNA	-	+	-	-
Control-siRNA	-	-	-	+

Figure 4.4: Silencing of MEF2A expression blocks the increase in GLUT4 content in NRF-1 overexpressing cells. C2C12-Tet-On myotubes that were transfected with MEF2A-siRNA or control siRNA were cultured in medium containing Dox (+) or vehicle (-) for 60 h. **A**: MEF2A protein (54 kDa) is increased by Dox treatment but significantly decreased by MEF2A-siRNA. **B**: GLUT4 protein (45 kDa) is also increased by Dox treatment and decreased by MEF2A-siRNA. Control siRNA did not decrease MEF2A expression (as expected) and had no effect on GLUT4 expression. Representative western blot for MEF2A (54 kDa) *P = 0.002 vs MEF2-siRNA & * P = 0.005 vs control siRNA, GLUT4 (45 kDa) *P = 0.009 vs MEF2-siRNA & * P = 0.001 vs control siRNA and α-tubulin (51 kDa) are shown below the graphs. n = 4, * $P < 0.05$. Data is presented as means ± SD.

4.3.5. Dox increases the binding of NRF-1 and MEF2A to mef2a and glut4 promoters, respectively. To explain the increases in MEF2A and GLUT4 expression in Dox-treated C2C12-Tet-NRF-1 myotubes, we measured the contents of NRF-1 and MEF2A that were bound to *mef2a* and and *glut4* promoters, respectively. Myotubes were treated for 6 h with 1 μg/ml Dox and ChIP assays performed 6 h or 8 h later. Specificity of the the ChIP assay was verified as previously described in Chapter 3, Section 3.9.3.1: i.e. a) there was no evidence of NRF-1 binding at the *mef2a* coding region in position +2904 - +3154 which has no NRF-1 binding element (Figure 3.12), and b) only the anti-NRF-1, but not IgG, was able to co-immunoprecipitate the MEF2A binding domain (Fig 3.12 lanes 2 and 3, respectively). Validity of the assay was verified when we showed that there was nearly ~2.8-fold more *δalas*-bound NRF-1 in Dox-treated myotubes compared to vehicle-treated controls (Figure 4.5A) because the result is consistent with previous finding by Li et al. (135) who showed, by EMSA, that NRF-1 overexpression in mice increased NRF-1 binding to the *δalas* gene. Figure 4.5A indicates that there was ~2.8-fold increase in *mef2a*-bound NRF-1 due to Dox compared to controls. This result is not surprising since NRF-1 content was also increased at this time point (6 h). It is well documented that binding of a transcription factor to DNA is influenced by its abundance (75; 112). Figure 4.5C shows that *glut4*-bound MEF2A was also increased ~2.7-fold at the 8 h time point. Again this result is not surprising since MEF2A was already elevated at this time point (Figure 4.3B). GLUT4 content was increased at 18 h but not at 6 h (Figure 4.3 C); indicating that MEF2A binding to the gene preceed transcription and translation of the *glut4* gene as expected. We suspect that the dramatic reduction in GLUT4 expression that occurred when MEF2A expression was silenced (Fig 4.4A & B) was a result of a reduction in the level of *glut4*-bound MEF2A. Collectively these results indicate that the increases in GLUT4 that occur when NRF-1 is overexpressed are mediated by increased binding of NRF-1 to the *mef2a* gene and MEF2A to the *glut4* gene resulting from increased

abundance of NRF-1 and MEF2A in cells. Thes results are consistent with the general observation that an increase in the total content of a transcription factor in cells often reflects a rise in nuclear content as well, and is often accompanied by enhanced binding to appropriate DNApromoter sequences (94; 162; 223) to promote transcriptional activity. For example, a study by Holmes et al. (94) showed that when the total content of MEF2A protein was increased in rat muscle as a result of AICAR injection, a significant increase in nuclear MEF2A content also occurred and this ultimately resulted in ~2-fold increase in MEF2A binding to the *glut4* promoter.

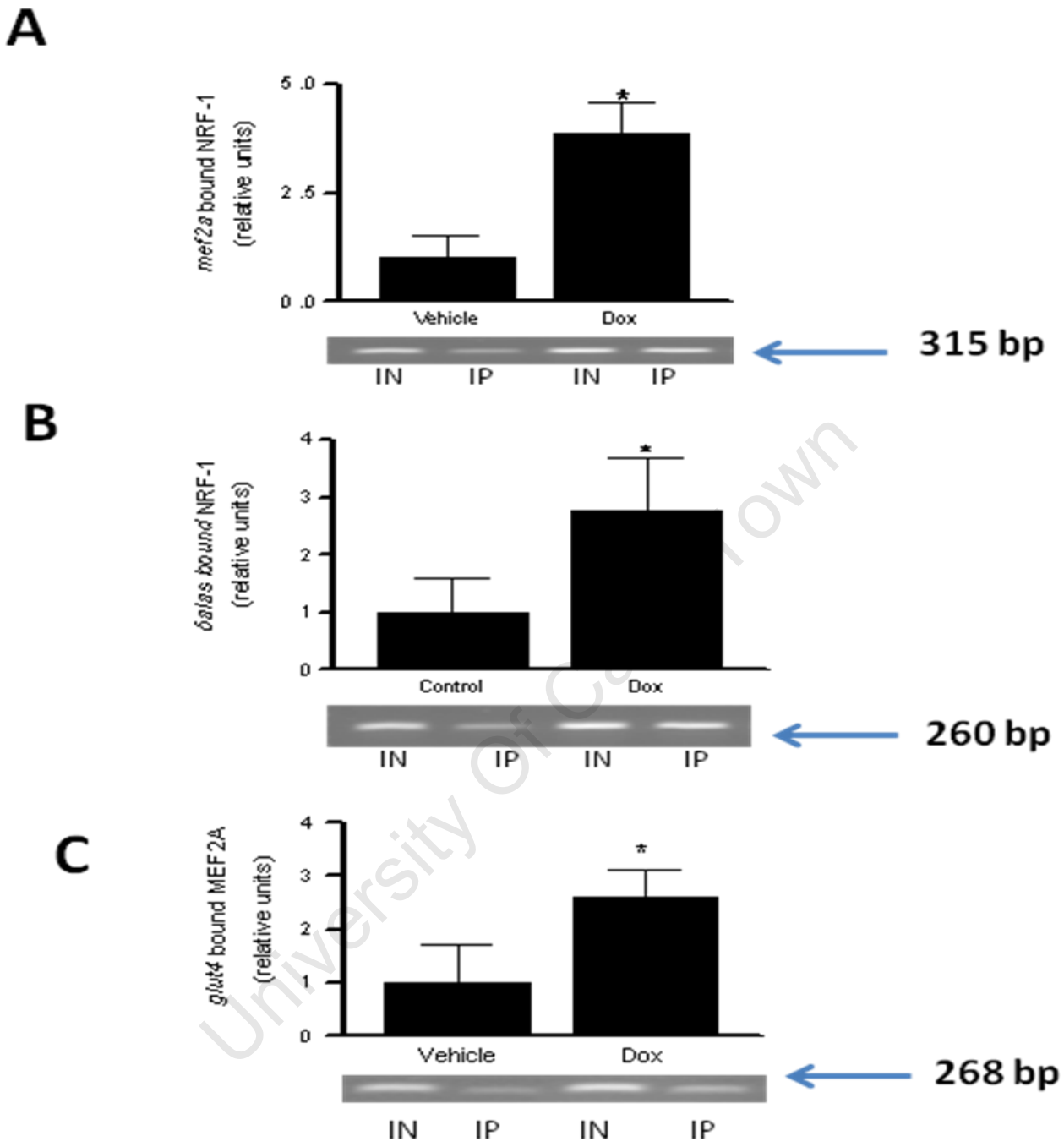

Figure 4.5: Overexpression of NRF-1 increases NRF-1 binding to the *mef2a* and *δalas* promoters. ChIP assays were used to assess *mef2a*-bound NRF-1*P = 0.01 vs vehicle (A), *δalas*-bound NRF-1 * P = 0.009 vs control (B) and *glut4*-bound MEF2A * P = 0.02 vs vehicle (C) in C2C12-Tet-ON-NRF-1 myotubes that were incubated in medium containing 1 µg/ml Dox or vehicle for 6 h, using appropriate antobodies. Co-immunoprecipitated promoter sections and DNA from an equal volume of input (non-immunoprecipitated) sample were PCR amplified using appropriate primers (section 3.9.3) and electrophoresed using 2% agarose gel. The graphs show the amplified co-immunoprecipitated promoter sections (IP) normalized to corresponding input (IN) signals. Representative PCR gels are shown below the graphs. n = 4, * P < 0.05. Data presented as means ± SD.

4.4. Summary and concluding remarks

Results from this study provide preliminary support for the hypothesis that overexpression of NRF-1 increases GLUT4 content through a cascade of events involving NRF-1→ *mef2a*→ MEF2A → *glut4* → GLUT4 in C2C12-Tet-On-NRF-1 myotubes. Suport for the cascade was provided by: a) the temporal relationships between the expression of NRF-1, MEF2A and GLUT4; b) abolishion of GLUT4 expression in NRF-1 overexpressing C2C12 myotubes when MEF2A was silenced, and c) increases in *mef2a*-bound NRF-1 and *glut4*-bound MEF2A with NRF-1 overexpression. However, more confirmatory pieces of evidence for the hypothesis are still needed: Firstly, the timelines of MEF2A and GLUT4 mRNA levels should be determined to indicate whether or not the observed increases in binding cause increased transcriptional activity. Secondly, *mef2a*-bound NRF-1 and *glut4*-bound MEF2A should be assessed at more time points after treatment, especially between 0-6 h after treatment, to indicate whether on not these events occur sequencially as predicted by the hypothesis. We were unable to perform these experiments because of financial constraints.

As mentioned in the text, we used an anti-MEF2A antibody which was raised against amino acids 1-300 of MEF2A (Santa Cruz Biotechnology) in most of our ChIP assays for *glut4*-bound MEF2A. Although this antibody reacts strongly with MEF2A, it also crossreacts to a lesser extent with the MEF2D and MEF2C isoforms, which are also expressed in skeletal muscle (162). The crossreactivity of this antibody to these MEF2 isoforms could have confounded some of our ChIP assay results. However, results using an anti-MEF2A antibody from Cell signalling (Cat no: 9736), which is reported not to crossreact with MEF2D or MEF2C were not different from those obtained using the Santa Cruz antibody; indicating that our ChIP assay results are still valid.

In conclusion, not withstanding the preliminary nature of some of our data, our results confirm that NRF-1 regulates GLUT4 expression and suggests that interventions that increase its

expression or its interaction with the *mef2a* gene could be useful in the treatment and management of type II diabetes.

CHAPTER 5

Study two:

Increased binding of NRF-1 to the *mef2a* promoter requires CaMK II activation in C2C12 myocytes

5.1. Introduction

In the previous chapter we showed that overexpression of NRF-1 in cultured muscle cells (C2C12 myotubes) enhanced the binding of NRF-1 to the *mef2a* gene and increased MEF2A protein content. Similar increases in MEF2A content have previously been reported in L6 myotubes that were treated with caffeine (173). In those studies, caffeine was used to activate CaMK II since it increases cytosolic calcium levels (172; 173). Inclusion of KN93 (an inhibitor of CaMK II) in the medium together with caffeine blocked the increase in MEF2A. This observation led the authors to conclude that the caffeine-induced increase in MEF2A was dependent on CaMK II activation. Although the mechanism by which CaMK II regulates MEF2A expression has not been well defined, there is some evidence to support the notion that it affects the binding of transcription factors, such as NRF-1, to their elements on genes. For example, Ojuka et al., (172; 173) showed that treatment of myotubes with caffeine increased NRF-1 binding to a *δalas* promoter sequence in a CaMK II - dependent manner. Marechal et al. (152) also demonstrated that DNA binding activity of hGT-1 to BoxII on *rbcS* (Ribulose-1, 5-bisphosphate carboxylase) promoter is increased ~10-20 -fold in the presence of purified activated CaMK II when measured by electrophoretic DNA mobility shift assay. Addition of KN93 blocked the increase in hGT-1 binding to Box II region. Similarly, CaMK II activation also increased AP-1 binding to *c-fos* promoter (240). In light of these observations, and because NRF-1 regulates MEF2A expression (10), we hypothesized that CaMK II activation by caffeine might increase MEF2A expression via increased NRF-1 binding to the *mef2a* gene.

Binding of transcription factors to DNA depends on the compactness of chromatin at the binding site, which depends on the interplay between the activities of HDACs and HATs (76; 143). HDACs remove acetyl moieties from lysine residues on histone tails in chromatin and cause chromatin to become more compact (3; 217), whereas HATs acetylate the same residues and relaxes chromatin. A number of studies have shown that activation of CaMK II in fibroblasts (10T1/2) and *Cos* cells (monkey kidney cells) cause phosphorylation and nuclear export of HDAC4/5 (136; 143; 158). Reduced nuclear content of HDACs increases nuclear HAT activity which remodels chromatin to favour increased accessibility of transcription factors to their respective binding domains on DNA. Whether CaMK II activation by caffeine promotes NRF-1 binding to the *mef2a* gene via a similar mechanism is currently not known. The purpose of the present study was therefore to test the hypotheses that CaMK II activation by caffeine: a) causes hyperacetylation of histones in the neighbourhood of the NRF-1 binding site on the *mef2a* gene, b) increases *mef2a*-bound NRF-1, and c) increases MEF2A transcription.

5.2. Methodology

5.2.1. Treatment of myotubes: C2C12 myotubes, which were allowed to differentiate in medium containing 2 % horse serum for 9-13 days, were treated with 10 mM caffeine for 2 h and harvested at 0, 3, 6, 9, 12 or 18 h post treatment. The level of phosphorylated CaMKII (pCaMK II) and total CaMK II were assayed by western blot. For ChIP and qRT-PCR analysis, myotubes were treated with 10 mM caffeine or 10 mM caffeine + 25 μM KN93, for 2 h and harvested 6 h later. For MEF2A protein assessment, myotubes were treated with 10 mM caffeine or 10 mM caffeine + 25 μM KN93 for 2 h per day for 4 days. Untreated cells served as controls in all cases.

5.2.2. Western Blot. After the treatments, myotubes were washed 2x with PBS, scraped loose form the culture plate in 300 μl RIPA buffer (56 mM Tris-HCl pH 7.4, 150 mM NaCl, 1 mM EDTA,

0.1 % SDS, 1 % Triton-X100, 10 mM $Na_4P_2O_4$, 20 mM NaF, 0.15 μM okadaic acid, 4 mM Na_3VO_4, 1 x complete protease inhibitors) and homogenized using a dounce homogenizer. The contents of pCaMK II, CaMKII, MEF2A and α-tubulin in the crude extracts were measured by western blot as described previously in Section 3.7.3.

***5.2.3. ChIP assay*:** ChIP assay was used to measure the amount of NRF-1 that was bound to its *cis* element on the *mef2a* gene and the extent of acetylation of histone H3 in the neighbourhood of this domain. Briefly, myotubes were fixed with formaldehyde, sonicated to fragments of 300-1000 DNA bp and the chromatin fragments immunoprecipitated using anti-NRF-1 (Abcam), anti-acetyl histone H3 or anti-histone H3 antibodies (Cell signalling). IgG (Cell signalling) was used as a negative control antibody in all cases. Co-immunoprecipitated DNA was PCR amplified using primers that recognize the NRF-1 sites on the *mef2a* gene. Control primers that targeted regions which do not contain the NRF-1 binding site on the *mef2a* gene, were also used as negative controls. PCR products were electrophoresed on 2 % agarose gels and the sizes of resulting bands quantified by densitometry. Signals from immunoprecipitated chromatin (IP) were normalised to corresponding input (chromatin that did not undergo immunoprecipitation) signal (IN). The assay protocol is described in detail in Section 3.9.1-3

***5.2.4. Quantitative RT-PCR*.** After treatments, total RNA from harvested myotubes was extracted using 1 ml Trizol as described in Section 3.10.2. One μg of RNA was mixed with 0.5 μg of 22-mer oligo-dT primer and incubated at 70 ^{o}C for 5 min to denature RNA secondary structures. Genomic DNA was eliminated from the samples by digestion with 1 U DNAse-1 (Promega) for 90 min at 37 ^{o}C and DNAse-1 was subsequently deactivated by incubation at 75 ^{o}C for 5 min. cDNA was synthesized using 200 U of M-MLV reverse transcriptase (Promega) for 1 h at 42 ^{o}C. Quantitative real time PCR (qRT-PCR), using 1 μl cDNA, was performed to measure MEF2A

mRNA by a Light Cycler PCR machine (Roche) using SYBR Green PCR reagents (Roche) and primers which amplify a 187 bp region of the mouse *mef2a* gene (see table 3.5). The concentration of MEF2A mRNA relative to GAPDH or Ribosome S12 (internal controls) were calculated using the method described by Livak & Schmittgen (140) and mean values of the triplicate samples were normalized to the mRNA level of a control untreated sample (see Section 3.10.2.)

5.3. Results

5.3.1. Caffeine activates CaMK II in C2C12 myotubes. It is widely accepted that CaMK II activation is achieved via phosphorylation (34; 82; 131; 141). To verify that caffeine activated CaMK II in C2C12 myotubes, we measured the level of phosphorylation of CaMK II at Thr286 (pCaMK II) at 0, 3, 6, 9, 12 and 18 h after 2 h treatment with 10 mM caffeine. Total CaMK II was also measured at these time points for comparison (Fig 5.1B). Figures 5.1A and B, showing the graph and western blot of pCaMK II for these time points, indicates that immediately after caffeine treatment (0 h) pCaMK II level was ~3.5-fold higher than control values and declined progressively thereafter. Total CaMK II content remained constant at all time points. These results indicate that 10 mM caffeine activated CaMK II in the myotubes.

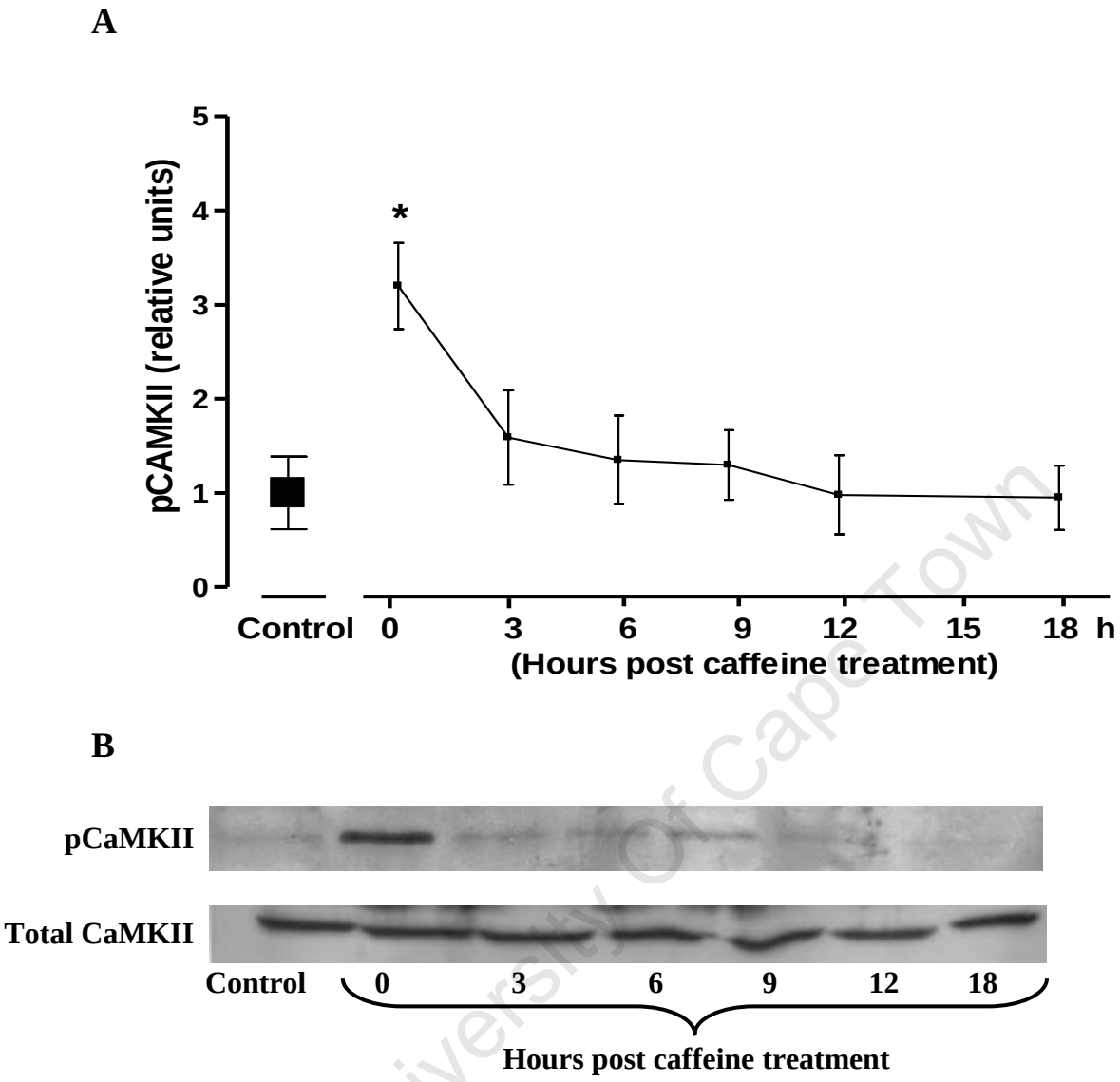

Figure 5.1: Phosphorylation of CaMK II in C2C12 myotubes after treatment with caffeine. **A**: Quantitative analysis of pCaMK II relative to total CaMK II from myotubes that were treated for 2 h with caffeine and analysed at time points 0-18 h post treatment. Signals were nomalized to control (without caffeine treatment). * P = 0.001 vs control. **B**: Western blot of the contents of pCaMK II and total CaMK II levels before and after caffeine treatment (0-18 h). pCaMK II signal was normalized to total CaMK II. N=3. *P<0.05. Data presented as means ± SD.

5.3.2. CaMK II activation increases NRF-1 binding to the mef2a promoter in C2C12 myotubes.

Although previous studies have shown that activation of CaMK II by caffeine increases

MEF2A content in myotubes (173), the mechanism(s) involved have not been identified. Our observation, reported in the previous chapter, that increased binding of NRF-1 to the *mef2a* gene is associated with MEF2A expression, led us to suspect that CaMK II activation by caffeine might increase MEF2A expression via increased NRF-1 binding to the *mef2a* promoter. To test this hypothesis, we incubated C2C12 myotubes with caffeine in the presence or absence of KN93 for 2 h and measured the content of *mef2a* promoter-bound NRF-1 6 h post treatment using ChIP assay. The gel in Figure 5.2 shows a typical pattern of PCR products from immunoprecipitated (IP) and input (IN) samples. The ratio of signal intensities between IP and IN for each treatment was normalized to control and is depicted graphically in Figure 5.2. As shown, caffeine caused ~2.5–fold increase in the amount of NRF-1 that bound to the *mef2a* promoter; and incubation of myotubes with 25 μM KN93 abolished the effect of caffeine. These results indicate that caffeine increases NRF-1 binding to the *mef2a* promoter via a CaMK II- dependent mechanism.

The specificity of the ChIP assay was verified by the following observations: a) there was no evidence of NRF-1 binding at the *mef2a* coding region in position +2904 - +3154 which has no NRF-1 binding element as indicated in Chapter 3 (Figure 3.12), b) only the anti-NRF-1, but not IgG, was able to co-immunoprecipitate the MEF2A binding domain (Fig 3.12 lanes 2 and 3 respectively).

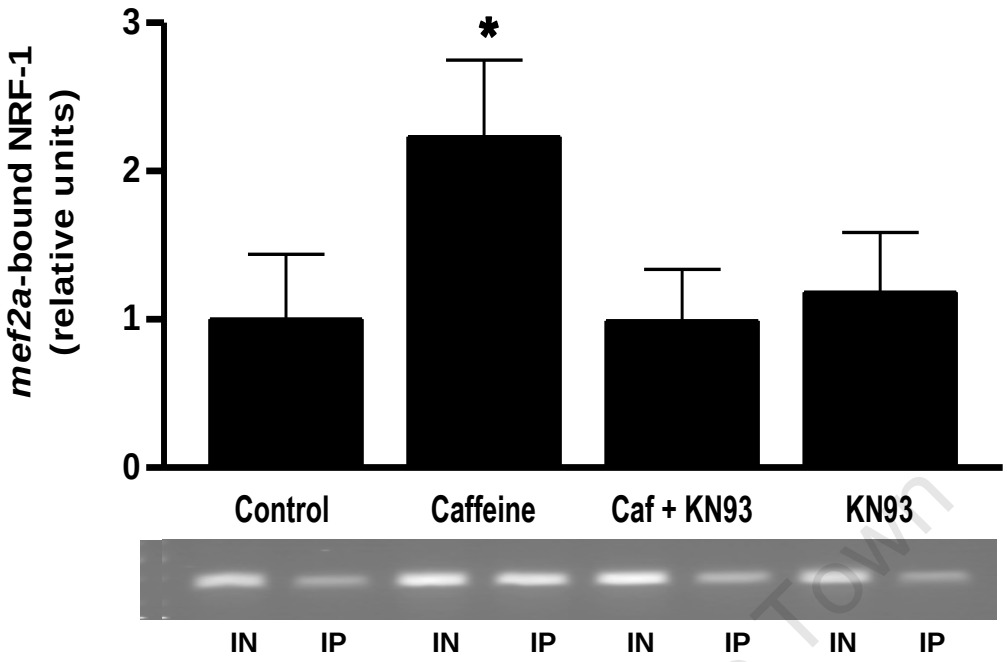

Figure 5.2: CaMK II activation increases NRF-1 binding to the *mef2a* gene in C2C12 myotubes. Myotubes were treated with 10 mM caffeine in presence or absence of KN93 for 2 h and chromatin immunoprecipitation determined 6 h post incubation PCR signals for ChIP assay to detect the levels of NRF-1 binding to the *mef2a* gene assessed from IP (immunoprecipitation) samples were normalized to IN (Input) samples as shown below the graph. The bars represent the IP/IN ratio normalized to control. * P = 0.003 vs Control, * P = 0.009 vs Caf+KN93, *P = 0.001 vs KN93. N = 4. * P<0.05. Data represented as means ± SD.

5.3.3. CaMK II activation induces hyper-acetylation of histones at the neighbourhood of the NRF-1 binding site on the mef2a promoter. It is now well established that CaMK activation induces nuclear export of HDACs in a variety of cell types (143; 158). A decrease in HDAC nuclear content has been shown to induce hyperacetylation of histones in nucleosomes because the level of acetylation of histones in nucleosomes is dependent on the balance between the activities of HATs and HDACs (13). Because binding of transcription factors to DNA *in vivo* is enhanced by hyper-acetylation of histones in close proximity to their binding domains (168), we reasoned that the increase in *mef2a*-bound NRF-1 that we observed after caffeine treatment might be associated with

hyperacetylation of histones in the neighbourhood of the NRF-1 binding site on the *mef2a* promoter region. To test this view, we measured the contents of acetyl histone H3 in the region which encompasses the NRF-1 binding site at the *mef2a* promoter by ChIP assay in C2C12 myotubes that were treated with caffeine in the presence or absence of KN93. Representative agarose gels showing PCR products from control, caffeine, and caffeine + KN93 -treated myotubes are shown in figure 5.3 A. Signals from input (IN) sample, representing the total NRF-1 site in the sample, and from immunoprecipitated (IP) samples, representing the fraction that contain acetylated H3 histones, are shown adjacent to each other (for each treatment group) to facilitate comparison. The fraction, IP NRF-1 site/Total NRF-1 site (i.e acetylated histone/histone H3), which represent the relative levels of H3 acetylation under different treatments, are graphed in figures 5.3 B & C. The data shows that caffeine treatment increased the level of acetylation of histone H3 in the vicinity of the NRF-1 site on the *mef2a* promoter compared to control, but the increase was abolished by KN93.

Because acetylation of histones remodels chromatin, it may be argued that the observed differences in signal intensities from the various treatments were due to inequalities in cross-linking efficiencies or antibody accessibility to histones. Therefore, we performed control experiments using an antibody against histone H3 (Cell signalling). As can be seen from Figure 5.3 C (histone H3), the signal intensity was similar in all treatments when this antibody was used; demonstrating that there were no differences in cross-linking efficiencies and/or antibody accessibility.

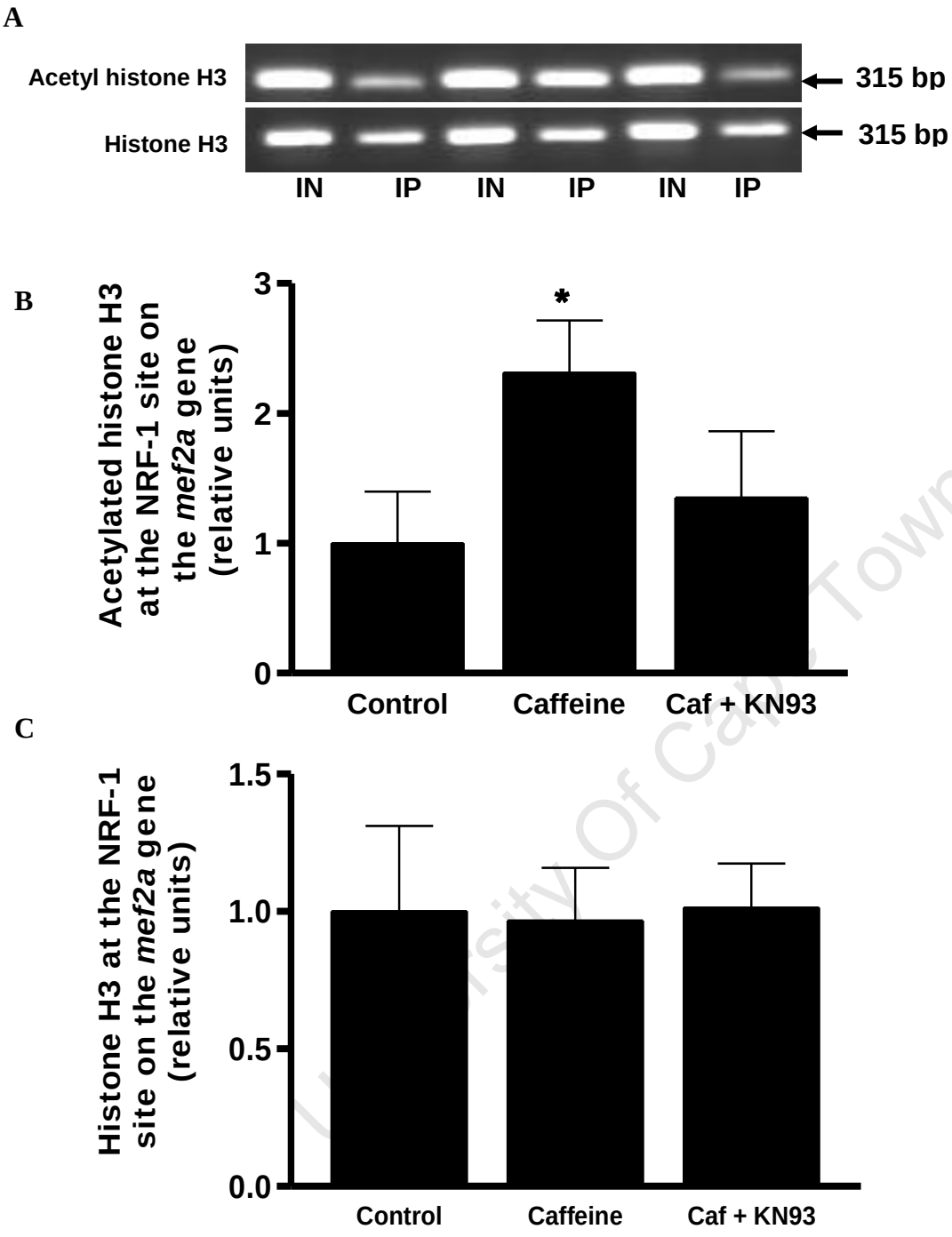

Figure 5.3: Acetylation of histone H3 in the neighbourhood of NRF-1 site on the *mef2a* gene. Caffeine induced an increase in acetylation of NRF-1 sites on the *mef2a* genes in C2C12 myotubes. Myotubes were treated with 10 mM caffeine (caf) in the presence or absence of KN93 for 2 h and chromatin immunoprecipitation determined 6 h post incubation. A: Shows gels for acetylation of histones on the neighbourhood of NRF-1 binding sites on the *mef2a* promoter with AcH3 (acetylated H3) and histone H3 control experiment. Bar graph representing acetylated histone H3 (AcH3) * P = 0.001 vs Control, * P = 0.007 vs Caf+KN93, and histone H3 are shown in B and C, respectively. N = 4. * P<0.05. Data represented as means ± SD.

5.3.4. Caffeine increases MEF2A expression in a CaMK II-dependent manner: It has previously been shown that chronic treatment of L6 myotubes with caffeine increased MEF2A content in L6 myotubes in a CaMK II-dependent manner (173). Our observation of increased binding of NRF-1 to the *mef2a* promoter in C2C12 myotubes caused us to suspect that the increased level of MEF2A that is seen after caffeine treatment results from increased transcription. We therefore measured MEF2A mRNA at 6 h post incubation by qRT-PCR. Figure 5.4A shows that MEF2A mRNA was increased ~2-fold by caffeine relative to control. Inclusion of KN93 in the medium together with caffeine prevented the increase in MEF2A mRNA; suggesting that the increase in MEF2A mRNA is also CaMK II driven. GAPDH did not change under the experimental conditions used. Consistent with previous observation in L6 myotubes, incubation of C2C12 myotubes with caffeine for 2 h per day for 4 days increased MEF2A protein ~2-fold, and inclusion of KN93 in the medium abolished the increase due to caffeine (Fig 5.4B).

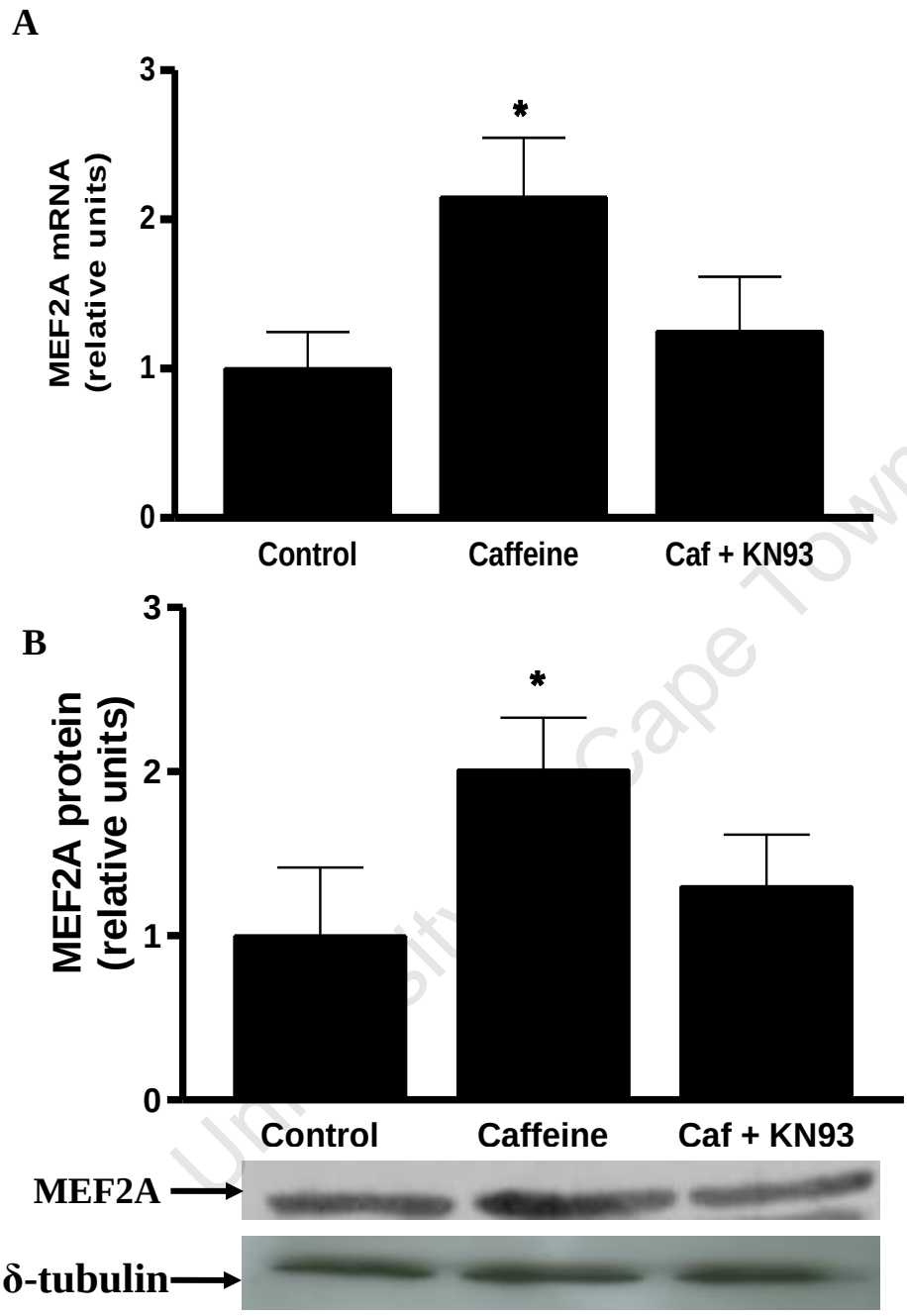

Figure 5.4: CaMK II activation increases MEF2A mRNA and protein levels in C2C12 myotubes. Myotubes were treated with 10 mM caffeine in the presence or absence of KN93 (Caf +KN93). **A**: MEF2A mRNA was measured by quantitative RT-PCR as described in experimental procedure. Well differentiated myotubes were treated for 2 h and cells harvested 6 h post treatment (* P = 0.001 vs Control & Caf+ KN93). **B**: Western blot showing MEF2A protein levels. Myotubes were treated for 2 h for 4 days with caffeine in the presence or absence of KN93 (Caf + KN93). The bars represent relative units normalized with the control (*P = 0.02 vs Control, * P = 0.009 vs Caf+KN93). (N=4). * P<0.05. Data represented as means ± SD.

5.4. Discussion and Conclusion

The main findings from the present study are that CaMK II activation by caffeine increased: a) MEF2A expression, b) the level of acetylation of histone H3 in the vicinity of the NRF-1 binding site on the *mef2a* promoter and c) *mef2a* promoter- bound NRF-1. Ramachandran et al. (185) recently provided overwhelming evidence that NRF-1 is a key regulator of *mef2a* gene expression when they showed that: a) the 5' *mef2a* regulatory region within ~0.8 kb upstream of the transcription start site, which is highly conserved among mammals, contains MEF2, NRF-1 and E-box elements, b) endogenous NRF-1 binds to the *mef2a* promoter element, c) MEF2A mRNA was strongly induced in cells that overexpressed $NRF1_{VP16}$ (NRF-1 fused to the trans-activating domain from viral VP16), d) *mef2a* promoters are highly responsive to forced expression of NRF-1 or $NRF1_{VP16}$ in mammalian (HeLa) and *Drosophila* cells and e) myocyte *mef2a* mRNA is reduced with *nrf-1* interference. Our finding that, CaMK II influences the acetylation state of histones in the region encompassing the NRF-1 binding domain on the *mef2a* gene, adds new insights onto the mechanism of *mef2a* gene regulation by NRF-1: It supports the hypothesis that CaMK II activation remodels chromatin to favour increased accessibility of NRF-1 to its binding domain on the *mef2a* gene to favour *mef2a* transcription.

The level of acetylation of histones in nucleosomes depends on the balance between the activities of HATs, which acetylate histones, and HDACs, which remove acetyl groups from histones. There is a growing body of evidence showing that CaMK II phosphorylates class II histone deacetylases, such as HDAC4 and HDAC5, and induces their nuclear export (143; 156; 158). Decreased nuclear HDAC content due to CaMK II activation would favour increased nuclear HATs activity resulting in hyperacetylation of histones in nucleosomes and enhanced accessibility of transcription factors to their binding domains on DNA. There is also evidence that some HATs, e.g.

p300, are substrates of CaMK II: Yuan et al, (239) have shown that p300 is phosphorylated and activated when acted upon by CaMK II. Our observation, of ~2.5-fold increase (compared to control) in the level of acetylation of histone H3 surrounding the NRF-1 binding domain on the *mef2a* gene, and a similar increase in the the content of *mef2a*-bound NRF-1, provide evidence that these effects of CaMK occur at the *mef2a* promoter region. However, the effect of CaMK activation by caffeine on nuclear HDAC content has not been studied, nor is the species of HDAC that are affected known. Moreover, the specific HAT that is responsible for hyperacetylation of histones surrounding the NRF-1 binding domain has not yet been identified, although p300 and cyclic AMP response element-binding (CREB) protein associated factor (CAF) are likely candidates because they are capable of acetylating all four histones (14; 171) and have been shown to associate with NRF-1 and MEF2 (89; 110; 147; 198).

Although our data clearly show that CaMK II activation caused hyperacetylation of histone H3 on the region encompassing NRF-1 binding site on the *mef2a* promoter and increased NRF-1 binding to the site, we are unable to conclude that the increased binding was due to the observed histone hyperacetylation. Other factors, such as increased NRF-1 acetylation, may have contributed to the increased binding. Indeed, Izumi et al., (110) showed that treatment of human breast cancer cells (MCF-7) with sodium butyrate increased NRF-1 binding activity via increased acetylation of NRF-1 at the N-terminal domain (which contains 17-clustered lysine residues) by p300/CAF associated factor (110). The observed CaMK II inhibition by KN93 on caffeine-induced: a) hyperacetylation of histones surrounding the NRF-1 binding sites on the *mef2a* promoter, b) increase in NRF-1 binding to the *mef2a* promoter and c) increase in MEF2A protein expression, does not exclude the possibility that other non-CaMK II stimuli (such as AMPK which has a similar substrate specificity to CaMK II) may have been involved in these processes.

Consistent with previous observations in L6 myotubes (173), we have shown in the present study that caffeine also increases MEF2A expression in C2C12 myotubes. Because the increase in MEF2A expression was blocked when KN93 was included in the medium together with caffeine, it follows that the increase in MEF2A expression by caffeine is CaMK II-driven. Our finding that CaMK activation increased MEF2A expression is consistent with findings from several other studies: Passier et al., (176) showed that CaMKIV overexpression in the heart resulted in >100-fold increase in MEF2A expression (176). Likewise, Zhang et al., (241) found that CaMK II activation in cardiomyocytes induced ~ 7-fold increase in MEF2 gene expression. The increase in MEF2A content appears to affect the expression of *glut4* and some mitochondrial genes: With regard to *glut4* gene, Smith et al., (212) showed that CaMK II activation by exercise resulted in increased MEF2A binding to the *glut4* gene and ~2-fold increase in GLUT4 expression. Activation of CaMK II with caffeine also increased GLUT4 expression (173) and mitochondrial proteins such as δALAS, citrate synthase, cyclooxygenase-1 (COX-1) and cytochrome *c* (172) in L6 myotubes. Incubation of L6 myotubes with A23187, a Ca^{2+} ionophore which increases cytosolic Ca^{2+} levels and activates CaMK II (173) increases the expressions of malate dehydrogenase F_1-ATPase and cytochrome *c* (58). Transgenic mice that selectively express a constitutive active CaMKIV in skeletal muscle have increased expression of enzymes involved in fatty acids metabolism and electron transport chain (234). Given that many of these mitochondrial enzymes, are encoded by genes that are regulated by NRF-1, we speculate that CaMK activation might have caused hyperacetylation of histones at NRF-1 binding sites on these mitochondrial genes and increased NRF-1 binding to these sites.

Several studies have shown that exercise increases MEF2A expression (54; 227). Although the mechanism responsible has not been investigated, the findings from the present study lead us to speculate that it might be CaMK II driven. Indeed, several studies have shown that exercise activates

CaMK II (6; 55; 57; 193-195). Furthermore, since CaMK II activation by caffeine induces histone H3 hyperacetylation in the region surrounding the NRF-1 binding site, we are led to speculate that exercise might also induce histone hyperacetylation and increase NRF-1 binding in the same region. These speculations remain to be tested empirically.

In summary, our results shed new insights on CaMK's involvement in the regulation of MEF2A expression by NRF-1. We have demonstrated that CaMK II activity is necessary for NRF-1 binding to the *mef2a* gene and is associated with increased acetylation of histones surrounding the NRF-1 binding sites on the *mef2a* promoter.

Chapter 6

Study 3:

CaMK II activation exports HDAC5 from the nucleus and induces hyperacetylation of histones in the vicinity of the MEF2 *cis*-element on the *glut4* promoter in C2C12 myotubes

6.1. Introduction

Previous studies have reported that CaMK activation regulates GLUT4 expression. For example, Ojuka et al., (173) activated CaMK II in C2C12 myotubes using caffeine and observed ~2-fold increase in GLUT4 content. Jensen et al., (114) also showed that mice that expressed constitutively active CaMKIV had 30 % higher GLUT4 in skeletal muscle. Although the mechanism through which CaMK II regulate *glut4* expression has not been investigated, it is well known that GLUT4 expression is regulated by the binding of MEF2 to its consensus binding element on the *glut4* promoter (223). Therefore we reasoned that CaMK II activation might increase GLUT4 by improving the easy with which MEF2 factors bind to the *glut4* promoter.

There are four isoforms of MEF2 transcription factors, namely MEF2A, MEF2B, MEF2C and MEF2D. All of these isoforms possess a signature domain that specify MEF2 binding to a highly conserved AT-rich sequence [CTA(T/A)$_4$TAG] found in human, rat and mouse *glut4* gene (18; 139). It is reported that MEF2A binds to the *glut4* gene as a heterodimer with MEF2D (223) and when bound they recruit other transcriptional regulators such as p300/CBP (210), PGC-1 (160), GLUT4 enhancer factor (GEF), and MAPK such as p38 (80; 158; 160). The multimeric transcriptional complex that forms around MEF2 then attracts and activates RNA polymerase II, which initiates the *glut4* gene transcription.

MEF2 transcription factors also interact with Class II HDACs such as HDAC4 and 5 (143; 158) and HATs (49; 198; 210). Association of HDACs with MEF2 appears to suppress GLUT4 and other MEF2-dependent transcription (158; 214). For example, McGee & Hargreaves (156) reported a strong reverse correlation between nuclear MEF2A/HDAC content and GLUT4 mRNA and Czubryt et al., (40) showed that expression of a mutant form of HDAC5 which constitutively localizes in the nucleus results in a 3-fold decrease in GLUT4 expression. Stimuli such as exercise or overexpression of CaMK IV have been shown to dissociate MEF2A/HDAC complexes and induce export of HDACs out of the nucleus to the cytoplasm (143; 156). This nucleo-cytoplasmic shuttling of HDACs, which is dependent on phosphorylation of two serine motifs on HDACs by CaMKs, seem to promote association of MEF2 factors with HATs (41; 79; 237) and de-repressed MEF2-dependent genes (143). Indeed it is now known that the binding site of HDAC5 on MEF2 overlaps that of HAT p300/CPB; suggesting that dissociation of HDAC5 from MEF2 allows the association with p300/CBP (49; 143; 198). HATs acetylate histones, which relaxes chromatin and promotes transcription by increasing the accessibility of binding domains for transcriptional factors and other transcriptional regulators.

Because caffeine has been shown to activate CaMK II (see section 5.3.1) and increase GLUT4 expression (173) in L6 myotubes, we hypothesised that caffeine would: a) induce HADC5 nuclear export, b) promote hyperacetylation of histones on the MEF2 binding site on the *glut4* gene, and c) increase binding of MEF2A to the *glut4* promoter. To test these hypotheses, we incubated C2C12 myotubes with caffeine in the presence or absence of KN93 or dantrolene and assessed: a) HDAC5 abundance in the nucleus and cytosol, b) acetylation of histone H3 in the vicinity of the MEF2 site on the *glut4* promoter, c) the extent to which MEF2A was bound to its *cis* element on the GLUT4 promoter, and e) GLUT4 expression.

6.2. Methodology

6.2.1. Treatment of myotubes: C2C12 myoblasts were cultured in DMEM containing 2 % horse serum for 13 days to form well differentiated myotubes. They were then incubated for 2 h in medium containing10 mM caffeine, 10 mM caffeine +25 μM KN93, or 10 mM caffeine +10 μM Dantrolene. After treatment, they were harvested immediately or after 6 h for immunocytochemical analysis or for ChIP and qRT-PCR assays, respectively. For assessment of the effects of these treatments on the contents of HDAC5, MEF2A, GLUT4 and α-tubulin, myotubes were treated for 2 h per day for 4 consecutive days and harvested 18 h after the last treatment. Untreated myotubes served as controls in all cases.

6.2.2. Western Blot: After treatments, myotubes were washed 2x with PBS, scraped loose form the culture plate in 300 μl RIPA buffer (56 mM Tris-HCl pH 7.4, 150 mM NaCl, 1 mM EDTA, 0.1 % SDS, 1 % Triton-X100, 10 mM $Na_4P_2O_4$, 20 mM NaF, 0.15 μM okadaic acid, 4 mM Na_3VO_4, 1 x complete protease inhibitors) and homogenized using a dounce homogenizer. Total, nuclear and cytosolic proteins were extracted as described in section 3.7 and the protein content in each component measured using the Bradford assay. The activity of LDH (Santa Cruz), and the contents of α-tubulin and histone H3, was measured in both nuclear and cytosolic extracts to ascertain that our method effectively separated the nuclear and cytosolic compartments. The contents of HDAC5, MEF2A, GLUT4 and α-tubulin in the crude and nuclear extracts were measured by western blot as described previously in Section 3.7.3.

6.2.3. Immunocytochemistry analysis: Immediately after treatments, myotubes were washed in ice-cold PBS and fixed with 3:1 methanol/glacial acetic acid at –20 °C for 10 min. Thereafter, they were washed in PBS, blocked in 1 % BSA for 30 min, and incubated overnight at 4 °C with antibodies against HDAC5 (Sant Cruz) and MEF2A (Cell signalling). The following day, cells were

washed and incubated with fluorochrome-conjugated anti-rabbit (Cy3) and goat anti-mouse (Alexa) secondary antibodies (diluted 1:1000) for 2 h at room temperature. Nuclei were stained with a 1:50 dilution of 0.05 µg/ml DAPI for 10 min at room temperature. After being washed, a coverslip was mounted on the cells with a solution consisting of 40 % glycerol, 20 % Mowiol, 8 % n-propyl gallate, and 0.2 M Tris buffer (pH 7.4). Subcellular location of HDAC5 and MEF2A was viewed using a Zeiss Axiovert 200M fluorescence microscope equipped with plan-neofluar optics set at 15 (Cy3), 10 (Alexa 488), and 1 (DAPI) as well as an Axiocam HR charge-coupled device camera. Adobe Photoshop 7 software was used for image processing.

6.2.4. ChIP assay*:* In order to measure the content of MEF2A that was bound to its binding sequence on the *glut4* gene and the extent of acetylation of histone H3 in the neighbourhood of the MEF2A binding domain on the *glut4* gene, ChIP assays were used. Briefly, myotubes were fixed with formaldehyde, sonicated to fragment the chromatin to 300-1000 bp and the chromatin fragments co-immunoprecipitated using anti-MEF2A, anti-acetyl histone H3 or anti-histone H3 antibodies (Cell signalling). IgG (Cell signalling) was used as a negative control antibody. Co-immunoprecipitated DNA was PCR amplified using primers that recognize a sequence with the MEF2A sites on the *glut4* gene (refer to Section 3.9.3.3). Control primers that targeted regions which do not contain the MEF2A binding site on the *glut4* gene, were also used as negative controls. PCR products were separated by electrophoresis on a 2 % agarose gel and the signals quantified by densitometry. Signal from the immunoprecipitated chromatin (IP) was normalised to its corresponding input (chromatin that did not undergo immunoprecipitation) signal (IN). The assay protocol is described in detail in Section 3.9.1-3.

6.2.5. Quantitative RT-PCR*:* After treatments, total RNA from myotubes that were harvested from 10 cm plate was extracted using 1 ml Trizol (Ambion) as described in Section 3.10.2. One µg of

RNA was mixed with 0.5 μg of 22-mer oligo-dT primers and incubated at 70 ^{o}C for 5 min to denature RNA secondary structures. Genomic DNA was eliminated from the samples by digestion with 1 U DNAse-1 (Promega) for 90 min at 37 ^{o}C. DNAse-1 was subsequently deactivated by incubation at 75 ^{o}C for 5 min. cDNA was synthesized using 200 U M-MLV reverse transcriptase (Promega) for 1 h at 42 ^{o}C and stored at -20 ^{o}C. Quantitative real time PCR (qRT-PCR), using 1 μl cDNA, was performed to measure GLUT4 mRNA by a Light Cycler PCR machine (Roche) using SYBR Green PCR reagents (Roche) and primers which amplify a 270 bp region of the mouse GLUT4 gene (see table 3.5). The concentration of GLUT4 mRNA relative to GAPDH or Ribosome S12 (internal controls) were calculated using the method described by (291) and mean values of the triplicate samples were normalized to the mRNA level of a control untreated sample (see Section 3.10.2.)

6.3. Results

6.3.1. CaMK II activation by caffeine induces HDAC5 nuclear export. It has previously been shown that expression of constitutively active CaMK IV in fibroblasts (10T1/2) and *Cos* cells caused nuclear export of HDAC5 and stimulated MEF2-dependent differentiation of these cells. These observations led us to suspect that CaMK II activation by caffeine might also induce HDAC5 nuclear export in differentiated myotubes. To confirm this suspicion, we performed immunocytochemical studies on HDAC5 and MEF2A proteins to determine if caffeine affected their localization within myotubes via a Ca^{2+}-dependent activation of CaMK II.

C2C12 myotubes were incubated for 2 h with 10 mM caffeine in the presence or absence of 10 μM dantrolene or 25 μM KN93. Representative images from immunocytochemical analysis and western blot are shown in figures 6.1 A and B, respectively. Immunocytochemical images revealed that MEF2A was located predominantly in the nucleus under all conditions, i.e. in untreated cells and

in caffeine-treated cells in the absence or presence of dantrolene or KN93 (Fig. 6.1A: panels D, L and P). In contrast, whereas HDAC5 was found in both the nucleus and the cytosol in untreated cells, incubation with caffeine caused a decrease in intra-nuclear but an increase in peri-nuclear HDAC5 density (Fig 6.1A; *G*). Inclusion of KN93 or dantrolene in the medium together with caffeine blocked the effect of caffeine (Fig. 6.1A: panel I-L and M-P). These results provide evidence that caffeine causes HDAC5 to traffic out of the nucleus in a calcium- and CaMK II-dependent manner. Western blot of HDAC5 and MEF2A form nuclear extracts (Figure 6.1 B) confirmed the observations from immunocytochemical analyses. Caffeine reduced the nuclear contents of HDAC5 ($P < 0.05$) but not MEF2A, resulting in a diminished HDAC5/MEF2A ratio, compared with untreated controls (Fig. 6.1B). Inclusion of dantrolene or KN93 together with caffeine attenuated the decreases in nuclear HDAC5 content and HDAC5/MEF2A ratio.

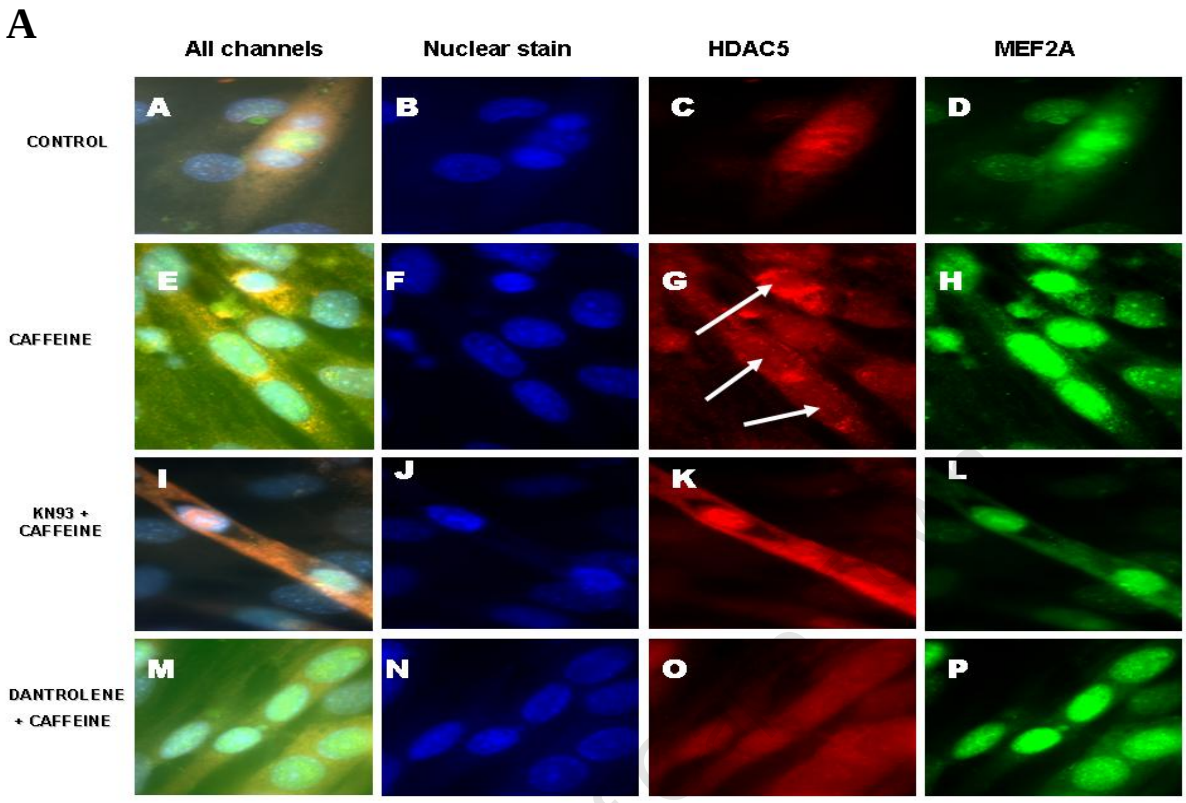

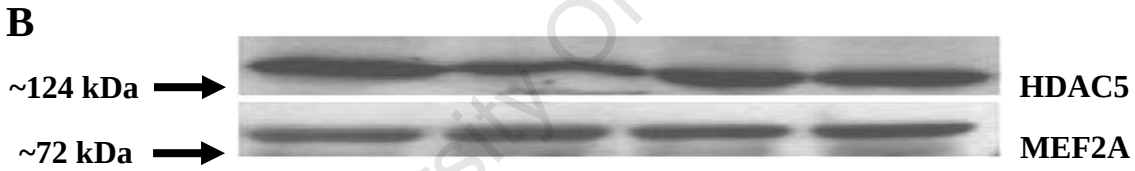

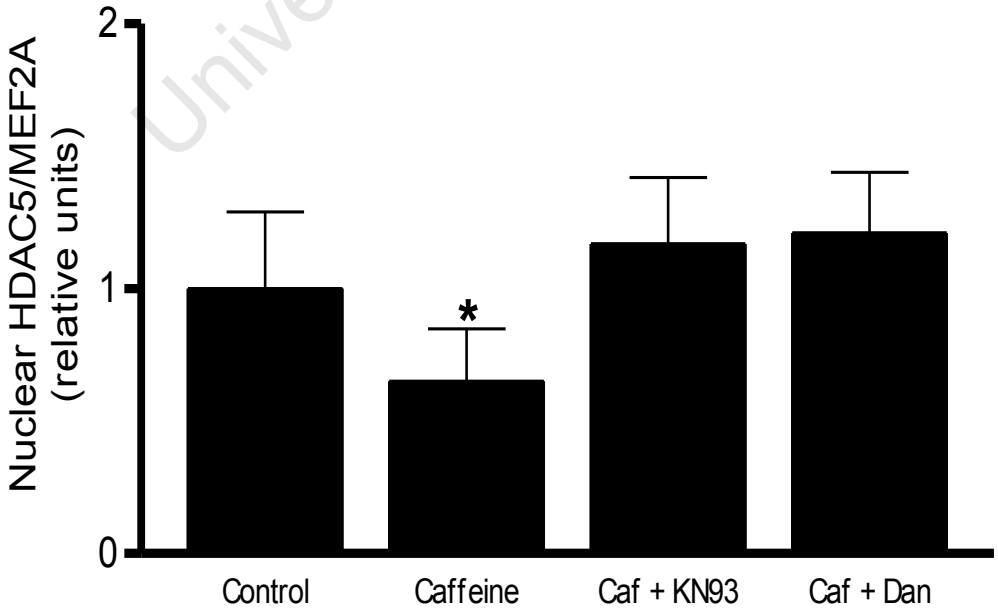

Figure 6.1: Representative Immunocytochemical images and western blot showing the localization of HDAC5 and MEF2A in C2C12 myotubes. ***A****:* After incubation in medium containing 10 mM caffeine (Caf) in the presence or absence of 10 µM dantrolene (Dan) or 25 µM KN93 for 2 h, subcellular localization of the nucleus, HDAC5, and MEF2A was determined using the immunocytochemical technique described in section 3.8.3. *A–D*: control untreated myotubes. *E–H*: myotubes incubated with 10 mM caffeine.*I-L*: myotubes treated with caffeine+25 µM KN93. *M-P*: myotubes incubated with caffeine+10 mM dantrolene. Blue: 4, 6-diamidino-2-phenylindole (DAPI) nuclear stain; red, HDAC5; green, MEF2A. Arrows indicate decreased intranuclear HDAC5 and arrowheads increased perinuclear HDAC5 levels. Scale bar, 10 µm. N = 4. ***B***: Western blot analysis of nuclear contents of MEF2A and HDAC5. Representative western blots of MEF2A and HDAC5 from nuclear extracts and a histogram of the HDAC5/MEF2A ratio for the various treatments. The histogram reflects the abundance of HDAC5 relative to MEF2A in the nucleus. *P = 0.002 vs. Control, * P = 0.005 vs Caf+KN93 & Caf+Dan; *n* = 5 independent experiments. Data represented as means ± SD.

6.3.2. CaMK II activation induces hyperacetylation of histones at the MEF2A site on the glut4 promoter

The level of nucleosomal acetylation results from the balance between the activities of HDACs, which removes acetyl moieties from histones proteins and HATs which adds the acetyl groups to the histones. The CaMK II-driven nuclear export of HDAC5 that was observed (Fig 6.1) suggested to us that that nuclear HAT activity might be increased and prompted us to check if the level of acetylation of histones in the vicinity of the MEF2 binding element on the *glut4* promoter was increased. Figure 6.2A and 6.2B shows ChIP assay results for various treatment groups following immunoprecipitation by antibodies directed against acetylated histone H3 and histone H3. Signals from input sample (IN), representing the total MEF2 binding sites in the sample, and from immunoprecipitated samples (IP), showing the fraction of the sites that contained acetylated histone H3, are shown adjacent to each other (for each treatment group) to facilitate comparison. The fraction, IP /IN, which represents the levels of acetylation of histones in the vicinity of the MEF2A binding domain under different treatments, is depicted in Fig. 6.2 B. Here we see that caffeine treatment increased the amount of AcH3 (acetylated histone H3) in the vicinity of MEF2 *cis*-element, but this effect of caffeine was abolished by dantrolene or KN93. Differences in cross-linking efficiencies and in the accessibility of antibody to histones that may result from the treatments can

influence the interpretation of ChIP assay results. To check if such differences existed in our experiments, we conducted control experiments using an antibody against histone H3. As depicted in Fig. 6.2A and 6.2C, ChIP assay results were similar in all treatment groups: Indicating that there were no differences in cross-linking efficiencies and/or antibody accessibility in our protocol. In summary, our results confirm that caffeine increases a) the binding of MEF2A to the *glut4* promoter and b) acetylation of histone H3 in the vicinity of the MEF2A site on the *glut4* promoter in a calcium- and CaMK II-dependent manner.

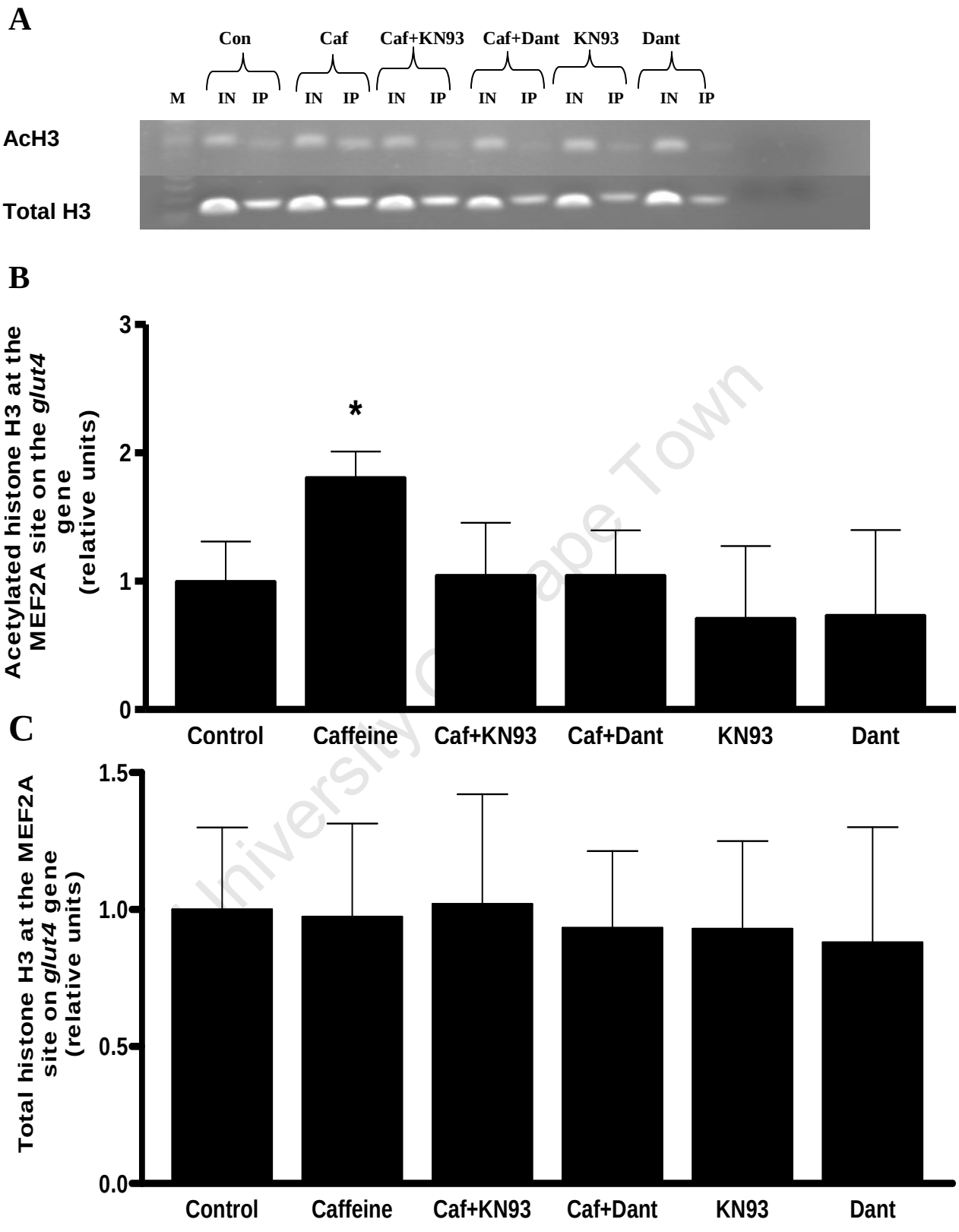

Figure 6.2: Caffeine induced hyperacetylation of histone H3 at the MEF2A site on the *glut4* promoter in a calcium and CaMK II dependent manner. Myotubes were treated with 10 mM CAF (caffeine) in the presence and absence 10 µM DAN (Dantrolene) or 25 µM KN93 for 2 h. The level of acetylation of histone H3 at the MEF2A binding site on the *glut4* promoter by chromatin immunoprecipitation assay 6 h post incubation. **A**: a section of the *glut4* promoter spanning the MEF2A binding site was PCR amplified from DNA that was coimmunoprecipitated (IP) with acetylated histone H3 (AcH3) or histone H3 antibody and from corresponding input (IN) samples. **B**: relative amounts of acetylated histones at the MEF2A site on the *glut4* gene **C:** relative amounts of non-acetylated H3 at the MEF2A site. The bars represent the IP/IN ratio normalized to control, * P = 0.001 vs Caf+KN93, * P = 0.006 vs Caf+Dant, * P = 0.009 vs KN93 & Dant. *$P < 0.05$ vs. control. M: molecular weight marker. Data represented as means ± SD. N=4.

6.3.3. CaMK II activation increases MEF2A binding to the glut4 gene. Hyperacetylation of histones is associated with increased accessibility of transcriptional factors to their DNA binding domains and the recruitment of transcriptional regulators to the site. Since we observed increased acetylation of histones on the neighbourhood of MEF2 binding domain on the *glut4* promoter, we assessed the level of MEF2A that was bound to the site. Figure 6.3 shows typical agarose gel of the 268 bp DNA that was PCR amplified from DNA that was co-immunoprecipitated with MEF2A antibody (IP) and DNA from input sample. The graph shows the signals after they were quantified by densitometry. Caffeine increased the *glut4*-bound MEF2A by ~2.3-fold compared with controls. However, when CaMK II activity was blocked by KN93, the amount of bound MEF2A was attenuated significantly. Moreover, when dantrolene was used to block caffeine-induced increases in cytosolic calcium (173), the increase in *glut4*-bound MEF2A was also blocked; implying that the increase in *glut4* bound MEF2A depends on Ca^{2+}-dependent CaMK II activation.

The specificity of the ChIP assay was verified by the following observations: a) there was no evidence of MEF2A binding at the *glut4* coding region in position +2868- +3183 which has no MEF2A binding element as indicated in the previous chapter 3 (Figure 3.13), b) only the anti-MEF2A, but not IgG, was able to co-immunoprecipitate the *glut4*-MEF2 binding domain (Fig 3.12 lanes 2 and 3 respectively).

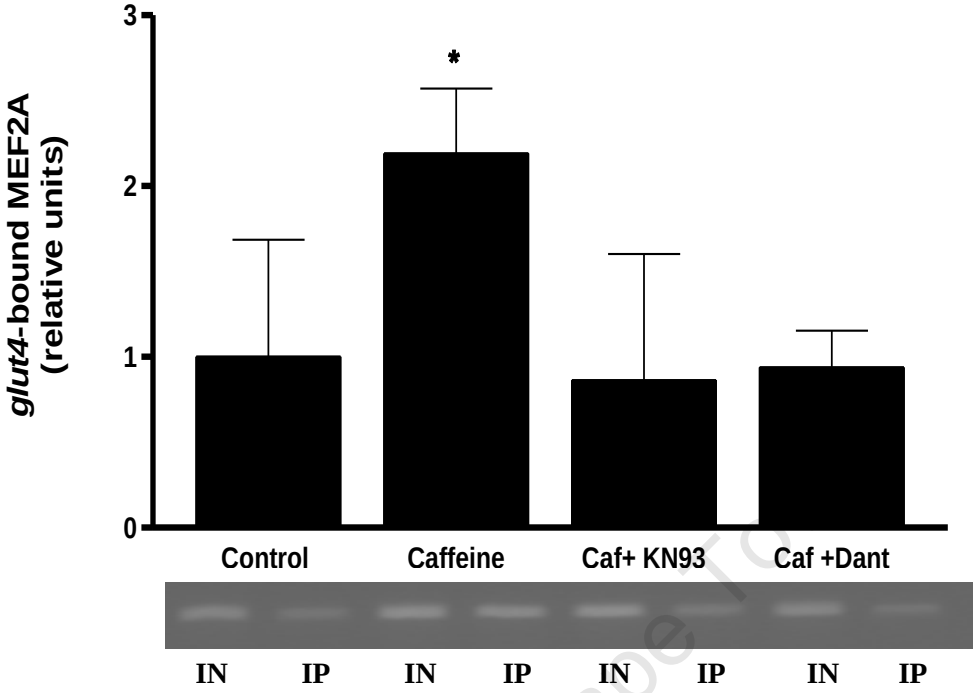

Figure 6.3: CaMK II activation induces an increase in the binding of MEF2A to the *glut4* promoter. Myotubes were treated with 10 mM caffeine (Caf) in the presence and absence 10 µM Dant (dantrolene) or 25 µM KN93 for 2 h and ChIP assay performed 6 h later. Relative amounts of *glut4* promoter-bound MEF2A was calculated from signal densities from PCR reactions in both IN and IP. The bars represent the IP/IN ratio normalized to control. * P = 0.0011 vs Control, * P = 0.005 vs Caf+KN93, * P = 0.009 vs Caf+Dant. N=4. Data represented as means ± SD. *P<0.05.

6.3.4. CaMK II activation increases GLUT4 mRNA and protein. After observing increased acetylation of histones and MEF2A binding to the *glut4* promoter, we next assessed the level of GLUT4 expression. We treated C2C12 myotubes with 10 mM caffeine or vehicle for 2 h and harvested the cells 6 h later for GLUT4 mRNA measurement. We found that CaMK II activation resulted in increased GLUT4 mRNA by ~2.6-fold ($P < 0.05$; Fig 6.4A); however GAPDH did not change under all experimental conditions. In myotubes that had been treated for 2 h for 4 consecutive days, GLUT4 protein was ~2.7-fold higher compared to controls. The caffeine-induced increases in GLUT4 mRNA and protein were significantly reduced when caffeine and KN93 were included in the growth medium; indicating that these increases require CaMK II.

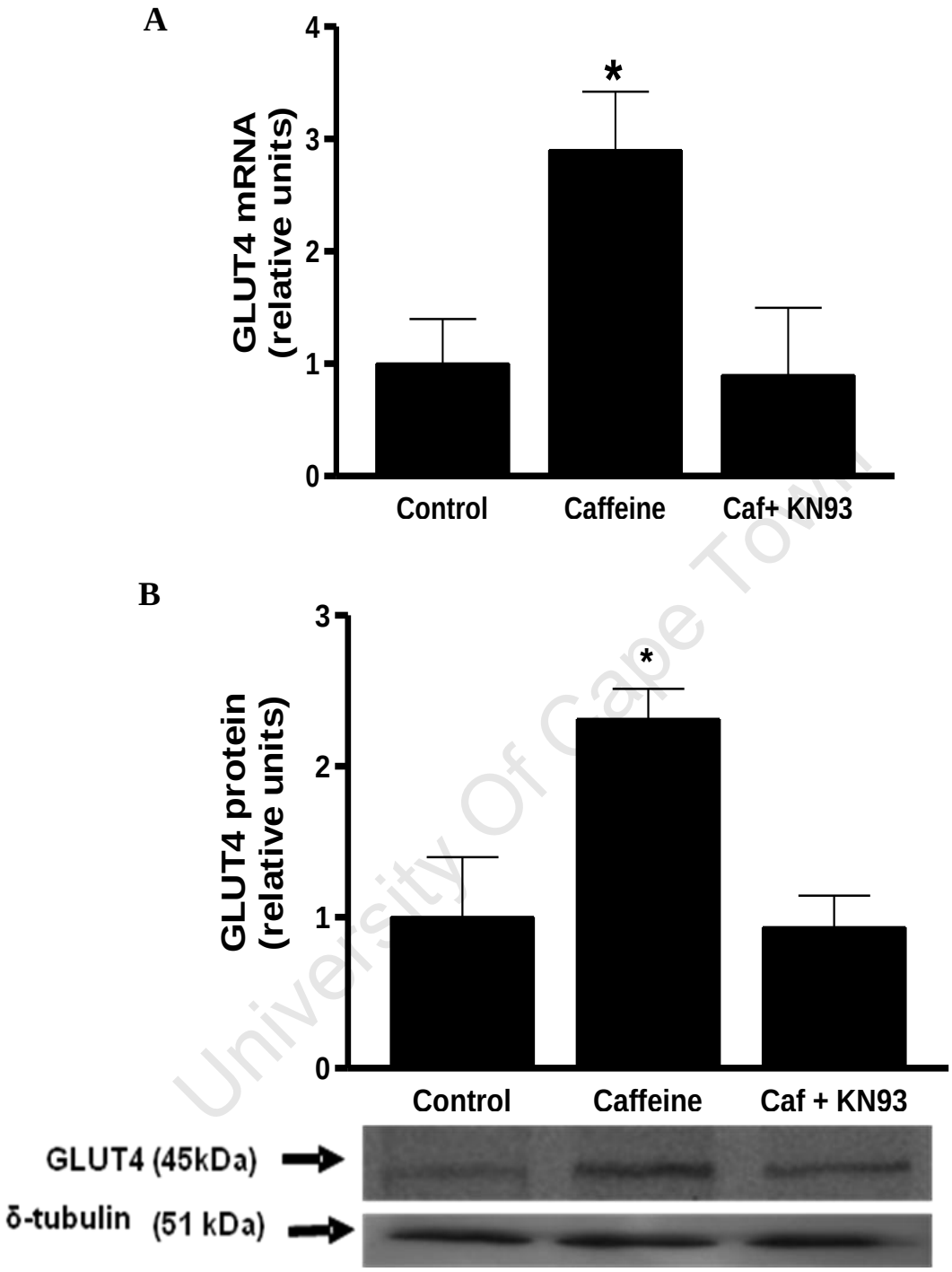

Figure 6.4: GLUT4 protein and mRNA is increased by caffeine (CAF) in C2C12 myotubes. Well-differentiated myotubes were incubated with 10 mM CAF in the presence or absence of 25 µM KN93 or 10 µM dantrolene (DAN) in serum-free medium for 2 h. **A.** Myotubes were harvested 6 h after the last treatment. GLUT4 mRNA was measured by real-time PCR as described in experimental procedures. * P = 0.0015 vs Control, * P = 0.001 vs Caf+KN93. **B**. Western blot for GLUT4 protein from myotubes that were treated for 2 h per day for 4 consecutive days. Data represented as means ± SD. N=6. *$P < 0.05$.

6.5. Discussion and Conclusion

Previous studies have shown that CaMK II regulates GLUT4 expression in L6 myotubes (173). The current study was designed to explore the mechanism involved. Here, we present evidence that CaMK II activation with caffeine: a) exports HDAC5 from the nucleus, b) induces hyperacetylation of histones on the neighbourhood of MEF2 domain on the *glut4* promoter, c) increases MEF2A binding to the *glut4* promoter, and d) increases GLUT4 expression. All the above changes were attenuated by inclusion of KN93 or dantrolene in the medium, indicating that these changes occur via a Ca^{2+}- and a CaMK II-dependent pathway.

Acetylation of histones by HATs, and deacetylation by HDACs are recognized as important opposing mechanisms in controlling gene expression (130). Normally genes are expressed when surrounding histones are hyperacetylated, a process which is facilitated by HATs (217). They are normally repressed when surrounding histones are deacetylated by HDACs (130). In this study we have found that histone H3 in the vicinity of the MEF2A binding site on the *glut4* promoter were hyperacetylated when caffeine was used to activate CaMK II in C2C12 myotubes and hypoacetylated when KN93 was included in the medium together with caffeine to inactivate CaMK II. This finding indicates that CaMK II increases the activity of some HAT which acetylates histone H3. Indeed we have shown that CaMK II activation decreased HDAC5 nuclear content (Figure 6.1), which would conceivably give rise to the observed increase in HAT activity. Although the HAT concerned has not been identified, it has been reported that CaMK II directly phosphorylates and activates p300 (239), a HAT that acetylates all four histones and most non histone proteins (14; 23). Acetylation of histones relaxes chromatin thereby enhancing access of transcriptional factors and RNA polymerases to the DNA site to increase gene transcription. Hyperacetylated histones ensure super induction of genes because they have increased ability to interact with transcriptional factors and to anchor

transcriptional coactivator complexes to gene promoters (217; 224). For example, hyperacetylated histones surrounding the MEF2 site on myogenic genes, such as MyoD, result in increased myogenesis in C2 cells (143). In contrast, accumulation of HDAC5 in the nucleus suppresses MEF2 dependent *glut4* promoter activity (214). Czybryt et al (40) confirmed this by showing that HDAC5 which constitutively localizes in the nucleus result in ~3-fold down-regulation of GLUT4 expression. It appears that nuclear HDAC5 forms a complex with MEF2 and deters MEF2-dependent transcription (158; 214).

MEF2A binding to the *glut4* was increased ~2-fold with caffeine treatment but the increase was blocked by inclusion of KN93; indicating that CaMK II also plays a role in MEF2A binding to the *glut4* gene. The increase in binding, which correlated with induced hyperacetylation at the same DNA site, could have been a consequence of increased accessibility of DNA to transcriptional factors. It could also have been due to acetylation of MEF2 because there are reports which indicate that p300 acetylates MEF2 factors and increases their DNA binding activity (5; 147; 198). Further studies are needed to ascertain which of those factors was responsible for the observed increased binding.

Because caffeine was able to increase GLUT4 expression by ~2.7-fold in this present study, it is reasonable to assume that it activates both binding and trans-activation domains of MEF2A. Although, the mechanism by which caffeine increased MEF2A trans-activation remains to be explored, it appears to activate other downstream kinases, including MAP kinases p38, which are known to activate MEF2 trans-activation domain (187; 233-235; 242). Further studies of the role of caffeine in MEF2A trans-activation are warranted.

In summary, we propose the following mechanisms to explain how CaMK activation increases GLUT4 expression in C2C12: CaMK II activation induces nuclear export of HDAC5

which increased nuclear HATs activity, resulting in hyperacetylation of histones on sections of the *glut4* promoter. Hyperacetylation of histones in the vicinity of MEF2 binding domain on the *glut4* promoter increases the accessibility of the domain to MEF2A transcription factors resulting in enhanced binding and transcriptional activity of MEF2A.

CHAPTER 7

Summary of the main findings, probable mechanisms and potential avenues for future research

The studies reported in this thesis investigated the molecular mechanisms by which GLUT4 expression is regulated by NRF-1 and CaMK II in C2C12 myotubes. The studies are important because knowledge of the molecular mechanisms involved could reveal targets for new therapeutic modalities for type II diabetes, a disease condition which can be prevented or treated by increasing GLUT4 expression. The studies showed that NRF-1 increases GLUT4 expression via a cascade involving NRF-1→*mef2a*→MEF2A→*glut4*→GLUT4; i.e NRF-1 binds to the *mef2a* gene and increases MEF2A expression, and MEF2A in turn binds to the *glut4* gene and increases its expression. Consistent with our observations, others have shown that NRF-1 overexpression significantly increased MEF2A mRNA (185) and protein expression (10). The importance of MEF2A in the cascade was demonstrated when it was shown that silencing MEF2A expression in NRF-1 overexpressing cells resulted in significant reduction in GLUT4 protein expression. It had previously been reported that MEF2A expression is increased by CaMK II activation (173). We have now shown that CaMK II activation by caffeine: a) increases NRF-1 binding to the *mef2a* gene in C2C12 myotubes, b) induces hyperacetylation of histones in the vicinity of the NRF-1 binding site on the *mef2a* gene, c) causes nuclear export of HDAC5, d) increases MEF2A expression, and e) results in GLUT4 expression. All the above changes were significantly reduced when KN93 was included in the medium together with caffeine, indicating that CaMK II was involved in these processes. Collectively, the results from this thesis support the hypothesis that NRF-1 increases GLUT4 expression via MEF2A and CaMK II activation facilitates these processes.

The increases in *mef2a*-bound NRF-1 and *glut4*-bound MEF2A that were reported in this thesis may have resulted from one or more of the following factors: a) increased abundance of NRF-1 and MEF2A (8; 94; 112; 135), b) increased accessibility of their binding domains on *glut4* and *mef2a* genes, respectively (128; 130; 132; 168), and c) increased binding activity of NRF-1 and MEF2A. Once synthesized in the cytosol, MEF2A and NRF-1 transcription factors translocate to the nucleus because they possess nuclear localization sequences on their N-terminal domains (20; 200). Increased expression, therefore, improves the probability of their interaction with *cis* elements on DNA of target genes. Once bound, the transcription factors recruit other gene regulators, including PGC-1 (40; 80; 160; 234), which in turn recruits general transcription factors such as transcription factor D (TFIID) that are required by RNA pol II, and HATs such as p300/CBP (183) and P/CAF (70; 190) which acetylate neighbouring histone tails. These acetylated histones attract and tether to more HATs, i.e. p300/CBP, p/CAF or GCN5, via bromodomain within the HATs (111; 113; 175; 217; 221). The interaction between acetylated histones and these HATs may results in: a) acetylation of more neighbouring histone tails and increased binding of more transcription factors through increased accessibility of binding sites, and b) acetylation of MEF2A and NRF-1 to increase their binding activity. In support of the latter mechanism, Izumi et al., (110) showed that NRF-1 binding is increased by P/CAF acetylation. Others have also shown that MEF2 binding to DNA is increased by p300/CBP (5; 147). In light of these observations, we envison that the increases in *mef2a*-bound NRF-1 and *glut4*-bound MEF2A may have been initiated by the increased abundance of NRF-1 and MEF2A, respectively, but the robust increases in binding that was observed may have been sustained by: a) increases in the abundance of transcription factors and accessibility of elements, and b) increased binding activities of MEF2A and NRF-1 due to acetylation. However, assessment of these mechanisms was beyond the scope of this thesis. Future studies should: a) assess the accessibility

DNA binding sites of these transcription factors to see if this correlates with the increased binding and transcription, b) identify the HATs responsible for the observed acetylation of histones, and c) characterize the transcription coactivators that may be recruited by NRF-1 and MEF2A transcription factors.

We found that overexpression of NRF-1 induced a large increase in NRF-1 binding to *mef2a* and *δalas* genes but relatively small increases in MEF2A and δALAS proteins (Figure 4.3). Similar findings have been reported previously: For example, Baar et al., (10), found that there was ~10-fold higher binding of NRF-1 to target genes in transgenic mice (compared to wild-type mice) but < 2-fold higher contents of cytochrome c, δALAS, MEF2A and GLUT4 proteins. In contrast, exercise or caffeine causes comparable increases in promoter-bound NRF-1 and the corresponding protein: For example, there was ~1.9-fold increase in NRF-1 binding to *δalas* promoter in L6 myotubes that were treated with caffeine and a corresponding ~2-fold increase in δALAS protein (172). In rats, *δalas*-bound NRF-1 and δALAS were both increased ~1.5 fold with exercise (11). The reason for the discrepancy between the magnitude of NRF-1 binding and gene expression in NRF-1 overexpression studies is not clear. We speculate that all the signals that are essential for gene expression might not have been activated sufficiently by NRF-1 overexpression. For example, protein kinases, such as AMPK, which phosphorylate the transactivational domain of NRF-1 and increase its transcriptional activity (16; 77), may not have been fully activated by NRF-1 overexpression. On the other hand, exercise or caffeine triggers a multitude of signals which may account for the coordinated increases in binding and transcriptional activities of NRF-1 (94; 115; 116).

Several studies have reported down regulation of *mef2a, glut4* and *nrf-1* genes in individuals with type II diabetes (161; 177; 180). The findings from this study, which show that increasing the expression of NRF-1 also increases *mef2a* and *glut4* expression, suggest that chemicals, such as

isoflavines (Genistein) that target the *nrf-1* gene and increase its expression (88), might also improve the expression of *mef2a* and *glut4* genes and enhance glucose transport capacity. Moreover, such drugs may also increase mitochondrial biogenesis since NRF-1 drives the expression of many mitochondrial proteins; thus improving lipid oxidation and insulin sensitivity (127). Therefore future studies of anti-diabetic drugs that target the *nrf-1* gene are warranted. We also observed that CaMK II activation increased the expression of both mitochondrial and GLUT4 proteins; suggesting that CaMK may also be a worthwhile candidate target for drug modalities to alleviate type II diabetes and insulin resistance. Therefore chemicals such as carbachol (12) or histamine (135) which activate CaMK II should be investigated to see if they might increase both GLUT4 and mitochondrial proteins and alleviate symptoms of type II diabetes. In conclusion, this thesis has confirmed that NRF-1 overexpression increases GLUT4 expression and has shown that this effect occurs via the *mef2a* gene. It provides evidence for a transcriptional cascade involving NRF-1→*mef2a*→MEF2A→g*lut4*→GLUT4. The thesis has also shown that CaMK activation increases GLUT4 expression by a process that involves histone hyperacetylation in the vicinity of the NRF-1 binding domain on the *mef2a* gene. These findings were observed in a cell culture model and further studies need to be conducted in animal models to confirm them.

Reference List

1. **Aguirre V, Uchida T, Yenush L, Davis R and White MF. The c-Jun NH2-terminal kinase promotes insulin resistance during association with insulin receptor substrate-1 and phosphorylation of Ser(307). *Journal of Biological Chemistry* 275: 9047-9054, 2000.**

2. **Al-Khalili L, Cartee GD and Krook A. RNA interference-mediated reduction in GLUT1 inhibits serum-induced glucose transport in primary human skeletal muscle cells. *Biochem Biophys Res Commun* 307: 127-132, 2003.**

3. **Allfrey VG and Mirsky AE. Structural Modifications of Histones + Their Possible Role in Regulation of Rna Synthesis. *Science* 144: 559-&, 1964.**

4. **Andersen PH, Lund S, Vestergaard H, Junker S, Kahn BB and Pedersen O. Expression of the major insulin regulatable glucose transporter (GLUT4) in skeletal muscle of noninsulin-dependent diabetic patients and healthy subjects before and after insulin infusion. *J Clin Endocrinol Metab* 77: 27-32, 1993.**

5. **Angelelli C, Magli A, Ferrari D, Ganassi M, Matafora V, Parise F, Razzini G, Bachi A, Ferrari S and Molinari S. Differentiation-dependent lysine 4 acetylation enhances MEF2C binding to DNA in skeletal muscle cells. *Nucleic Acids Res* 36: 915-928, 2008.**

6. **Antipenko A, Frias JA, Parra J, Cadefau JA and Cusso R. Effect of chronic electrostimulation of rabbit skeletal muscle on calmodulin level and protein kinase activity. *Int J Biochem Cell Biol* 31: 303-310, 1999.**

7. **Araki E, Lipes MA, Patti ME, Bruning JC, Haag B, III, Johnson RS and Kahn CR. Alternative pathway of insulin signalling in mice with targeted disruption of the IRS-1 gene. *Nature* 372: 186-190, 1994.**

8. **Aurell E, d'Herouel AF, Malmnas C and Vergassola M. Transcription factor concentrations versus binding site affinities in the yeast S. cerevisiae. *Phys Biol* 4: 134-143, 2007.**

9. **Ausubel FM, Brent R, Kingston RE, Moore DD, Seidman JG, Smith JA and Struhl K.** Current Protocols in Molecular Biology. **New York: John Wiley & Sons, Inc., 1998.**

10. **Baar K, Song Z, Semenkovich CF, Jones TE, Han DH, Nolte LA, Ojuka EO, Chen M and Holloszy JO. Skeletal muscle overexpression of nuclear respiratory factor 1 increases glucose transport capacity. *FASEB J* 17: 1666-1673, 2003.**

11. **Baar K, Wende AR, Jones TE, Marison M, Nolte LA, Chen M, Kelly DP and Holloszy JO. Adaptations of skeletal muscle to exercise: rapid increase in the transcriptional coactivator PGC-1. *FASEB J* 16: 1879-1886, 2002.**

12. **Babb EL, Tarpley J, Landt M and Easom RA. Muscarinic activation of Ca2+/calmodulin-dependent protein kinase II in pancreatic islets. Temporal dissociation of kinase activation and insulin secretion.** ***Biochem J*** **317 (Pt 1): 167-172, 1996.**

13. **Backs J and Olson EN. Control of cardiac growth by histone acetylation/deacetylation.** ***Circulation Research*** **98: 15-24, 2006.**

14. **Bannister AJ and Kouzarides T. The CBP co-activator is a histone acetyltransferase.** ***Nature*** **384: 641-643, 1996.**

15. **Baron U, Freundlieb S, Gossen M and Bujard H. Co-regulation of two gene activities by tetracycline via a bidirectional promoter.** ***Nucleic Acids Res*** **23: 3605-3606, 1995.**

16. **Bergeron R, Ren JM, Cadman KS, Moore IK, Perret P, Pypaert M, Young LH, Semenkovich CF and Shulman GI. Chronic activation of AMP kinase results in NRF-1 activation and mitochondrial biogenesis.** ***American Journal of Physiology-Endocrinology and Metabolism*** **281: E1340-E1346, 2001.**

17. **Berthon P, Freyssenet D, Chatard JC, Castells J, Mujika I, Geyssant A, Guezennec CY and Denis C. Mitochondrial Atp Production-Rate in 55-Year-Old to 73-Year-Old Men - Effect of Endurance Training.** ***Acta Physiologica Scandinavica*** **154: 269-274, 1995.**

18. **Black BL and Olson EN. Transcriptional control of muscle development by myocyte enhancer factor-2 (MEF2) proteins. *Annu Rev Cell Dev Biol* 14: 167-196, 1998.**

19. **Boirie Y. Insulin regulation of mitochondrial proteins and oxidative phosphorylation in human muscle. *Trends Endocrinol Metab* 14: 393-394, 2003.**

20. **Borghi S, Molinari S, Razzini G, Parise F, Battini R and Ferrari S. The nuclear localization domain of the MEF2 family of transcription factors shows member-specific features and mediates the nuclear import of histone deacetylase 4. *J Cell Sci* 114: 4477-4483, 2001.**

21. **Bourey RE, Koranyi L, James DE, Mueckler M and Permutt MA. Effects of altered glucose homeostasis on glucose transporter expression in skeletal muscle of the rat. *J Clin Invest* 86: 542-547, 1990.**

22. **Braidotti G, Borthwick IA and May BK. Identification of regulatory sequences in the gene for 5-aminolevulinate synthase from rat. *J Biol Chem* 268: 1109-1117, 1993.**

23. **Braunstein M, Rose AB, Holmes SG, Allis CD and Broach JR. Transcriptional Silencing in Yeast Is Associated with Reduced Nucleosome Acetylation. *Genes & Development* 7: 592-604, 1993.**

24. **Bruce CR, Thrush AB, Mertz VA, Bezaire V, Chabowski A, Heigenhauser GJF and Dyck DJ. Endurance training in obese humans improves glucose tolerance and mitochondrial fatty acid oxidation and alters muscle lipid content.** ***American Journal of Physiology-Endocrinology and Metabolism*** **291: E99-E107, 2006.**

25. **Brush MH, Guardiola A, Connor JH, Yao TP and Shenolikar S. Deactylase inhibitors disrupt cellular complexes containing protein phosphatases and deacetylases.** ***Journal of Biological Chemistry*** **279: 7685-7691, 2004.**

26. **Burchfiel CM, Sharp DS, Curb JD, Rodriguez BL, Hwang LJ, Marcus EB and Yano K. Physical-Activity and Incidence of Diabetes - the Honolulu Heart Program.** ***American Journal of Epidemiology*** **141: 360-368, 1995.**

27. **Cam H, Balciunaite E, Blais A, Spektor A, Scarpulla RC, Young R, Kluger Y and Dynlacht BD. A common set of gene regulatory networks links metabolism and growth inhibition.** ***Mol Cell*** **16: 399-411, 2004.**

28. **Campbell JE, Fediuc S, Hawke TJ and Riddell MC. Endurance exercise training increases adipose tissue glucocorticoid exposure: adaptations that facilitate lipolysis.** ***Metabolism*** **58: 651-660, 2009.**

29. **Camps M, Castello A, Munoz P, Monfar M, Testar X, Palacin M and Zorzano A. Effect of diabetes and fasting on GLUT-4 (muscle/fat) glucose-transporter expression in insulin-sensitive tissues. Heterogeneous response in heart, red and white muscle. *Biochem J* 282 (Pt 3): 765-772, 1992.**

30. **Cantley LC. The phosphoinositide 3-kinase pathway. *Science* 296: 1655-1657, 2002.**

31. **Chen ZJ and Pikaard CS. Epigenetic silencing of RNA polymerase I transcription: a role for DNA methylation and histone modification in nucleolar dominance. *Genes Dev* 11: 2124-2136, 1997.**

32. **Chen ZP, McConell GK, Michell BJ, Snow RJ, Canny BJ and Kemp BE. AMPK signaling in contracting human skeletal muscle: acetyl-CoA carboxylase and NO synthase phosphorylation. *Am J Physiol Endocrinol Metab* 279: E1202-E1206, 2000.**

33. **Chibalin AV, Yu M, Ryder JW, Song XM, Galuska D, Krook A, Wallberg-Henriksson H and Zierath JR. Exercise-induced changes in expression and activity of proteins involved in insulin signal transduction in skeletal muscle: differential effects on insulin-receptor substrates 1 and 2. *Proc Natl Acad Sci U S A* 97: 38-43, 2000.**

34. **Chin ER. Role of Ca2+/calmodulin-dependent kinases in skeletal muscle plasticity. *J Appl Physiol* 99: 414-423, 2005.**

35. Choi YS, Kim S, Kyu LH, Lee KU and Pak YK. In vitro methylation of nuclear respiratory factor-1 binding site suppresses the promoter activity of mitochondrial transcription factor A. *Biochem Biophys Res Commun* 314: 118-122, 2004.

36. Christ CY, Hunt D, Hancock J, Garcia-Macedo R, Mandarino LJ and Ivy JL. Exercise training improves muscle insulin resistance but not insulin receptor signaling in obese Zucker rats. *J Appl Physiol* 92: 736-744, 2002.

37. Christ-Roberts CY, Pratipanawatr T, Pratipanawatr W, Berria R, Belfort R, Kashyap S and Mandarino LJ. Exercise training increases glycogen synthase activity and GLUT4 expression but not insulin signaling in overweight nondiabetic and type 2 diabetic subjects. *Metabolism* 53: 1233-1242, 2004.

38. Coderre L, Kandror KV, Vallega G and Pilch PF. Identification and characterization of an exercise-sensitive pool of glucose transporters in skeletal muscle. *J Biol Chem* 270: 27584-27588, 1995.

39. Cortez MY, Torgan CE, Brozinick JT, Jr. and Ivy JL. Insulin resistance of obese Zucker rats exercise trained at two different intensities. *Am J Physiol* 261: E613-E619, 1991.

40. **Czubryt MP, McAnally J, Fishman GI and Olson EN. Regulation of peroxisome proliferator-activated receptor gamma coactivator 1 alpha (PGC-1 alpha) and mitochondrial function by MEF2 and HDAC5. *Proc Natl Acad Sci U S A* 100: 1711-1716, 2003.**

41. **Davis FJ, Gupta M, Camoretti-Mercado B, Schwartz RJ and Gupta MP. Calcium/calmodulin-dependent protein kinase activates serum response factor transcription activity by its dissociation from histone deacetylase, HDAC4 - Implications in cardiac muscle gene regulation during hypertrophy. *Journal of Biological Chemistry* 278: 20047-20058, 2003.**

42. **Defronzo RA. Pathogenesis of type 2 (non-insulin dependent) diabetes mellitus: a balanced overview. *Diabetologia* 35: 389-397, 1992.**

43. **Defronzo RA, Ferrannini E, Sato Y, Felig P and Wahren J. Synergistic interaction between exercise and insulin on peripheral glucose uptake. *J Clin Invest* 68: 1468-1474, 1981.**

44. **Dela F, Holten M and Jensen CM. Insulin action, training, and aging. *Int J Sport Nutr Exerc Metab* 11 Suppl: S78-S85, 2001.**

45. **Dela F, Ploug T, Handberg A, Petersen LN, Larsen JJ, Mikines KJ and Galbo H. Physical training increases muscle GLUT4 protein and mRNA in patients with NIDDM. *Diabetes* 43: 862-865, 1994.**

46. **Dhar SS, Ongwijitwat S and Wong-Riley MT. Nuclear respiratory factor 1 regulates all ten nuclear-encoded subunits of cytochrome c oxidase in neurons.** ***J Biol Chem*** **283: 3120-3129, 2008.**

47. **Douen AG, Ramlal T, Rastogi S, Bilan PJ, Cartee GD, Vranic M, Holloszy JO and Klip A. Exercise induces recruitment of the "insulin-responsive glucose transporter". Evidence for distinct intracellular insulin- and exercise-recruitable transporter pools in skeletal muscle.** ***J Biol Chem*** **265: 13427-13430, 1990.**

48. **Dresner A, Laurent D, Marcucci M, Griffin ME, Dufour S, Cline GW, Slezak LA, Andersen DK, Hundal RS, Rothman DL, Petersen KF and Shulman GI. Effects of free fatty acids on glucose transport and IRS-1-associated phosphatidylinositol 3-kinase activity.** ***Journal of Clinical Investigation*** **103: 253-259, 1999.**

49. **Eckner R, Yao TP, Oldread E and Livingston DM. Interaction and functional collaboration of p300/CBP and bHLH proteins in muscle and B-cell differentiation.** ***Genes Dev*** **10: 2478-2490, 1996.**

50. **Elbashir SM, Lendeckel W and Tuschl T. RNA interference is mediated by 21- and 22-nucleotide RNAs.** ***Genes Dev*** **15: 188-200, 2001.**

51. **Eriksson KF and Lindgarde F. Prevention of type 2 (non-insulin-dependent) diabetes mellitus by diet and physical exercise. The 6-year Malmo feasibility study.** ***Diabetologia*** **34: 891-898, 1991.**

52. **Evans MJ and Scarpulla RC. Interaction of nuclear factors with multiple sites in the somatic cytochrome c promoter. Characterization of upstream NRF-1, ATF, and intron Sp1 recognition sequences.** ***J Biol Chem*** **264: 14361-14368, 1989.**

53. **Evans MJ and Scarpulla RC. NRF-1: a trans-activator of nuclear-encoded respiratory genes in animal cells.** ***Genes Dev*** **4: 1023-1034, 1990.**

54. **Fan M, Rhee J, St Pierre J, Handschin C, Puigserver P, Lin J, Jaeger S, Erdjument-Bromage H, Tempst P and Spiegelman BM. Suppression of mitochondrial respiration through recruitment of p160 myb binding protein to PGC-1alpha: modulation by p38 MAPK.** ***Genes Dev*** **18: 278-289, 2004.**

55. **Ferretti G. The effect of prolonged bed rest on maximal instantaneous muscle power and its determinants.** ***Int J Sports Med*** **18 Suppl 4: S287-S289, 1997.**

56. **FitzGerald PC, Shlyakhtenko A, Mir AA and Vinson C. Clustering of DNA sequences in human promoters.** ***Genome Res*** **14: 1562-1574, 2004.**

57. **Fluck M, Booth FW and Waxham MN. Skeletal muscle CaMKII enriches in nuclei and phosphorylates myogenic factor SRF at multiple sites.** ***Biochem Biophys Res Commun*** **270: 488-494, 2000.**

58. **Freyssenet D, Irrcher I, Connor MK, Di CM and Hood DA. Calcium-regulated changes in mitochondrial phenotype in skeletal muscle cells.** ***Am J Physiol Cell Physiol*** **286: C1053-C1061, 2004.**

59. **Friedman JE, de Vente JE, Peterson RG and Dohm GL. Altered expression of muscle glucose transporter GLUT-4 in diabetic fatty Zucker rats (ZDF/Drt-fa).** ***Am J Physiol*** **261: E782-E788, 1991.**

60. **Friedman JE, Dohm GL, Leggett-Frazier N, Elton CW, Tapscott EB, Pories WP and Caro JF. Restoration of insulin responsiveness in skeletal muscle of morbidly obese patients after weight loss. Effect on muscle glucose transport and glucose transporter GLUT4.** ***J Clin Invest*** **89: 701-705, 1992.**

61. **Friedman JE, Sherman WM, Reed MJ, Elton CW and Dohm GL. Exercise training increases glucose transporter protein GLUT-4 in skeletal muscle of obese Zucker (fa/fa) rats.** ***FEBS Lett*** **268: 13-16, 1990.**

62. **Frisch RE, Wyshak G, Albright TE, Albright NL and Schiff I. Lower Prevalence of Diabetes in Female Former College Athletes Compared with Nonathletes.** ***Diabetes*** **35: 1101-1105, 1986.**

63. **Fryer LG, Foufelle F, Barnes K, Baldwin SA, Woods A and Carling D. Characterization of the role of the AMP-activated protein kinase in the stimulation of glucose transport in skeletal muscle cells.** ***Biochem J*** **363: 167-174, 2002.**

64. **Gao Z, Zhang X, Zuberi A, Hwang D, Quon MJ, Lefevre M and Ye J. Inhibition of insulin sensitivity by free fatty acids requires activation of multiple serine kinases in 3T3-L1 adipocytes. *Mol Endocrinol* 18: 2024-2034, 2004.**

65. **Garvey WT, Maianu L, Hancock JA, Golichowski AM and Baron A. Gene expression of GLUT4 in skeletal muscle from insulin-resistant patients with obesity, IGT, GDM, and NIDDM. *Diabetes* 41: 465-475, 1992.**

66. **Garvey WT, Maianu L, Zhu JH, Brechtel-Hook G, Wallace P and Baron AD. Evidence for defects in the trafficking and translocation of GLUT4 glucose transporters in skeletal muscle as a cause of human insulin resistance. *J Clin Invest* 101: 2377-2386, 1998.**

67. **Gaudilliere B, Shi Y and Bonni A. RNA interference reveals a requirement for myocyte enhancer factor 2A in activity-dependent neuronal survival. *J Biol Chem* 277: 46442-46446, 2002.**

68. **Gibbs EM, Stock JL, McCoid SC, Stukenbrok HA, Pessin JE, Stevenson RW, Milici AJ and McNeish JD. Glycemic improvement in diabetic db/db mice by overexpression of the human insulin-regulatable glucose transporter (GLUT4). *J Clin Invest* 95: 1512-1518, 1995.**

69. **Gill JMR and Cooper AR. Physical Activity and Prevention of Type 2 Diabetes Mellitus. *Sports Medicine* 38: 807-824, 2008.**

70. **Glass CK and Rosenfeld MG. The coregulator exchange in transcriptional functions of nuclear receptors. *Genes Dev* 14: 121-141, 2000.**

71. **Goodyear LJ, Giorgino F, Balon TW, Condorelli G and Smith RJ. Effects of contractile activity on tyrosine phosphoproteins and PI 3- kinase activity in rat skeletal muscle. *Am J Physiol* 268: E987-E995, 1995.**

72. **Goodyear LJ and Kahn BB. Exercise, glucose transport, and insulin sensitivity. *Annu Rev Med* 49: 235-261, 1998.**

73. **Gopalakrishnan L and Scarpulla RC. Structure, expression, and chromosomal assignment of the human gene encoding nuclear respiratory factor 1. *J Biol Chem* 270: 18019-18025, 1995.**

74. **Gossen M, Freundlieb S, Bender G, Muller G, Hillen W and Bujard H. Transcriptional activation by tetracyclines in mammalian cells. *Science* 268: 1766-1769, 1995.**

75. **Griffin JB, Rodriguez-Melendez R and Zempleni J. The nuclear abundance of transcription factors Sp1 and Sp3 depends on biotin in Jurkat cells. *J Nutr* 133: 3409-3415, 2003.**

76. Grozinger CM and Schreiber SL. Regulation of histone deacetylase 4 and 5 and transcriptional activity by 14-3-3-dependent cellular localization. *Proc Natl Acad Sci U S A* 97: 7835-7840, 2000.

77. Gugneja S and Scarpulla RC. Serine phosphorylation within a concise amino-terminal domain in nuclear respiratory factor 1 enhances DNA binding. *J Biol Chem* 272: 18732-18739, 1997.

78. Gulve EA and Spina RJ. Effect of 7-10 days of cycle ergometer exercise on skeletal muscle GLUT-4 protein content. *J Appl Physiol* 79: 1562-1566, 1995.

79. Han AD, He J, Wu YQ, Liu JO and Chen L. Mechanism of recruitment of class II histone deacetylases by myocyte enhancer factor-2. *Journal of Molecular Biology* 345: 91-102, 2005.

80. Handschin C, Rhee J, Lin J, Tarr PT and Spiegelman BM. An autoregulatory loop controls peroxisome proliferator-activated receptor gamma coactivator 1alpha expression in muscle. *Proc Natl Acad Sci U S A* 100: 7111-7116, 2003.

81. Hansen PA, Nolte LA, Chen MM and Holloszy JO. Increased GLUT-4 translocation mediates enhanced insulin sensitivity of muscle glucose transport after exercise. *J Appl Physiol* 85: 1218-1222, 1998.

82. **Hanson PI, Meyer T, Stryer L and Schulman H. Dual role of calmodulin in autophosphorylation of multifunctional CaM kinase may underlie decoding of calcium signals. *Neuron* 12: 943-956, 1994.**

83. **Hawley JA. Exercise as a therapeutic intervention for the prevention and treatment of insulin resistance. *Diabetes-Metabolism Research and Reviews* 20: 383-393, 2004.**

84. **Hayashi T, Hirshman MF, Kurth EJ, Winder WW and Goodyear LJ. Evidence for 5' AMP-activated protein kinase mediation of the effect of muscle contraction on glucose transport. *Diabetes* 47: 1369-1373, 1998.**

85. **Hayashi T, Wojtaszewski JF and Goodyear LJ. Exercise regulation of glucose transport in skeletal muscle. *Am J Physiol* 273: E1039-E1051, 1997.**

86. **Helmrich SP, Ragland DR, Leung RW and Paffenbarger RS, Jr. Physical activity and reduced occurrence of non-insulin-dependent diabetes mellitus. *N Engl J Med* 325: 147-152, 1991.**

87. **Henriksson J. Influence of exercise on insulin sensitivity. *J Cardiovasc Risk* 2: 303-309, 1995.**

88. **Hernandez-Montes E, Pollard SE, Vauzour D, Jofre-Montseny L, Rota C, Rimbach G, Weinberg PD and Spencer JP. Activation of glutathione peroxidase via Nrf1 mediates genistein's protection against oxidative endothelial cell injury.** ***Biochem Biophys Res Commun*** **346: 851-859, 2006.**

89. **Herzig RP, Scacco S and Scarpulla RC. Sequential serum-dependent activation of CREB and NRF-1 leads to enhanced mitochondrial respiration through the induction of cytochrome c.** ***J Biol Chem*** **275: 13134-13141, 2000.**

90. **Hirshman MF, Wallberghenriksson H, Wardzala LJ, Horton ED and Horton ES. Acute Exercise Increases the Number of Plasma-Membrane Glucose Transporters in Rat Skeletal-Muscle.** ***Febs Letters*** **238: 235-239, 1988.**

91. **Holloszy JO. Regulation by exercise of skeletal muscle content of mitochondria and GLUT4.** ***J Physiol Pharmacol*** **59 Suppl 7: 5-18, 2008.**

92. **Holmes B and Dohm GL. Regulation of GLUT4 gene expression during exercise.** ***Medicine and Science in Sports and Exercise*** **36: 1202-1206, 2004.**

93. **Holmes BF, Kurth-Kraczek EJ and Winder WW. Chronic activation of 5'-AMP-activated protein kinase increases GLUT-4, hexokinase, and glycogen in muscle.** ***J Appl Physiol*** **87: 1990-1995, 1999.**

94. Holmes BF, Sparling DP, Olson AL, Winder WW and Dohm GL. Regulation of muscle GLUT4 enhancer factor and myocyte enhancer factor 2 by AMP-activated protein kinase. *Am J Physiol* 289: E1071-E1076, 2005.

95. Holten MK, Zacho M, Gaster M, Juel C, Wojtaszewski JF and Dela F. Strength training increases insulin-mediated glucose uptake, GLUT4 content, and insulin signaling in skeletal muscle in patients with type 2 diabetes. *Diabetes* 53: 294-305, 2004.

96. Hood DA, Irrcher I, Ljubicic V and Joseph AM. Coordination of metabolic plasticity in skeletal muscle. *Journal of Experimental Biology* 209: 2265-2275, 2006.

97. Houmard JA, Egan PC, Neufer PD, Friedman JE, Wheeler WS, Israel RG and Dohm GL. Elevated skeletal muscle glucose transporter levels in exercise-trained middle-aged men. *Am J Physiol* 261: E437-E443, 1991.

98. Houmard JA, Hickey MS, Tyndall GL, Gavigan KE and Dohm GL. Seven days of exercise increase GLUT-4 protein content in human skeletal muscle. *J Appl Physiol* 79: 1936-1938, 1995.

99. Houmard JA, Shinebarger MH, Dolan PL, Leggett-Frazier N, Bruner RK, McCammon MR, Israel RG and Dohm GL. Exercise training increases GLUT-4 protein concentration in previously sedentary middle-aged men. *Am J Physiol* 264: E896-E901, 1993.

100. Hu G, Lakka TA, Kilpelainen TO and Tuomilehto J. Epidemiological studies of exercise in diabetes prevention. *Applied Physiology Nutrition and Metabolism-Physiologie Appliquee Nutrition et Metabolisme* 32: 583-595, 2007.

101. Hu G, Qiao Q, Silventoinen K, Eriksson JG, Jousilahti P, Lindstrom J, Valle TT, Nissinen A and Tuomilehto J. Occupational, commuting, and leisure-time physical activity in relation to risk for Type 2 diabetes in middle-aged Finnish men and women. *Diabetologia* 46: 322-329, 2003.

102. Huo L and Scarpulla RC. Multiple 5'-untranslated exons in the nuclear respiratory factor 1 gene span 47 kb and contribute to transcript heterogeneity and translational efficiency. *Gene* 233: 213-224, 1999.

103. Ikemoto S, Thompson KS, Itakura H, Lane MD and Ezaki O. Expression of an insulin-responsive glucose transporter (GLUT4) minigene in transgenic mice: effect of exercise and role in glucose homeostasis. *Proc Natl Acad Sci U S A* 92: 865-869, 1995.

104. Irrcher I, Adhihetty PJ, Joseph AM, Ljubicic V and Hood DA. Regulation of mitochondrial biogenesis in muscle by endurance exercise. *Sports Medicine* 33: 783-793, 2003.

105. Itani SI, Ruderman NB, Schmieder F and Boden G. Lipid-induced insulin resistance in human muscle is associated with changes in diacylglycerol, protein kinase C, and IkappaB-alpha. *Diabetes* 51: 2005-2011, 2002.

106. Ivy JL. Role of exercise training in the prevention and treatment of insulin resistance and non-insulin-dependent diabetes mellitus. *Sports Med* 24: 321-336, 1997.

107. Ivy JL, Brozinick JT, Torgan CE and Kastello GM. Skeletal-Muscle Glucose-Transport in Obese Zucker Rats After Exercise Training. *Journal of Applied Physiology* 66: 2635-2641, 1989.

108. Ivy JL and Holloszy JO. Effect of Training on Glucose-Uptake by Striated-Muscle. *Medicine and Science in Sports and Exercise* 13: 90, 1981.

109. Ivy JL and Holloszy JO. Persistent Increase in Glucose-Uptake by Rat Skeletal-Muscle Following Exercise. *American Journal of Physiology* 241: C200-C203, 1981.

110. Izumi H, Ohta R, Nagatani G, Ise T, Nakayama Y, Nomoto M and Kohno K. p300/CBP-associated factor (P/CAF) interacts with nuclear respiratory factor-1 to regulate the UDP-N-acetyl-alpha-d-galactosamine: polypeptide N-acetylgalactosaminyltransferase-3 gene. *Biochem J* 373: 713-722, 2003.

111. Jacobson RH, Ladurner AG, King DS and Tjian R. Structure and function of a human TAFII250 double bromodomain module. *Science* 288: 1422-1425, 2000.

112. Jalinot P, Devaux B and Kedinger C. The abundance and in vitro DNA binding of three cellular proteins interacting with the adenovirus EIIa early promoter are not modified by the EIa gene products. *Mol Cell Biol* 7: 3806-3817, 1987.

113. Jeanmougin F, Wurtz JM, Le DB, Chambon P and Losson R. The bromodomain revisited. *Trends Biochem Sci* 22: 151-153, 1997.

114. Jensen EB, Zheng D, Russell RA, Bassel-Duby R, Williams RS, Olson AL and Dohm GL. Regulation of GLUT4 expression in denervated skeletal muscle. *Am J Physiol Regul Integr Comp Physiol* 296: R1820-R1828, 2009.

115. Jensen TE, Rose AJ, Hellsten Y, Wojtaszewski JF and Richter EA. Caffeine-induced Ca(2+) release increases AMPK-dependent glucose uptake in rodent soleus muscle. *Am J Physiol Endocrinol Metab* 293: E286-E292, 2007.

116. Jorgensen SB, Richter EA and Wojtaszewski JF. Role of AMPK in skeletal muscle metabolic regulation and adaptation in relation to exercise. *J Physiol* 574: 17-31, 2006.

117. Jorgensen SB, Treebak JT, Viollet B, Schjerling P, Vaulont S, Wojtaszewski JF and Richter EA. Role of AMPKalpha2 in basal, training-, and AICAR-induced GLUT4, hexokinase II, and mitochondrial protein expression in mouse muscle. *Am J Physiol Endocrinol Metab* 292: E331-E339, 2007.

118. Kao H, Verdel A, Tsai C, Simon C, Juguilon H and Kochbin S. Mechanism for Nucleocytoplasmic Shuttling of Histone Deacetylase 7. *Journal of Biological Chemistry* 276: 47496-47507, 2001.

119. Kawanaka K, Tabata I, Katsuta S and Higuchi M. Changes in insulin-stimulated glucose transport and GLUT-4 protein in rat skeletal muscle after training. *Journal of Applied Physiology* 83: 2043-2047, 1997.

120. Kennedy JW, Hirshman MF, Gervino EV, Ocel JV, Forse RA, Hoenig SJ, Aronson D, Goodyear LJ and Horton ES. Acute exercise induces GLUT4 translocation in skeletal muscle of normal human subjects and subjects with type 2 diabetes. *Diabetes* 48: 1192-1197, 1999.

121. Kim JK, Fillmore JJ, Sunshine MJ, Albrecht B, Higashimori T, Kim DW, Liu ZX, Soos TJ, Cline GW, O'Brien WR, Littman DR and Shulman GI. PKC-theta knockout mice are protected from fat-induced insulin resistance. *J Clin Invest* 114: 823-827, 2004.

122. King PA, Betts JJ, Horton ED and Horton ES. Exercise, unlike insulin, promotes glucose transporter translocation in obese Zucker rat muscle. *Am J Physiol* 265: R447-R452, 1993.

123. Kislinger T, Gramolini AO, Pan Y, Rahman K, MacLennan DH and Emili A. Proteome dynamics during C2C12 myoblast differentiation. *Mol Cell Proteomics* 4: 887-901, 2005.

124. Knight JB, Eyster CA, Griesel BA and Olson AL. Regulation of the human GLUT4 gene promoter: interaction between a transcriptional activator and myocyte enhancer factor 2A. *Proc Natl Acad Sci U S A* 100: 14725-14730, 2003.

125. Knutti D and Kralli A. PGC-1, a versatile coactivator. *Trends Endocrinol Metab* 12: 360-365, 2001.

126. Koranyi L, James D, Mueckler M and Permutt MA. Glucose transporter levels in spontaneously obese (db/db) insulin-resistant mice. *J Clin Invest* 85: 962-967, 1990.

127. Koves TR, Li P, An J, Akimoto T, Slentz D, Ilkayeva O, Dohm GL, Yan Z, Newgard CB and Muoio DM. Peroxisome proliferator-activated receptor-gamma co-activator 1 alpha-mediated metabolic remodeling of skeletal myocytes mimics exercise training and reverses lipid-induced mitochondrial inefficiency. *Journal of Biological Chemistry* 280: 33588-33598, 2005.

128. Krajewski WA. Histone hyperacetylation facilitates chromatin remodelling in a Drosophila embryo cell-free system. *Mol Gen Genet* 263: 38-47, 2000.

129. Kump DS and Booth FW. Alterations in insulin receptor signalling in the rat epitrochlearis muscle upon cessation of voluntary exercise. *Journal of Physiology-London* 562: 829-838, 2005.

130. Kuo MH and Allis CD. Roles of histone acetyltransferases and deacetylases in gene regulation. *Bioessays* 20: 615-626, 1998.

131. Lai Y, Nairn AC and Greengard P. Autophosphorylation reversibly regulates the Ca2+/calmodulin-dependence of Ca2+/calmodulin-dependent protein kinase II. *Proc Natl Acad Sci U S A* 83: 4253-4257, 1986.

132. Lee DY, Hayes JJ, Pruss D and Wolffe AP. A positive role for histone acetylation in transcription factor access to nucleosomal DNA. *Cell* 72: 73-84, 1993.

133. Lenka N, Vijayasarathy C, Mullick J and Avadhani NG. Structural organization and transcription regulation of nuclear genes encoding the mammalian cytochrome c oxidase complex. *Prog Nucleic Acid Res Mol Biol* 61: 309-344, 1998.

134. Leturque A, Loizeau M, Vaulont S, Salminen M and Girard J. Improvement of insulin action in diabetic transgenic mice selectively overexpressing GLUT4 in skeletal muscle. *Diabetes* 45: 23-27, 1996.

135. Li B, Holloszy JO and Semenkovich CF. Respiratory uncoupling induces delta-aminolevulinate synthase expression through a nuclear respiratory factor-1-dependent mechanism in HeLa cells. *J Biol Chem* 274: 17534-17540, 1999.

136. Linseman DA, Bartley CM, Le SS, Laessig TA, Bouchard RJ, Meintzer MK, Li M and Heidenreich KA. Inactivation of the myocyte enhancer factor-2 repressor histone deacetylase-5 by endogenous Ca(2+) //calmodulin-dependent kinase II promotes depolarization-mediated cerebellar granule neuron survival. *J Biol Chem* 278: 41472-41481, 2003.

137. Lipton RB, Liao Y and Cao G. Determinants of Non-Insulin-Dependent Diabetes-Mellitus Among Blacks and Whites in A National Sample - the Nhanes-I Epidemiologic Follow-Up-Study (Vol 138, Pg 826, 1993). *American Journal of Epidemiology* 139: 964-966, 1994.

138. Lipton RB, Liao YL, Cao GC, Cooper RS and Mcgee D. Determinants of Incident Non-Insulin-Dependent Diabetes-Mellitus Among Blacks and Whites in A National Sample - the Nhanes-I Epidemiologic Follow-Up-Study. *American Journal of Epidemiology* 138: 826-839, 1993.

139. Liu ML, Olson AL, Edgington NP, Moyerowley WS and Pessin JE. Myocyte Enhancer Factor-2 (Mef2) Binding-Site Is Essential for C2C12 Myotube-Specific Expression of the Rat Glut4 Muscle-Adipose Facilitative Glucose-Transporter Gene. *J Biol Chem* 269: 28514-28521, 1994.

140. Livak KJ and Schmittgen TD. Analysis of relative gene expression data using real-time quantitative PCR and the 2(T)(-Delta Delta C) method. *Methods* 25: 402-408, 2001.

141. Lou LL, Lloyd SJ and Schulman H. Activation of the multifunctional Ca2+/calmodulin-dependent protein kinase by autophosphorylation: ATP modulates production of an autonomous enzyme. *Proc Natl Acad Sci U S A* 83: 9497-9501, 1986.

142. Lowell BB and Shulmanz GI. Mitochondrial dysfunction and type 2 diabetes. *Science* 307: 384-387, 2005.

143. Lu JR, McKinsey TA, Nicol RL and Olson EN. Signal-dependent activation of the MEF2 transcription factor by dissociation from histone deacetylases. *Proc Natl Acad Sci U S A* 97: 4070-4075, 2000.

144. Lund S, Pryor PR, Ostergaard S, Schmitz O, Pedersen O and Holman GD. Evidence against protein kinase B as a mediator of contraction-induced glucose transport and GLUT4 translocation in rat skeletal muscle. *FEBS Lett* 425: 472-474, 1998.

145. Lyons GE, Micales BK, Schwarz J, Martin JF and Olson EN. Expression of mef2 genes in the mouse central nervous system suggests a role in neuronal maturation. *J Neurosci* 15: 5727-5738, 1995.

146. Ma H, Shang Y, Lee DY and Stallcup MR. Study of nuclear receptor-induced transcription complex assembly and histone modification by chromatin immunoprecipitation assays. *Methods Enzymol* 364: 284-296, 2003.

147. Ma K, Chan JK, Zhu G and Wu Z. Myocyte enhancer factor 2 acetylation by p300 enhances its DNA binding activity, transcriptional activity, and myogenic differentiation. *Mol Cell Biol* 25: 3575-3582, 2005.

148. Magas S, Poljicanin T, Sekerija M, Ajdukovic D, Metelko Z, Car N and Kern J. Lifestyle Habits of Croatian Diabetic Population: Observations from the Croatian Adult Health Survey. *Collegium Antropologicum* 33: 115-119, 2009.

149. Manco M, Mingrone G, Greco AV, Capristo E, Gniuli D, De Gaetano A and Gasbarrini G. Insulin resistance directly correlates with increased saturated fatty acids in skeletal muscle triglycerides. *Metabolism-Clinical and Experimental* 49: 220-224, 2000.

150. Manson JE, Rimm EB, Colditz GA, Stampfer MJ, Willett WC, Arky RA, Rosner B, Hennekens CH and Speizer FE. Parity and Incidence of Non-Insulin-Dependent Diabetes-Mellitus. *American Journal of Medicine* 93: 13-18, 1992.

151. Manson JE, Rimm EB, Stampfer MJ, Colditz GA, Willett WC, Krolewski AS, Rosner B, Hennekens CH and Speizer FE. Physical-Activity and Incidence of Non-Insulin-Dependent Diabetes-Mellitus in Women. *Lancet* 338: 774-778, 1991.

152. Marechal E, Hiratsuka K, Delgado J, Nairn A, Qin J, Chait BT and Chua NH. Modulation of GT-1 DNA-binding activity by calcium-dependent phosphorylation. *Plant Mol Biol* 40: 373-386, 1999.

153. Marette A, Richardson JM, Ramlal T, Balon TW, Vranic M, Pessin JE and Klip A. Abundance, localization, and insulin-induced translocation of glucose transporters in red and white muscle. *Am J Physiol* 263: C443-C452, 1992.

154. Mayer-Davis EJ, D'Agostino R, Karter AJ, Haffner SM, Rewers MJ, Saad M and Bergman RN. Intensity and amount of physical activity in relation to insulin sensitivity - The Insulin Resistance Atherosclerosis Study. *Jama-Journal of the American Medical Association* 279: 669-674, 1998.

155. McGarry JD. Dysregulation of fatty acid metabolism in the etiology of type 2 diabetes. *Diabetes* 51: 7-18, 2002.

156. Mcgee SL and Hargreaves M. Exercise and myocyte enhancer factor 2 regulation in human skeletal muscle. *Diabetes* 53: 1208-1214, 2004.

157. Mcgee SL, Sparling D, Olson AL and Hargreaves M. Exercise increases MEF2- and GEF DNA-binding activities in human skeletal muscle. *FASEB J* 2005.

158. McKinsey TA, Zhang CL, Lu JR and Olson EN. Signal-dependent nuclear export of a histone deacetylase regulates muscle differentiation. *Nature* 408: 106-111, 2000.

159. McKinsey TA, Zhang CL and Olson EN. Control of muscle development by dueling HATs and HDACs. *Curr Opin Genet Dev* 11: 497-504, 2001.

160. Michael LF, Wu Z, Cheatham RB, Puigserver P, Adelmant G, Lehman JJ, Kelly DP and Spiegelman BM. Restoration of insulin-sensitive glucose transporter (GLUT4) gene expression in muscle cells by the transcriptional coactivator PGC-1. *Proc Natl Acad Sci U S A* 98: 3820-3825, 2001.

161. Mootha VK, Lindgren CM, Eriksson KF, Subramanian A, Sihag S, Lehar J, Puigserver P, Carlsson E, Ridderstrale M, Laurila E, Houstis N, Daly MJ, Patterson N, Mesirov JP, Golub TR, Tamayo P, Spiegelman B, Lander ES, Hirschhorn JN, Altshuler D and Groop LC. PGC-1 alpha-responsive genes involved in oxidative phosphorylation are coordinately downregulated in human diabetes. *Nature Genetics* 34: 267-273, 2003.

162. Mora S and Pessin JE. The MEF2A isoform is required for striated muscle-specific expression of the insulin-responsive GLUT4, glucose transporter. *J Biol Chem* 275: 16323-16328, 2000.

163. Morino K, Neschen S, Bilz S, Sono S, Tsirigotis D, Reznick RM, Samuel V, Philbrick WM and Shulman GI. IRS-1 serine phosphorylation is a key molecular event in the pathogenesis of fat-induced insulin resistance in skeletal muscle in vivo. *Diabetes* 54: A339, 2005.

164. Morrish F, Giedt C and Hockenbery D. c-MYC apoptotic function is mediated by NRF-1 target genes. *Genes Dev* 17: 240-255, 2003.

165. Naya FJ, Black BL, Wu H, Bassel-Duby R, Richardson JA, Hill JA and Olson EN. Mitochondrial deficiency and cardiac sudden death in mice lacking the MEF2A transcription factor. *Nat Med* 8: 1303-1309, 2002.

166. Nedachi T, Fujita H and Kanzaki M. Contractile C2C12 myotube model for studying exercise-inducible responses in skeletal muscle. *Am J Physiol Endocrinol Metab* 295: E1191-E1204, 2008.

167. Neufer PD and Dohm GL. Exercise induces a transient increase in transcription of the GLUT-4 gene in skeletal muscle. *Am J Physiol* 265: C1597-C1603, 1993.

168. Norton VG, Marvin KW, Yau P and Bradbury EM. Nucleosome linking number change controlled by acetylation of histones H3 and H4. *J Biol Chem* 265: 19848-19852, 1990.

169. O'Gorman DJ, Karlsson HKR, McQuaid S, Yousif O, Rahman Y, Gasparro D, Glund S, Chibalin AV, Zierath JR and Nolan JJ. Exercise training increases insulin-stimulated glucose disposal and GLUT4 (SLC2A4) protein content in patients with type 2 diabetes. *Diabetologia* 49: 2983-2992, 2006.

170. Oakes ND, Bell KS, Furler SM, Camilleri S, Saha AK, Ruderman NB, Chisholm DJ and Kraegen EW. Diet-induced muscle insulin resistance in rats is ameliorated by acute dietary lipid withdrawal or a single bout of exercise: parallel relationship between insulin stimulation of glucose uptake and suppression of long-chain fatty acyl-CoA. *Diabetes* 46: 2022-2028, 1997.

171. Ogryzko VV, Schiltz RL, Russanova V, Howard BH and Nakatani Y. The transcriptional coactivators p300 and CBP are histone acetyltransferases. *Cell* 87: 953-959, 1996.

172. Ojuka EO, Jones TE, Han DH, Chen M and Holloszy JO. Raising Ca2+ in L6 myotubes mimics effects of exercise on mitochondrial biogenesis in muscle. *FASEB J* 17: 675-681, 2003.

173. Ojuka EO, Jones TE, Nolte LA, Chen M, Wamhoff BR, Sturek M and Holloszy JO. Regulation of GLUT4 biogenesis in muscle: evidence for involvement of AMPK and Ca(2+). *Am J Physiol* 282: E1008-E1013, 2002.

174. Oshel KM, Knight JB, Cao KT, Thai MV and Olson AL. Identification of a 30-base pair regulatory element and novel DNA binding protein that regulates the human GLUT4 promoter in transgenic mice. *J Biol Chem* 275: 23666-23673, 2000.

175. Owen DJ, Ornaghi P, Yang JC, Lowe N, Evans PR, Ballario P, Neuhaus D, Filetici P and Travers AA. The structural basis for the recognition of acetylated histone H4 by the bromodomain of histone acetyltransferase gcn5p. *EMBO J* 19: 6141-6149, 2000.

176. Passier R, Zeng H, Frey N, Naya FJ, Nicol RL, McKinsey TA, Overbeek P, Richardson JA, Grant SR and Olson EN. CaM kinase signaling induces cardiac hypertrophy and activates the MEF2 transcription factor in vivo. *J Clin Invest* 105: 1395-1406, 2000.

177. Patti ME, Butte AJ, Crunkhorn S, Cusi K, Berria R, Kashyap S, Miyazaki Y, Kohane I, Costello M, Saccone R, Landaker EJ, Goldfine AB, Mun E, Defronzo R, Finlayson J, Kahn CR and Mandarino LJ. Coordinated reduction of genes of oxidative metabolism in humans with insulin resistance and diabetes: Potential role of PGC1 and NRF1. *Proceedings of the National Academy of Sciences of the United States of America* 100: 8466-8471, 2003.

178. Pelosi M and Donella-Deana A. Localization, purification, and characterization of the rabbit sarcoplasmic reticulum associated calmodulin-dependent protein kinase. *Biochemistry (Mosc)* 65: 259-268, 2000.

179. Perseghin G, Price TB, Petersen KF, Roden M, Cline GW, Gerow K, Rothman DL and Shulman GI. Increased glucose transport-phosphorylation and muscle glycogen synthesis after exercise training in insulin-resistant subjects. *N Engl J Med* 335: 1357-1362, 1996.

180. Petersen KF, Befroy D, Dufour S, Dziura J, Ariyan C, Rothman DL, DiPietro L, Cline GW and Shulman GI. Nuclear magnetic resonance spectroscopic studies of mitochondrial oxidative phosphorylation activity and insulin resistance in the elderly. *Journal of Investigative Medicine* 51: S370-S371, 2003.

181. Petersen KF, Dufour S, Befroy D, Garcia R and Shulman GI. Impaired mitochondrial activity in the insulin-resistant offspring of patients with type 2 diabetes. *New England Journal of Medicine* 350: 664-671, 2004.

182. Pownall ME, Gustafsson MK and Emerson CP, Jr. Myogenic regulatory factors and the specification of muscle progenitors in vertebrate embryos. *Annu Rev Cell Dev Biol* 18: 747-783, 2002.

183. Puigserver P, Adelmant G, Wu Z, Fan M, Xu J, O'Malley B and Spiegelman BM. Activation of PPARgamma coactivator-1 through transcription factor docking. *Science* 286: 1368-1371, 1999.

184. Puntschart A, Claassen H, Jostarndt K, Hoppeler H and Billeter R. Messenger-Rnas of Enzymes Involved in Energy-Metabolism and Mtdna Are Increased in Endurance-Trained Athletes. *American Journal of Physiology-Cell Physiology* 38: C619-C625, 1995.

185. Ramachandran B, Yu GS and Gulick T. Nuclear respiratory factor 1 controls myocyte enhancer factor 2A transcription to provide a mechanism for coordinate expression of respiratory chain subunits. *Journal of Biological Chemistry* 283: 11935-11946, 2008.

186. Rasmussen BB, Hancock CR and Winder WW. Postexercise recovery of skeletal muscle malonyl-CoA, acetyl-CoA carboxylase, and AMP-activated protein kinase. *J Appl Physiol* 85: 1629-1634, 1998.

187. Rauch C and Loughna PT. Static stretch promotes MEF2A nuclear translocation and expression of neonatal myosin heavy chain in C2C12 myocytes in a calcineurin- and p38-dependent manner. *Am J Physiol Cell Physiol* 288: C593-C605, 2005.

188. Ren B and Dynlacht BD. Use of chromatin immunoprecipitation assays in genome-wide location analysis of mammalian transcription factors. *Methods Enzymol* 376: 304-315, 2004.

189. Richter EA, Garetto LP, Goodman MN and Ruderman NB. Muscle Glucose-Metabolism Following Exercise in the Rat - Increased Sensitivity to Insulin. *Journal of Clinical Investigation* 69: 785-793, 1982.

190. Robyr D, Wolffe AP and Wahli W. Nuclear hormone receptor coregulators in action: diversity for shared tasks. *Mol Endocrinol* 14: 329-347, 2000.

191. Rockl KS, Hirshman MF, Brandauer J, Fujii N, Witters LA and Goodyear LJ. Skeletal muscle adaptation to exercise training: AMP-activated protein kinase mediates muscle fiber type shift. *Diabetes* 56: 2062-2069, 2007.

192. Rodnick KJ, Henriksen EJ, James DE and Holloszy JO. Exercise training, glucose transporters, and glucose transport in rat skeletal muscles. *Am J Physiol* 262: C9-14, 1992.

193. Rose AJ, Frosig C, Kiens B, Wojtaszewski JF and Richter EA. Effect of endurance exercise training on Ca2+ calmodulin-dependent protein kinase II expression and signalling in skeletal muscle of humans. *J Physiol* 583: 785-795, 2007.

194. Rose AJ and Hargreaves M. Exercise increases Ca2+-calmodulin-dependent protein kinase II activity in human skeletal muscle. *J Physiol -Lond* 553: 303-309, 2003.

195. Rose AJ, Kiens B and Richter EA. Ca2+-calmodulin-dependent protein kinase expression and signalling in skeletal muscle during exercise. *Journal of Physiology-London* 574: 889-903, 2006.

196. **Ryder JW, Yang J, Galuska D, Rincon J, Bjornholm M, Krook A, Lund S, Pedersen O, Wallberg-Henriksson H, Zierath JR and Holman GD. Use of a novel impermeable biotinylated photolabeling reagent to assess insulin- and hypoxia-stimulated cell surface GLUT4 content in skeletal muscle from type 2 diabetic patients.** ***Diabetes*** **49: 647-654, 2000.**

197. **Santalucia T, Moreno H, Palacin M, Yacoub MH, Brand NJ and Zorzano A. A novel functional co-operation between MyoD, MEF2 and TRalpha1 is sufficient for the induction of GLUT4 gene transcription.** ***J Mol Biol*** **314: 195-204, 2001.**

198. **Sartorelli V, Huang J, Hamamori Y and Kedes L. Molecular mechanisms of myogenic coactivation by p300: direct interaction with the activation domain of MyoD and with the MADS box of MEF2C.** ***Mol Cell Biol*** **17: 1010-1026, 1997.**

199. **Scarpulla RC. Nuclear activators and coactivators in mammalian mitochondrial biogenesis.** ***Biochim Biophys Acta*** **1576: 1-14, 2002.**

200. **Schaefer L, Engman H and Miller JB. Coding sequence, chromosomal localization, and expression pattern of Nrf1: the mouse homolog of Drosophila erect wing.** ***Mamm Genome*** **11: 104-110, 2000.**

201. **Schenk S and Horowitz JF. Acute exercise increases triglyceride synthesis in skeletal muscle and prevents fatty acid-induced insulin resistance.** ***J Clin Invest*** **117: 1690-1698, 2007.**

202. Schmitz-Peiffer C. Signalling aspects of insulin resistance in skeletal muscle: mechanisms induced by lipid oversupply. *Cellular Signalling* 12: 583-594, 2000.

203. Schmitz-Peiffer C, Browne CL, Oakes ND, Watkinson A, Chisholm DJ, Kraegen EW and Biden TJ. Alterations in the expression and cellular localization of protein kinase C isozymes epsilon and theta are associated with insulin resistance in skeletal muscle of the high-fat-fed rat. *Diabetes* 46: 169-178, 1997.

204. Schranz A, Tuomilehto J, Marti B, Jarrett RJ, Grabauskas V and Vassallo A. Low physical activity and worsening of glucose tolerance: results from a 2-year follow-up of a population sample in Malta. *Diabetes Res Clin Pract* 11: 127-136, 1991.

205. Seki Y, Berggren JR, Houmard JA and Charron MJ. Glucose transporter expression in skeletal muscle of endurance-trained individuals. *Med Sci Sports Exerc* 38: 1088-1092, 2006.

206. Shen K and Meyer T. In vivo and in vitro characterization of the sequence requirement for oligomer formation of Ca2+/calmodulin-dependent protein kinase IIalpha. *J Neurochem* 70: 96-104, 1998.

207. Shen X, Collier JM, Hlaing M, Zhang L, Delshad EH, Bristow J and Bernstein HS. Genome-wide examination of myoblast cell cycle withdrawal during differentiation. *Dev Dyn* 226: 128-138, 2003.

208. Short KR, Vittone JL, Bigelow ML, Proctor DN, Rizza RA, Coenen-Schimke JM and Nair KS. Impact of aerobic exercise training on age-related changes in insulin sensitivity and muscle oxidative capacity. *Diabetes* 52: 1888-1896, 2003.

209. Slentz CA, Gulve EA, Rodnick KJ, Henriksen EJ, Youn JH and Holloszy JO. Glucose Transporters and Maximal Transport Are Increased in Endurance-Trained Rat Soleus. *Journal of Applied Physiology* 73: 486-492, 1992.

210. Slepak TI, Webster KA, Zang J, Prentice H, O'Dowd A, Hicks MN and Bishopric NH. Control of cardiac-specific transcription by p300 through myocyte enhancer factor-2D. *J Biol Chem* 276: 7575-7585, 2001.

211. Smith JA, Kohn TA, Chetty AK and Ojuka EO. CaMK activation during exercise is required for histone hyperacetylation and MEF2A binding at the MEF2 site on the Glut4 gene. *Am J Physiol Endocrinol Metab* 295: E698-E704, 2008.

212. Smith JAH, Collins M, Grobler LA, Magee CJ and Ojuka EO. Exercise and CaMK activation both increase the binding of MEF2A to the Glut4 promoter in skeletal muscle in vivo. *American Journal of Physiology-Endocrinology and Metabolism* 292: E413-E420, 2007.

213. Sobel RE, Cook RG, Perry CA, Annunziato AT and Allis CD. Conservation of deposition-related acetylation sites in newly synthesized histones H3 and H4. *Proc Natl Acad Sci U S A* 92: 1237-1241, 1995.

214. Sparling DP, Griesel BA, Weems J and Olson AL. GLUT4 enhancer factor (GEF) interacts with MEF2A and HDAC5 to regulate the GLUT4 promoter in adipocytes. *J Biol Chem* 283: 7429-7437, 2008.

215. Spiegelman BM, Puigserver P and Wu Z. Regulation of adipogenesis and energy balance by PPARgamma and PGC-1. *Int J Obes Relat Metab Disord* 24 Suppl 4: S8-10, 2000.

216. Storlien LH, Jenkins AB, Chisholm DJ, Pascoe WS, Khouri S and Kraegen EW. Influence of Dietary-Fat Composition on Development of Insulin Resistance in Rats - Relationship to Muscle Triglyceride and Omega-3-Fatty-Acids in Muscle Phospholipid. *Diabetes* 40: 280-289, 1991.

217. Strahl BD and Allis CD. The language of covalent histone modifications. *Nature* 403: 41-45, 2000.

218. Strahl BD, Huang HJ, Sebastian J, Ghosh BR and Miller WL. Transcriptional activation of the ovine follicle-stimulating hormone beta-subunit gene by gonadotropin-releasing hormone: involvement of two activating protein-1-binding sites and protein kinase C. *Endocrinology* 139: 4455-4465, 1998.

219. Sui G, Soohoo C, Affar eB, Gay F, Shi Y, Forrester WC and Shi Y. A DNA vector-based RNAi technology to suppress gene expression in mammalian cells. *Proc Natl Acad Sci U S A* 99: 5515-5520, 2002.

220. Taguchi T, Kishikawa H, Motoshima H, Sakai K, Nishiyama T, Yoshizato K, Shirakami A, Toyonaga T, Shirotani T, Araki E and Shichiri M. Involvement of bradgkinin in acute exercise-induced increase of glucose uptake and GLUT-4 translocation in skeletal muscle: Studies in normal and diabetic humans and rats. *Metabolism-Clinical and Experimental* 49: 920-930, 2000.

221. Tamkun JW, Deuring R, Scott MP, Kissinger M, Pattatucci AM, Kaufman TC and Kennison JA. brahma: a regulator of Drosophila homeotic genes structurally related to the yeast transcriptional activator SNF2/SWI2. *Cell* 68: 561-572, 1992.

222. Terada S, Yokozeki T, Kawanaka K, Ogawa K, Higuchi M, Ezaki O and Tabata I. Effects of high-intensity swimming training on GLUT-4 and glucose transport activity in rat skeletal muscle. *J Appl Physiol* 90: 2019-2024, 2001.

223. Thai MV, Guruswamy S, Cao KT, Pessin JE and Olson AL. Myocyte enhancer factor 2 (MEF2)-binding site is required for GLUT4 gene expression in transgenic mice. Regulation of MEF2 DNA binding activity in insulin-deficient diabetes. *J Biol Chem* 273: 14285-14292, 1998.

224. Turner BM. Histone acetylation and an epigenetic code. *Bioessays* 22: 836-845, 2000.

225. Usui K, Yamanouchi K, Asai K, Yajima M, Iriyama A, Okabayashi N, Sakakibara H, Kusunoki M, Kakumu S and Sato Y. The effect of low intensity bicycle exercise on the insulin-induced glucose uptake in obese patients with type 2 diabetes. *Diabetes Res Clin Pract* 41: 57-61, 1998.

226. Virbasius CA, Virbasius JV and Scarpulla RC. NRF-1, an activator involved in nuclear-mitochondrial interactions, utilizes a new DNA-binding domain conserved in a family of developmental regulators. *Genes Dev* 7: 2431-2445, 1993.

227. Vissing K, Mcgee SL, Roepstorff C, Schjerling P, Hargreaves M and Kiens B. Effect of sex differences on human MEF2 regulation during endurance exercise. *Am J Physiol Endocrinol Metab* 294: E408-E415, 2008.

228. Wan B and Moreadith RW. Structural characterization and regulatory element analysis of the heart isoform of cytochrome c oxidase VIa. *J Biol Chem* 270: 26433-26440, 1995.

229. Wannamethee SG, Shaper AG and Alberti KGMM. Physical activity, metabolic factors, and the incidence of coronary heart disease and type 2 diabetes. *Archives of Internal Medicine* 160: 2108-2116, 2000.

230. Watson RT, Kanzaki M and Pessin JE. Regulated membrane trafficking of the insulin-responsive glucose transporter 4 in adipocytes. *Endocr Rev* 25: 177-204, 2004.

231. Willems MET, Brozinick JT, Torgan CE, Cortez MY and Ivy JL. Muscle Glucose-Uptake of Obese Zucker Rats Trained at 2 Different Intensities. *Journal of Applied Physiology* 70: 36-42, 1991.

232. Wojtaszewski JF, Nielsen P, Hansen BF, Richter EA and Kiens B. Isoform-specific and exercise intensity-dependent activation of 5'-AMP-activated protein kinase in human skeletal muscle. *J Physiol* 528 Pt 1: 221-226, 2000.

233. Wright DC, Geiger PC, Han DH, Jones TE and Holloszy JO. Calcium induces increases in peroxisome proliferator-activated receptor gamma coactivator-1alpha and mitochondrial biogenesis by a pathway leading to p38 mitogen-activated protein kinase activation. *J Biol Chem* 282: 18793-18799, 2007.

234. Wu H, Kanatous SB, Thurmond FA, Gallardo T, Isotani E, Bassel-Duby R and Williams RS. Regulation of mitochondrial biogenesis in skeletal muscle by CaMK. *Science* 296: 349-352, 2002.

235. Yang SH, Galanis A and Sharrocks AD. Targeting of p38 mitogen-activated protein kinases to MEF2 transcription factors. *Mol Cell Biol* 19: 4028-4038, 1999.

236. Yin DX, Zhu L and Schimke RT. Tetracycline-controlled gene expression system achieves high-level and quantitative control of gene expression. *Anal Biochem* 235: 195-201, 1996.

237. Youn HD, Chatila TA and Liu JO. Integration of calcineurin and MEF2 signals by the coactivator p300 during T-cell apoptosis. *Embo Journal* 19: 4323-4331, 2000.

238. Yu C, Chen Y, Cline GW, Zhang D, Zong H, Wang Y, Bergeron R, Kim JK, Cushman SW, Cooney GJ, Atcheson B, White MF, Kraegen EW and Shulman GI. Mechanism by which fatty acids inhibit insulin activation of insulin receptor substrate-1 (IRS-1)-associated phosphatidylinositol 3-kinase activity in muscle. *J Biol Chem* 277: 50230-50236, 2002.

239. Yuan GX, Nanduri J, Bhasker CR, Semenza GL and Prabhakar NR. Ca2+/calmodulin kinase-dependent activation of hypoxia inducible factor 1 transcriptional activity in cells subjected to intermittent hypoxia. *Journal of Biological Chemistry* 280: 4321-4328, 2005.

240. Zayzafoon M, Fulzele K and McDonald JM. Calmodulin and calmodulin-dependent kinase IIalpha regulate osteoblast differentiation by controlling c-fos expression. *J Biol Chem* 280: 7049-7059, 2005.

241. Zhang T, Kohlhaas M, Backs J, Mishra S, Phillips W, Dybkova N, Chang S, Ling H, Bers DM, Maier LS, Olson EN and Brown JH. CaMKIIdelta isoforms differentially affect calcium handling but similarly regulate HDAC/MEF2 transcriptional responses. *J Biol Chem* 282: 35078-35087, 2007.

242. Zhao M, New L, Kravchenko VV, Kato Y, Gram H, di PF, Olson EN, Ulevitch RJ and Han J. Regulation of the MEF2 family of transcription factors by p38. *Mol Cell Biol* 19: 21-30, 1999.

243. Zierath JR, He L, Guma A, Odegoard WE, Klip A and Wallberg-Henriksson H. Insulin action on glucose transport and plasma membrane GLUT4 content in skeletal muscle from patients with NIDDM. *Diabetologia* 39: 1180-1189, 1996.